Design and Construction of Molecular Assemblies with Large Second-Order Optical Nonlinearities. Quantum Chemical Aspects

David R. Kanis,* Mark A. Ratner,* and Tobin J. Marks*

Department of Chemistry and the Materials Research Center, Northwestern University, Evanston, Illinois 60208-3113

Contents

I. Introduction

Nonlinear optics (NLO) deals with the interactions of applied electromagnetic fields in various materials to generate new electromagnetic fields, altered in frequency, phase, or other physical properties. Substances able to manipulate photonic signals efficiently are of importance in technologies such as optical communication, optical computing, and dynamic image processing.[1-15] In general, progress in these areas would be greatly enhanced by the availability of readily processed materials with sufficiently large NLO responses and having other desirable properties (vide infra). Thus, extensive research efforts have been directed at synthesizing more efficient photon-manipulating materials.[16-34]

There exist three generic classes of NLO materials: multilayered semiconductor structures, molecular-based macroscopic assemblies, and traditional inorganic solids. Each class possesses its own complement of favorable and unfavorable attributes,[35] and to date, the inorganic solids, such as $LiNbO_3$ and KH_2PO_4, have traditionally been the NLO materials of choice. However, recent results suggest that molecule-based macroscopic π-electron assemblies possess many attractive NLO characteristics. Specifically, these materials offer ultrafast response times, lower dielectric constants, better processability characteristics, and enhanced NLO responses relative to the traditional inorganic solids.[16-34] Since the NLO response of these molecule-based materials is ultimately governed by the NLO characteristics of the constituent molecular chromophores, the search for novel molecules capable of manipulating electric fields, especially photonic signals, is currently an intense area of research.

Traditionally, NLO-active molecules were discovered by laborious Edisonian searches with only rudimentary design rules to guide such synthetic explorations. Contemporary chromophore synthetic chemistry is highly labor, expendables, and facilities intensive, with the outcome of many tedious syntheses frequently being uncertain. In the past half-decade, chemically-oriented theoretical/computational quantum procedures have profoundly changed the science of chromophore design. Reliable computational techniques provide the basic understanding necessary to expeditiously target optimum chromophore structures and structural families. Experimentalists are able to apply chemical intuition in concert with insight provided by such contemporary computations to effectively guide synthetic strategies. Not surprisingly, a large number of publications reporting new NLO response formalisms have appeared in the recent literature. Due to the technological ramifications of this area and the evolution of "black-box"-type quantum chemical programs for NLO response computations, the reliable answers provided by such algorithms as well as our understanding of quadratic hyperpolarizabilities have markedly increased in the last several years, as evidenced by the dramatic increase in the publications devoted to understanding structure–property relationships in non-linear optics.
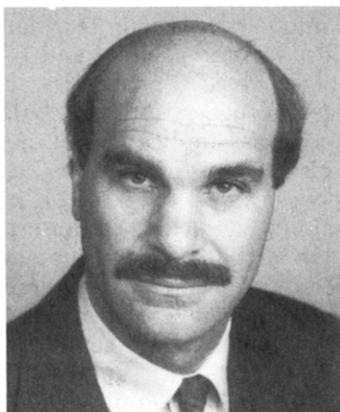
Within the general area of materials chemistry, an important challenge to electronic structure techniques
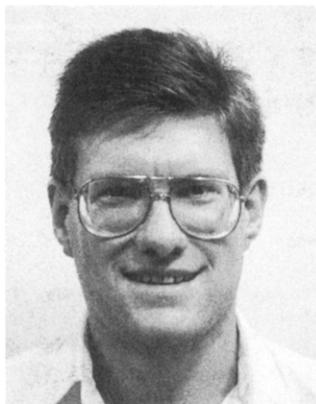
David R. Kanis was born in Rochester, NY, in 1961. He received a B.S. degree from Rensselaer Polytechnic Institute in 1983 and a Ph.D. from the University of Wisconsin—Madison in 1988, working with R. F. Fenske. He is presently a postdoctoral fellow at Northwestern University. His research interests center around theoretical inorganic chemistry and identifying structure–property relationships in materials chemistry.

Mark Ratner, Professor of Chemistry at Northwestern University, comes from Cleveland. His chemical education includes an undergraduate degree from Harvard, a doctoral degree from Northwestern, postdoctoral experiences in Denmark and Germany, and faculty positions in New York and at Northwestern. His research interests center on the use of theoretical methods to understand problems of chemical mechanism, structure, and behavior. More specific interests include molecular electronics, dynamics of coupled-mode systems, ion and electron transfer, nonlinear optics, and chemical education and science policy.

Tobin J. Marks was born in Washington, D.C., in 1944. He received a B.S. degree from the University of Maryland in 1966 and a Ph.D. from M.I.T. in 1970, working under F. A. Cotton. He moved to Northwestern University as an assistant professor in 1970. Tobin Marks is currently Charles E. and Emma H. Morrison Professor of Chemistry and Professor of Materials Science and Engineering at Northwestern. His research interests include the synthesis and properties of unusual molecules and molecule-derived materials.

lies not so much in performing extremely accurate calculations (as is required, say, for dissociation energies or ionization potentials), but rather in interpretation, correlation, and prediction of experimental observations. That is, the challenge is not necessarily to reproduce the frequency-dependent molecular hyper-polarizabilities to the second or third decimal place, but rather to understand what aspects of molecular electronic structure are responsible for the observed NLO response.

The field of nonlinear optical materials is, in many senses, a paradigm for modern materials chemistry: it embodies challenges in the design, synthesis, analysis, improvement, and utilization of molecule-based materials with designed microstructural organization for an ultimate application. To make progress toward this goal of materials by design, theoretical concepts must be used to understand the nonlinear response at the individual chromophore level, to model the modification of isolated chromophores caused by environmental

interactions (including those with solvent, host matrix, and other chromophores), and finally to describe the overall response of the macroscopic material. Each of these steps comprises a substantial challenge to theoretical chemistry; calculation of the nonlinear optical response of isolated molecules is itself difficult, and such calculations are both computationally demanding and methodologically challenging. Intermolecular and molecule/solvent interactions are generally modeled by molecular field approximations, the validity and utility of which are still not clear. Finally, even direct comparison of computation with experiment has been problematic, because the most common experiments (e.g., the solution-phase EFISH method) are performed in differing solvents at finite temperatures, because of problems in achieving reproducibility of experiments from laboratory to laboratory, and due to a number of currently unsettled conventions and definitions.[36-39]

This contribution is directed toward chemists interested in second-order NLO chromophores, but not possessing a comprehensive background in photonics, physics, or computational chemistry. In this review we seek to (1) describe and objectively evaluate the methods currently available for computing quadratic hydropolarizabilities and (2) report selected results derived from such computational studies through illustrative examples. Specifically, in section II we will present the fundamental concepts of the nonlinear optical phenomenon and discuss the theoretical approaches employed for computing second-order susceptibilities and their respective reliabilities. Section III highlights the various models for extracting chemical information from computational studies, while section IV surveys applications of *ab initio* procedures in understanding the origin of NLO responses in molecular chromophores. Section V is devoted to applications of semiempirical treatments. Both organic chromophores and the less investigated area of organometallic chromophores are discussed, as well as chromophore–chromophore interactions, nonlinear response of charge-transfer complexes, and supermolecule analysis of interchromophore behavior. Finally, some general comments are made in section VI.

The present volume of *Chemical Reviews* includes a number of papers the emphases of which are both complementary to and helpful for understanding this article. Shelton and Rice present an overall view of nonlinear responses, including discussions of atomic calculations, accurate calculations of the response of diatomics, symmetries among the various nonlinear responses of both second- and third-order, vibronic effects, and some discussion of the effect of external fields. In particular, their discussion of the effects of vibration, of finite temperature and of external fields on the nonlinear response covers this area adequately; we therefore will say nothing about these matters. Brédas and Walsh review the calculation of the cubic hyperpolarizability, and many of the conclusions reached there complement our discussion. Zyss provides an elegant discussion of nonlinear optics in nontraditional chromophores, as well as a treatment of nonlinear response in general; his contribution is an interesting complement to the more standard approach taken here.

II. Theoretical Methodologies for Computing Second-Order Responses

A. Fundamental Concepts

The rationalization, computation, and prediction of NLO responses centers on our understanding of how light interacts with matter. Comprehensive treatments (quantitative) of the physics of nonlinear optics originating from electron–photon interactions can be found elsewhere.[1-6] Here, we choose to introduce the NLO phenomenon through a qualitative, chemically-oriented picture.

Electric fields (F), such as an applied dc field or a propagating electromagnetic wave, always induce electron displacements in bulk media.[1-6,40] Electrons in a material are bound to nearby nuclei, however, their locations will be slightly perturbed by an external field. In an applied oscillatory field, the electrons will begin oscillating at the applied frequency. The magnitude of such an induced "polarization" at modest field strengths will be proportional to the applied field as sketched in Figure 1a. Quantitatively, the macroscopic polarization (P) is frequently expressed as a function of a medium-dependent susceptibility $\chi^{(1)}$, as given in eq 1. So long as the electric field strength is small

$$P = \chi^{(1)}F \qquad (1)$$

compared with interatomic coulombic fields (10^9 V/cm), the response of the electron cloud will be linear.

The nonlinear optical phenomenon arises from the breakdown of eq 1 at sufficiently intense fields.[1-6,40,41] As the applied field strengths increase, the polarization response of the medium is no longer linear as shown pictorially in Figure 1, parts b and c. Only after the advent of the laser could optical fields of sufficient intensity be produced to observe this effect.[42] To account for the "nonlinearity" of the medium response, the induced polarization is given as a schematic power series expansion in the electric field:

$$P = \chi^{(1)}F + \chi^{(2)}FF + \chi^{(3)}FFF + ... \qquad (2)$$

where the coefficients $\chi^{(2)}$ and $\chi^{(3)}$ represent the second- and third-order responses of the material, respectively.
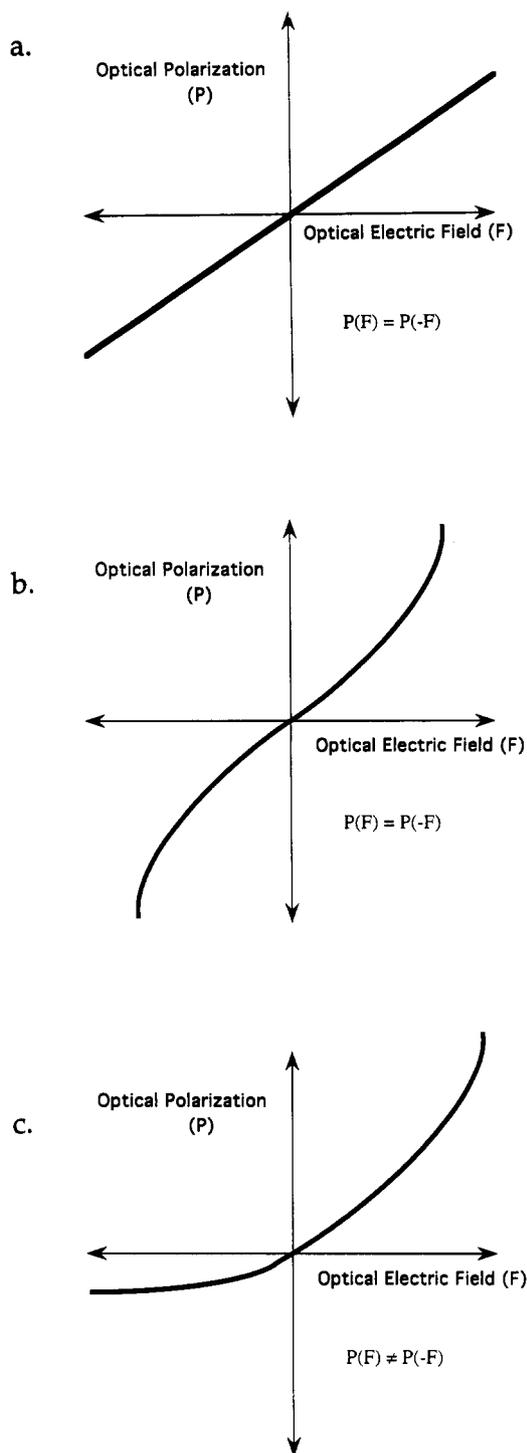
Figure 1. Schematic representation depicting the optical polarization in (a) linear, (b) centrosymmetric nonlinear, and (c) noncentrosymmetric nonlinear media.

In Figure 1b, the nonlinear polarization in the $+F$ direction ($P(+F)$) is identical to the induced polarization in the opposite direction ($P(-F)$), thus this diagram depicts the induced polarization in a centrosymmetric medium. One feature that follows from this symmetry property is that the power series expansion of P cannot contain even terms (i.e $\chi^{(2)} = \chi^{(4)} ... = 0$). In contrast, Figure 1c depicts the nonlinear polarization induced in a noncentrosymmetric material since $P(+F) \neq P(-F)$. From eq 2, we see that the second-order response ($\chi^{(2)}$) can only be nonzero in a noncentrosymmetric material $[P(+F) \neq P(-F)]$.

Figure 2. The polarization response $P(x)$ of a push/pull molecule in the x direction as a function of time due to an electric field oscillating at $F(\omega)$, and the Fourier components of $P(x)$ at frequencies ω, 2ω, and 0. (Reprinted from ref 32. Copyright 1984 Verlag.)

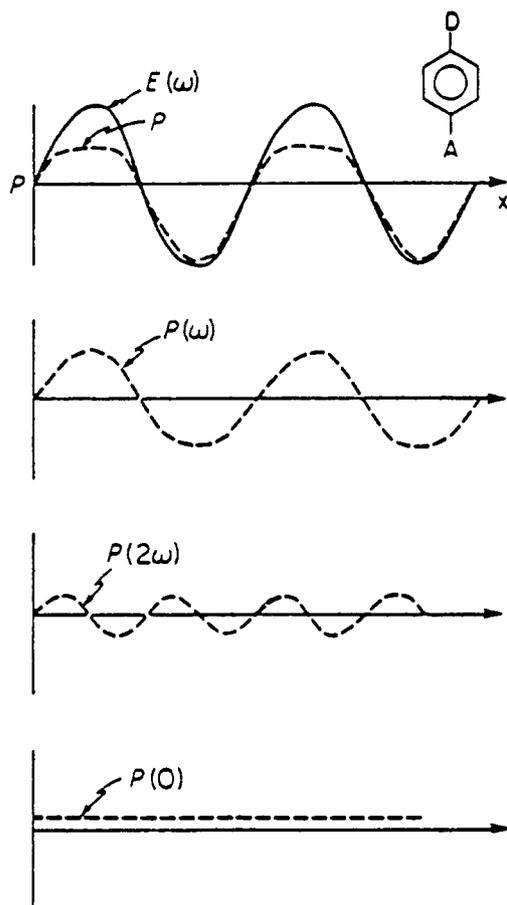The connection between the nonlinear polarization response described above and harmonic generation in NLO materials can be gained using a chemically-oriented picture put forth by Yariv[41] and Williams.[32] This instructive description considers an individual molecular unit rather than a collection of molecular units. In this representation, stronger optical fields compete more successfully with the interatomic binding forces, thereby permitting electrons to move further away from equilibrium locations. As a consequence, nearby environments will affect the microscopic polarizability of the molecule. For the prototypical electron donor/acceptor molecule (noncentrosymmetric) displayed in Figure 2, the molecule would exhibit an asymmetric polarization response to a symmetric electric field at intense field strengths since electron density is more easily displaced toward an acceptor substituent than toward a substituent donor. If the polarization response is asymmetric, it can be described as a summation of the Fourier components of frequencies ω, 2ω, 3ω, etc. as displayed in Figure 2. The harmonic components of the polarization, such as $P(2\omega)$, will produce a photonic electric field of harmonic frequencies $(F(2\omega))$. It is not difficult to envision an ensemble of microscopic units each contributing to the macroscopic polarization in a similar fashion, thus producing a macroscopic harmonic response. Thus, medium-dependent coefficients of the polarization

expansion that are directly linked to the nonlinear optical susceptibility of a material provide a quantitative measure of the ability of a bulk material to manipulate light and are the parameters that researchers in NLO materials seek to optimize.

This qualitative description must be slightly modified (eq 3) to account for the vectorial nature of electric fields and of the polarization (P_I). The nth order macroscopic electric susceptibilities $(\chi^{(n)})$ that relate components of the polarization to the applied field are therefore $(n + 1)$-order tensors.

$$P_I = \sum_J \chi^{(1)}_{IJ} F_J + \frac{1}{2}\sum_{J,K} \chi^{(2)}_{IJK} F_J F_K +$$
$$\frac{1}{6}\sum_{J,K,L} \chi^{(3)}_{IJKL} F_J F_K F_L + \dots \quad (3)$$

where the indices I, J, K, and L run over the macroscopic axes of the material.

If we are considering the nonlinear optical susceptibility of a molecular-based ensemble where each of the individual molecular units is contributing to the NLO tensors, a microscopic polarization analogue to eq 3 can be written. The macroscopic susceptibilities are related to the corresponding molecular susceptibilities by local field corrections $(f)^{43}$ and the molecular number density (N)

$$\chi^{(1)}_{IJ} = N \sum_{ij} f_I \langle\cos\theta_{Ii}\rangle f_J \langle\cos\theta_{Jj}\rangle \alpha_{ij}$$

$$\chi^{(2)}_{IJK} = N \sum_{ijk} f_I \langle\cos\theta_{Ii}\rangle f_J \langle\cos\theta_{Jj}\rangle f_K \langle\cos\theta_{Kk}\rangle \beta_{ijk} \quad (4)$$

$$\chi^{(3)}_{IJKL} = N \sum_{ijkl} f_I \langle\cos\theta_{Ii}\rangle f_J \langle\cos\theta_{Jj}\rangle f_K \langle\cos\theta_{Kk}\rangle f_L$$
$$\langle\cos\theta_{Ll}\rangle \gamma_{ijkl}$$

where the variables i, j, k, and l now span the molecular axes, and the angle between the macroscopic axis I and microscopic i is denoted as θ_{Ii}. The local field factors essentially correct for the difference between an applied field that would be felt by the molecule in free space and the local field detected in a material. These factors usually take the form of the well-known Onsager[44] or Lorentz[45] correction fields. The microscopic polarization (p_i) can then be expressed as

$$p_i = \sum_j \alpha_{ij} F_j + \frac{1}{2}\sum_{j,k} \beta_{ijk} F_j F_k + \frac{1}{6}\sum_{j,k,l} \gamma_{ijkl} F_j F_k F_l + \dots \quad (5)$$

or removing redundant summations to

$$p_i = \sum_j \alpha_{ij} F_j + \sum_{j\leq k} \beta_{ijk} F_j F_k + \sum_{j\leq k\leq l} \gamma_{ijkl} F_j F_k F_l + \dots \quad (6)$$

The frequency dependence of the polarization must be added to the expansion in eq 5 to complete the mathematical description of the nonlinear optical response. If the molecular polarization at frequency ω_1 is induced through applied fields of frequency ω_2, ω_3, ..., ω_s we have

$$p_i(\omega_1) = \sum_j \alpha_{ij}(-\omega_1;\omega_2)F_j(\omega_2)$$
$$+ \sum_{j \leq k} \beta_{ijk}(-\omega_1;\omega_2,\omega_3)F_j(\omega_2)F_k(\omega_3)$$
$$+ \sum_{j \leq k \leq l} \gamma_{ijkl}(-\omega_1;\omega_2,\omega_3,\omega_4)F_j(\omega_2)F_k(\omega_3)F_l(\omega_4)$$
$$+ ... \tag{7}$$

The molecular second-order response coefficient, generically denoted as β,[46] is also referred to as the first hyperpolarizability, the second-order NLO susceptibility, or the quadratic hyperpolarizability.[49] Four different second-order effects can be observed experimentally; they are second-harmonic generation [SHG; $\beta(-2\omega;\omega,\omega)$], the linear electrooptic effect [LEOE; $\beta(-\omega;\omega,0)$], sum-frequency generation [SFG; $\beta(-\omega_1-\omega_2;\omega_1,\omega_2)$], and optical rectification [OREC; $\beta(0;\omega,-\omega)$]. The great preponderance of results has been given for frequency doubling, and we will restrict our discussion to this property; experimentally, this property is both of greatest interest and most frequently measured.[53]

The challenges in computational second-order NLO materials research are to understand the origin of the $\beta(-2\omega;\omega,\omega)$ in microscopic structures, to design new structures with enhanced responses, and to understand how intermolecular interactions affect the local electric fields. Historically, chromophores possessing the largest β responses contain donor and acceptor substituents linked through an intervening π-backbone such as 1 or 2.
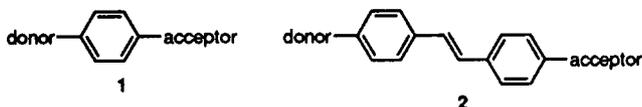

From empirical observations, researchers have learned that the second-order response can be enhanced by either increasing the electronic asymmetry (using more potent donating or accepting moieties) or increasing the conjugation length between the substituents.[16-34] Moreover, the effect of subtle variations in the molecular architecture can lead to enormous changes in the NLO response.[56,57] For π-molecular architectures of reasonable size (benzene derivatives and larger), β can span 3-4 orders of magnitude depending upon the input laser frequency ω.[56,57] If diatomic and triatomic molecules are included in the survey, β can range over 6 orders of magnitude! In Table 1 we present a somewhat subjective classification list of representative chromophores at a given wavelength of light (1.91 μm; $\hbar\omega$ = 0.65 eV). Note that the magnitude of the second-order response is very sensitive to the choice of laser frequency (vide infra), and therefore the arbitrary labels employed in Table 1 do not apply near resonant wavelengths. While empirical observations and associated "seat-of-the-pants" explanations have laid the ground work for contemporary studies, today molecular architecture–electronic structure–NLO response relationships are best deciphered by state-of-the art quantum chemical computations. Before we survey in detail the quantum chemical procedures now employed for this purpose, it is useful to review early models for interpreting β.

Table 1. Representative Molecules Illustrating the Magnitude of Second-Order Responses for an Incident Laser Beam of 1.91 μm ($\hbar\omega$ = 0.65 eV)[a,b]

β_{vec}	classification	representative molecules
0.001–0.1	negligible	diatomics, triatomics (HCl)
0.1–1.0	small	small organic molecules (urea)
1–10	modest	push/pull benzenes (p-nitroaniline)
10–100	large	push/pull stilbenes [4-(dimethylamino)-4'-nitrostilbene]
100–1000	very large	extended π-organics[c] dye molecules

[a] All NLO data are in units 10^{-30} cm^5 esu^{-1}. [b] Note that the quadratic hyperpolarizability is sensitive to the choice of input frequency; therefore the arbitrary classifications listed above will not hold for other input wavelengths.
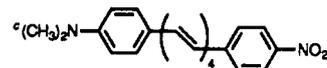
B. Early Models for Understanding β

The Equivalent Field Model (EIF), developed in 1975 by Oudar and Chemla,[58-60] was perhaps the first attempt at interpreting second-order responses. The EIF model sought to understand trends in β by quantifying the ground-state asymmetry of a π-network in a systematic fashion. It was proposed that a major portion of the second-order response in π-organic chromophores could be predicted from the ground-state deformation of the π-electron distribution due to appended substituents. The perturbation of the π-cloud caused by a particular substituent radical (R) was defined as a substituent's mesomeric moment (μ_R). The relationship between the π-distortion and the quadratic hyperpolarizability is given by:[58-60]

$$\beta_\pi = \frac{3\gamma\Delta\mu_R}{\alpha} \tag{8}$$

where α is the polarizability and γ is the second hyperpolarizability. Note the β_π used in eq 8 is a static ($\hbar\omega$ = 0.0 eV) value.

Determining the mesomeric moment ($\Delta\mu_R$, not to be confused with $\Delta\mu_{ground\rightarrow excited}$) is the principal complication in predicting β_π. For monosubstituted benzenes or stilbenes, the π-deformation caused by substituent R is defined as the difference between the ground-state dipole moment of the monosubstituted aromatic derivative and that for the analogous monosubstituted aliphatic molecule.[58-60] Obviously this prescription eliminates the σ-contributions to the dipole moment of the π-chromophore. Using published values of mesomeric moments,[61] the second-order responses for a considerable number of monosubstituted π-conjugated systems were predicted using this method, and the EIF-derived trends in β_π correlated well with experimental trends in the second-order response,[58-60,62] as illustrated in Figure 3. Since γ/α scales quadratically with the length of the molecule,[63] a quadratic dependence of β on conjugation length was rationalized.[64] The model also accounted for the negative sign in the second-order response when the added group was an acceptor and a positive β when the attached moiety was an electron donor.[58-60] Moreover, the linear relationship between the π-polarizability and the measured response was very encouraging (Figure 3).

The obvious next step toward the optimization of the NLO responses would be to use two substituents
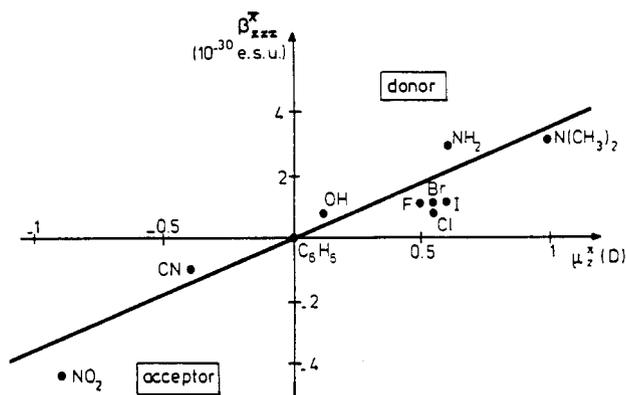
Figure 3. Measured β versus mesomeric dipole moment $(\Delta\mu_R)$ for a series of monosubstituted benzene derivatives. (Reprinted from ref 62. Copyright 1979 American Institute of Physics.)

connected by a π-electron bridge, the β_π values of which were of opposite sign (push/pull substituted benzenes). An extension of the EIF method was proposed to deal with disubstituted derivatives.[60,65,66] Conceptually, the total molecular nonlinearity for a complex molecule was proposed to be a tensorial sum of contributions from each of the important structural elements of the molecule.[67,68] For example, the quadratic hyperpolarizability of p-nitroaniline would be approximately equal to β_π(aniline) $- \beta_\pi$(nitrobenzene). Such an additivity model is quite successful at predicting the scalar portions of molecular *polarizabilities* in complicated systems,[69] and therefore it might work for hyperpolarizabilities. Later implementations of the additivity model used vector addition of experimental NLO responses for small molecules to predict responses of more complicated structures.[48,70]

The additivity model was found to work well for weakly coupled systems, such as donor/acceptor σ-networks,[71] but, in general, failed (qualitatively and quantitatively) for strongly-coupled disubstituted systems.[65,66,71,72] Specifically, the additivity models could not account for the large second-order responses consistently observed for highly asymmetric π-networks. The two difficulties with both the EIF and the related additivity models is the assumption that β is governed by ground-state electronic distributions and that the substituents act independently of each other.

In the high-β push/pull π-organic chromophores of interest in most NLO studies, however, excited states dictate the NLO response as elegantly shown by Oudar and Chemla.[65,66] They assumed that the anomalously large responses measured in these donor/acceptor chromophores were due an intramolecular charge-transfer interaction between acceptor and donor. The second-order response was then taken to be sum of two contributions

$$\beta = \beta_{add} + \beta_{ct} \tag{9}$$

where β_{add} is the additive portion, accounting for the interaction between the individual substituents and the conjugated π-network, and β_{ct} is the contribution arising from the interaction of donor and acceptor moieties. The charge-transfer "correction" term was described in terms of a two-level interaction between the ground state (g) and first excited state (n) as given in eq 10.[65,66]

Table 2. Two-Level (Charge-Transfer) Contribution β_{ct} Calculated From Eq 10 and Experimental Values β_{expt} for Some Conventional Push/Pull Chromophores[a,b]

chromophore	β_{ct}	β_{expt}
$H_2N-\langle\rangle-NO_2$	19	34.5
$(CH_3)_2N-\langle\rangle-\!\!=\!\!-NO_2$	217	220
$H_2N-\langle\rangle-\!\!=\!\!-\langle\rangle-NO_2$	227	260
$(CH_3)_2N-\langle\rangle-\!\!=\!\!-\langle\rangle-NO_2$	383	450
$(CH_3)_2N-\langle\rangle-\!\!=\!\!-\!\!=\!\!-NO_2$	715	650

[a] All NLO data are in units of 10^{-30} cm^5 esu^{-1} and were calculated/measured at 1064 nm ($\hbar\omega = 1.17$ eV). [b] Tabular data taken from ref 66, Table IV.

Table 3. Charge-Transfer β_{ct}[a] and Additive β_{add}[b] Contributions for Three Isomers of Nitroaniline (Experimental Values β_{expt} for Each Chromophore Are Also Included)[a,d]

isomer of nitroaniline	β_{ct}	β_{add}	β_{expt}
$H_2N-\langle\rangle-NO_2$	19.6	3.5	34.5
$H_2N-\langle\rangle-NO_2$ (meta)	4	3.1	6
$H_2N\ NO_2$ (ortho)	10.9	2.0	10.2

[a] Calculated from eq 10. [b] Computed from the second-order responses of nitrobenzene and aniline. [c] All NLO data are in units of 10^{-30} cm^5 esu^{-1} and were calculated/measured at 1064 nm ($\hbar\omega = 1.17$ eV). [d] Tabular data taken from ref 65, Table II.

$$\beta_{ct} = \frac{3e^2}{2m} \frac{\hbar\omega_{gn}f_{gn}\Delta\mu_{gn}}{[(\hbar\omega_{gn})^2 - (2\hbar\omega)^2][(\hbar\omega_{gn})^2 - (\hbar\omega)^2]} \tag{10}$$

Here $\hbar\omega$ is the energy of the laser photon, $\hbar\omega_{gn}$ in the energy difference between the ground state and first excited state, f_{gn} the oscillator strength of a g $\rightarrow$ n transition, and $\Delta\mu_{gn}$ the difference in dipole moments between the ground state and first excited state. By using readily available ω_{gn} and f_{gn} data in conjunction with a crude model for the $\Delta\mu$ term, it was shown that β_{ct} is responsible for a large portion of the experimentally-determined values of disubstituted polyenes[65] (Table 2) and isomers of nitroaniline[66] (Table 3). Theoretical studies by Zyss later confirmed the conclusions of Oudar and Chemla.[71] Thus, *the second-order response in high-β molecules is intrinsically related to charge-transfer excited states, and therefore any method that seeks to accurately predict second-order NLO responses must adequately represent the excitation to these states.*

C. Modern Quantum-Chemical Approaches

The phenomenological methods described above have been largely supplanted by modern quantum-chemical treatments.[73] Many such procedures exist, varying in
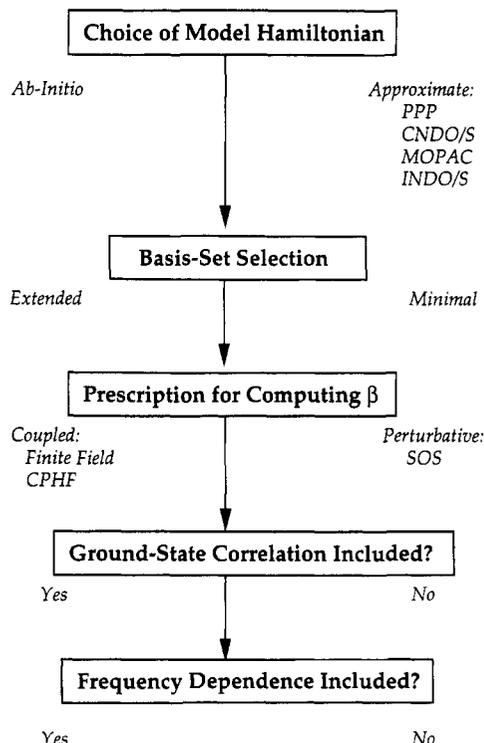
Choice of Model Hamiltonian

Ab-Initio   *Approximate:*
                                               PPP
                                               CNDO/S
                                               MOPAC
                                               INDO/S

Basis-Set Selection

Extended   *Minimal*

Prescription for Computing β

Coupled: *Perturbative:*
Finite Field   *SOS*
CPHF

Ground-State Correlation Included?

Yes   *No*

Frequency Dependence Included?

Yes   *No*

Figure 4. Flowchart delineating options in second-order response calculations.

the accuracy of the computed results,[74] computational demands, and potential for interpretation. In this section the formalisms and technical details for calculating β will be presented.

Molecular NLO response calculations require both the definition of a model Hamiltonian and the specification of a computational method to compute β. Obviously, the ideal treatment would employ an exact Hamiltonian in an extensive basis set and an exact computation of the second-order response with full-scale correlation and would permit an interpretation of the response in a chemical context for any size molecular unit at modest computational cost. Such exhaustive accuracy is not economically feasible at present, and therefore compromises must be devised in order to make the studies computationally tractable. A flowchart listing the computational model decisions discussed in some detail in this section is presented in Figure 4.

1. Model Hamiltonians Employed in Response Calculations

The choice of model Hamiltonian is crucial to the computation of NLO responses. Often an advantage such as computational efficiency must be weighed against a disadvantage such as exactness. Model Hamiltonians employed in NLO calculations are of two types, *ab initio* and semiempirical. Generally, the *ab initio* methods have the advantage of reduced arbitrariness and parameterization, while the semiempirical methods are generally less demanding, require substantially less computational resources, and produce results that are more easily interpreted in a chemical context.

It is most convenient and specific to describe electronic structure Hamiltonians using so-called second-quantization methods.[75-77] For readers unfamiliar with this notation, it is perhaps simplest to think of the

matrix elements in eq 11 as defining exactly which interactions are permitted within the particular model. The electronic structure model, then, used for nearly all calculations of β is given by

$$H = \sum_{ij} \sum_{\mu} t_{ij} \, a_{i\mu}^{+} a_{j\mu} + \frac{1}{2} \sum_{ijkl} \sum_{\mu\nu} \langle ij|kl \rangle a_{i\mu}^{+} a_{k\nu}^{+} a_{l\nu} a_{j\mu} \quad (11)$$

Here the Latin subscripts i, j, k, l label atomic basis functions, the Greek subscripts μ and ν label spin components, with the summands running over the specified basis set. The operator $a_{i\mu}$ destroys an electron in basis orbital i with spin μ, while the operator $a_{l\nu}^{+}$ similarly creates an electron with the appropriate quantum labels. The parameters t_{ij} and $\langle ij|kl \rangle$, each with the dimension of energy, describe one-electron and two-electron interactions, respectively. As shown in eqs 12 and 13, the t_{ij} term arises from the electronic kinetic energy and electron–nuclear attraction, while the $\langle ij|kl \rangle$ is the nonseparable term arising from the interelectronic repulsion. Once the t_{ij} and $\langle ij|kl \rangle$ terms

$$t_{ij} = \int u_i(1) \left(-\frac{1}{2}\nabla_1^2 - \sum_{\alpha}^{nuclei} \frac{Z_\alpha}{R_{1\alpha}} \right) u_j(1) \, dr_1 \quad (12)$$

$$\langle ij|kl \rangle = \int d^3r_1 \int d^3r_2 \, [u_i(1)u_j(1)] \frac{e^2}{r_{12}} [u_k(2)u_l(2)] \quad (13)$$

are specified, as well as the orbitals over which the Latin summations run, the Hamiltonian is almost completely defined. To complete the definition, we include the overlap integrals (S_{ij}, eq 16) between atomic basis functions u_i and u_j that enter into the anticommutation relationships (eqs 14 and 15).

$$[a_{i\mu}, a_{j\nu}^{+}]_{+} = S_{ij}\,\delta_{\mu\nu} \quad (14)$$

$$[a_{i\mu}, a_{j\nu}]_{+} = 0 \quad (15)$$

$$S_{ij} = \int u_i^{*}(1) u_j(1) dr_1 \quad (16)$$

Of the two types of Hamiltonians, the *ab initio* methods are easier to describe. In *ab initio* techniques, the integrals S_{ij}, t_{ij}, and $\langle ij|kl \rangle$ are calculated explicitly as three-dimensional and six-dimensional integrals without any approximations. Such widely-available *ab initio* software packages, as ACES II,[78] GAUSSIAN,[79] and HONDO[80,81] perform such electronic structure computations. Extensive arbitrariness, however, still exists in the definition of the basis functions (u_i) themselves: usually, these are optimized to fit particular properties of the isolated atom, and while this is a reasonable procedure, there is no guarantee that these are the optimal basis functions for *ab initio* calculations of nonlinear optical response. In so-called minimum basis calculations, these are the orbitals occupied in the simplest atomic aufbau scheme (1s for hydrogen, 1s, 2s, 2p for carbon; 1s, 2s, 2p, 3s, 3p, 3d, 4s for titanium; etc). Such a basis is usually insufficient for NLO response computations. Various extended basis sets, including polarization functions and diffuse functions, are generally required for computations of hyperpolarizability.[73] Construction of diffuse and polarization functions is generally even more arbitrary, so the simple statement that a calculation is at the *ab initio* level

does *not* mean that no arbitrary assumptions are made in the model Hamiltonian; it simply means that the molecular integrals are computed appropriately for the given choice of basis set. The influence of basis set size on the computed response will be discussed later in this section.

Semiempirical model Hamiltonians can be understood, again, on the basis of eq 11. The semiempirical parameterization of the molecular integrals both defines the model and is required if a simple, minimum basis semiempirical model is to describe the same behavior that requires extensive basis sets in the *ab initio* framework. The molecular integral parameterization must be chosen to take into account such effects as multiple electron screening, behavior of the core electrons that are not included in the basis, and the particular interactions that are not included in the model Hamiltonian. Like *ab initio* models, semiempirical models must define the atomic basis orbitals over which the summations run, and the values of the molecular integrals t_{ij}, S_{ij}, and $\langle ij|kl \rangle$. All commonly employed semiempirical schemes limit the basis set to valence orbitals of Slater-type. Indeed, many semiempirical models limit the basis to include, on each atom, only one atomic orbital of given (n, l, m_l) type—that is, one 2s orbital, one $2p_z$ orbital, one $3d_{z^2}$ orbital. Thus, the semiempirical basis set is generally much smaller than that required for accurate *ab initio* calculations. To obtain accuracy, then, the semiempirical schemes rely on a redefinition of the molecular integrals to obtain consistent predictions of the given property, or set of properties, for a set of sample molecules. Thus a semiempirical model, like an *ab initio* model, is defined by fixing the values of the molecular integrals; in semiempirical theory, however, some of these values are set not by actual computation of the three- and six-dimensional integrals entering eqs 12 and 13, but rather by physically reasonable approximations or fitting to particular experimental data sets.

While a large number of semiempirical models have been used for computation of β, the most common types are Hückel and extended-Hückel models, exchange-free models of the PPP and CNDO/S type, and models that include one-center exchange, such as MNDO, INDO/S, or ZINDO. These models are described extensively elsewhere in the literature,[77,82-84] but for clarity, important definitions will be summarized here.

In the Hückel[85] and extended-Hückel[86] models, all two-electron interactions are neglected. Thus, the Hückel model Hamiltonian is a sum of effective one-electron (valence-only) Hamiltonians. In Hückel theory, all one-electron integrals (t_{ij}) are parameterized arbitrarily and all overlap integrals $S_{ij} = \delta_{ij}$.[85] Specifically, t_{ij} is set equal to α for all diagonal matrix elements, β for nearest-neighbor interactions, and to 0 for all other matrix elements. In the extended-Hückel (EH) model popularized by Hoffmann and co-workers,[86] S_{ij} is computed based on Slater-type orbitals; a modified Wolfsberg–Helmholtz[87] relationship between the diagonal and off-diagonal matrix elements is assumed. The eigenstates and eigenenergies are computed by diagonalizing the matrix representation of the model Hamiltonian.

In Pariser–Parr–Pople (PPP)[88,89] and complete neglect of overlap/spectroscopy (CNDO/S) models,[90] the

sum is again restricted to valence orbitals, and electron repulsion is included by keeping specific two-electron $(\langle ij|kl \rangle)$ matrix elements. Both PPP and CNDO/S methods utilize the zero differential overlap (ZDO) approximation (eq 17) to reduce greatly the number of two-electron integrals evaluated. Equation 11 then

$$u_i(1)u_j(1) = \delta_{ij}u_i^2(1) \qquad (17)$$

becomes

$$H = \sum_{ij} \sum_{\mu} t_{ij}\, a_{i\mu}^+ a_{j\mu} + \frac{1}{2} \sum_{ij} \sum_{\mu\nu} \gamma_{ij}\, a_{i\mu}^+ a_{j\nu}^+ a_{j\nu} a_{i\mu} \qquad (18)$$

where the sums run over the valence basis and γ_{ij} are semiempirically determined repulsion integrals. If a valence basis set is employed and the semiempirical parameters are extracted from spectroscopic data, eq 18 is the CNDO/S version of the CNDO Hamiltonian. If the basis set is limited to one π-function per atom, the model is generally referred to as the PPP model. The PPP formalism is therefore applicable to computing properties of π-electron molecules. Note that the eigenfunctions and energies now include two-body interactions, and therefore an SCF procedure is required to solve the Schrödinger equation.

Electron exchange terms are absent from the CNDO and PPP models, and the only consequence of interelectronic repulsion is the energy-raising effect of the repulsion of Coulomb densities. In INDO/S (intermediate neglect of differential overlap/spectroscopy)[91] and ZINDO (INDO/S-based formalism) approximations,[92-95] the ZDO requirement is relaxed in that exchange terms are permitted on a single atom. This has the advantage of separating spin multiplets, and has proven useful both for computation of spin properties and, especially, for semiempirical calculations on inorganic molecules. Specifically, the INDO Hamiltonian has the form

$$H = \sum_{ij} \sum_{\mu} t_{ij}\, a_{i\mu}^+ a_{j\mu} + \frac{1}{2}\sum_{ij} \sum_{\mu\nu} \gamma_{ij}\, a_{i\mu}^+ a_{j\nu}^+ a_{j\nu} a_{i\mu} +$$
$$\frac{1}{2}\sum_{il}' \sum_{jk}' \sum_{\mu\nu} \langle ij|kl \rangle a_{i\mu}^+ a_{k\nu}^+ a_{l\nu} a_{j\mu} \qquad (19)$$

with the prime summations meaning that the exchange terms are restricted to one atom. Again, if the semiempirical parameters are determined by spectroscopic investigations, the INDO/S Hamiltonian emerges. The definitions of PPP, CNDO/S, or INDO/S are by no means unique. Several definitions for each method exist in the literature. The ZINDO algorithm is one such INDO parameterization scheme. ZINDO[92-95] is unique, however, in that it is parameterized for transition metal systems.

Another popular semiempirical algorithm used in NLO response computations is the MNDO (modified neglect of diatomic differential overlap)[96] and the associated parameterizations of AM-1,[97] and PM-3[98] readily available in the MOPAC software package. MNDO is essentially INDO in which the differential overlap is *only* neglected between atomic orbitals centered on different atoms. However, the MNDO model is not parameterized to reproduce either optical observations or *ab initio* wavefunctions as the other models; instead it is parameterized to reproduce gasphase $\Delta H_{f,298}^{\circ}$ values.

The semiempirical models have a historically important place in quantum chemistry,[82,99] but for the calculation of ground-state properties of small molecules, especially small organics, it is fair to say that they have been superseded by accurate *ab initio* techniques. The point to stress here is that calculations both of optical and of nonlinear optical properties are, in a sense, substantially more demanding than traditional ground-state calculations. As discussed earlier, they describe the response of a molecule to an applied field, and must include necessary information about the distortion of the wavefunction by the applied potential. Therefore, it is not surprising that the requirements both on basis set and on treatment of correlation among electrons are more severe than are required for simple calculations of, say, molecular geometries or ionization potentials. Semiempirical models, therefore, are still of major importance in prediction of molecular response properties, and indeed such calculations represent a very significant component of all electronic structure studies devoted to NLO response.

2. Molecular Geometry Considerations

Numerous studies have demonstrated that regardless of the computational algorithm used to compute β, the results can be sensitive to the choice of input geometry of the isolated molecule.[100] Three different strategies for defining metrical parameters can be found in the NLO literature: (1) employing experimental structures, (2) using geometries obtained through molecular energy minimization algorithms, or (3) using idealized molecular geometries constructed from experimental metrical parameters of related architectures. As a rule-of-thumb, contributions focusing on a handful of chromophores of limited size generally employ experimental geometries when available, while studies examining large numbers of complicated structural motifs tend to either optimize the structure via quantum mechanical routines or use molecular templates to build idealized structures.

If the input geometries to the electronic structure–NLO calculations are to be optimized via an additional computation, the sophistication of the energy minimization procedure, not surprisingly, usually mirrors the accuracy of the NLO computation. Thus, *ab initio* NLO computations usually employ fully-optimized geometries at the SCF *ab initio* level with fairly extensive basis sets (DZV or 6-31G for example). Similarly, semiempirical NLO computations typically employ a MOPAC Hamiltonian (MNDO or AM1) to optimize the ground-state geometry. At the semiempirical level, bond lengths and bond angles are typically optimized for π-organic chromophores, while the molecule is assumed to be planar (torsion angles not optimized). Brédas and co-workers[101] have used a different approach, whereby crucial portions of the geometry are optimized (*ab initio* SCF-level 3-21G basis set) and other sections (such as aromatic rings) are idealized.

As an alternative, recent theoretical studies of quadratic hyperpolarizabilities have employed idealized structures assembled from molecular templates.[100,102] These templates are specified by analyzing representative structures in structural databases, such as the
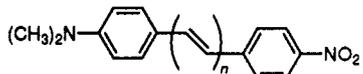
Table 4. Comparison of Experimental and ZINDO-Derived Molecular Hyperpolarizabilities (β_{vec}) for Idealized and Optimized Input Geometries[a,b]

Legend for the Input Structures

	structure 1	structure 2	structure 3
bonds	idealized	optimized	optimized
angles	idealized	idealized	optimized
torsion angles	idealized	idealized	idealized
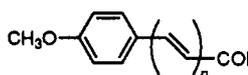
	β_{vec}^{calc}			
n^c	structure 1	structure 2	structure 3	$\beta_{vec}^{expt,d}$
1	8.42	8.70	10.7	12
2	17.0	16.3	19.4	28
3	28.0	25.1	30.0	42

	β_{vec}^{calc}			
n^c	structure 1	structure 2	structure 3	$\beta_{vec}^{expt,d}$
1	54.8	52.4	53.3	73
2	75.3	67.8	68.6	107
3	95.9	82.1	82.4	131

[a] Excerpts of table are taken from ref 100. [b] All NLO data are in units of 10^{-30} cm^5 esu^{-1} and were calculated at 1910 nm ($\hbar\omega$ = 0.65 eV). [c] n represents the number of nonaromatic ethyleneic units. [d] Experimental values taken from ref 56 and 57.

Cambridge Data Base.[103] The molecular geometry of *p*-nitroaniline, for example, would be resolved by systematically searching the database for π-molecules containing $C_{aromatic}$–NO_2 or $C_{aromatic}$–NH_2 moieties, then averaging over the appropriate bond distances, and idealizing the bond angles. Once transferable metrical parameters for a particular group or π-backbone are defined, the NLO response for large numbers of chromophores can be computed in a relatively facile manner. The INDO/S-derived responses for two conventional chromophoric structures for idealized, bonds-only-optimized, and bonds- and angles-optimized geometries are reported in Table 4. In the case of 4-(dimethylamino)-4′-nitrostilbene (DANS), for instance, the computed β_{vec} ($\hbar\omega$ = 0.65 eV) values are 54.8 × 10^{-30} cm^5 esu^{-1} (idealized), 52.4 × 10^{-30} cm^5 esu^{-1} (bond-only-optimized), and 53.3 × 10^{-30} cm^5 esu^{-1} (bonds- and angles-optimized) compared with an experimental β_{vec} of 73 × 10^{-30} cm^5 esu^{-1}. The data presented in this table and in a recent contribution[100] strongly suggest that appropriately chosen input coordinates are legitimate alternatives to optimizing molecular coordinates for all chromophores examined. That is, molecular geometries can be constructed in a systematic fashion using transferable fragment geometries; this strategy will prove particularly important in very exotic structures (such as organometallic motifs) where molecular energy minimizations are either too costly or not accurate. It could, perhaps, prove less useful when extremely acentric chromophores, such as the quinoidal motifs being studied by Marder and co-workers,[21] are examined, since the metrical parameters of the bridge unit can be rather sensitive to derivatization. Also, the transfer of geometry treatments might be expected to fail in small molecules (such as moving a C–H from methylamine to chloroform), and will be

best when the fragment is a well-defined donor or acceptor moiety, or a well-defined bridging unit.

3. Prescriptions for Calculating Molecular Nonlinear Optical Responses

Once a model Hamiltonian is defined, there are two basic methodologies that can be used in concert with an electronic structure method to compute β. These techniques are based either on perturbative schemes, in which the calculations are carried out on the free (independent of field) molecules and the response involves the coupling of excited states, or on generalized finite field elaborations of coupled Hartree–Fock schemes, in which the perturbation is included in the Hamiltonian. Both the field-independent and field-dependent schemes can be carried out using any model Hamiltonian, and also treating correlation effects at various levels of sophistication. In this section we will present a brief overview of the two prescriptions for computing the NLO response, specific Hamiltonian–NLO response algorithms, and appropriate considerations of basis set and correlation effects.

a. Coupled Treatments. Procedures with the field explicitly included in the Hamiltonian are broadly referred to as coupled procedures, but are more frequently labeled as finite-field (FF) or CPHF (coupled perturbed Hartree–Fock). In these formulations, the molecular Hamiltonian explicitly includes a term $(-\mathbf{r} \cdot \mathbf{F})$ describing the interaction between the external uniform *static* field and the electronic structure (eq 20).

$$H = \sum_{ij} \sum_{\mu} (t_{ij} - \mathbf{F} \cdot \mathbf{r}_{ij}) a_{i\mu}^{+} a_{j\mu} +$$
$$\frac{1}{2} \sum_{ijkl} \sum_{\mu\nu} \langle ij|kl \rangle a_{i\mu}^{+} a_{k\nu}^{+} a_{l\nu} a_{j\mu} \quad (20)$$

The $-\mathbf{r} \cdot \mathbf{F}$ term ($\mu \cdot \mathbf{F}$ in SI units) accounts for the isolated molecule-applied field interaction. At any given field strength, the molecular wavefunction $\psi(\mathbf{F})$ is found, from which the appropriate expectation values of the field-dependent molecular energy ($E(\mathbf{F})$) and the field-dependent dipole moment ($\mu(\mathbf{F})$) can be evaluated:

$$E(\mathbf{F}) = \langle \psi(\mathbf{F})|H(\mathbf{F})|\psi(\mathbf{F}) \rangle \quad (21)$$

$$\mu(\mathbf{F}) = \langle \psi(\mathbf{F})| \sum_i q_i(\mathbf{F}) \cdot \mathbf{r}_i(\mathbf{F}) |\psi(\mathbf{F}) \rangle \quad (22)$$

where q_i is the charge and $\mathbf{r}_i$ is the position vector of the ith particle, and i ranges over all nuclei and electrons.

Note that $\mu(\mathbf{F})$ is also related to the (hyper)-polarizabilities by

$$\mu(F)_i = \mu_i^0 + \sum_j \alpha_{ij} F_j + \frac{1}{2} \sum_{j,k} \beta_{ijk} F_j F_k +$$
$$\frac{1}{6} \sum_{j,k,l} \gamma_{ijkl} F_j F_k F_l + \dots \quad (23)$$

where μ_i^0 is the dipole moment in the absence of a field and $(\mu_i - \mu_i^0)$ is the polarization in the ith direction (p_i) as defined in eq 5. It is clear then, that by combining eqs 22 and 23, (hyper)polarizabilities of increasing order may be obtained by differentiating $\mu(\mathbf{F})$ with respect to $\mathbf{F}$ (eq 24) or equivalently (for wavefunctions satisfying the Hellmann–Feynman theorem) (eq 25), by differentiating the energy.[104-106] It is then clear that, for example, the partial derivative of the polarization with

respect to the field, evaluated at zero field, can give the polarizability, while the second partial derivative of the polarization with respect to field, again evaluated at zero field, gives the first hyperpolarizability. In

$$\alpha_{ij} = \frac{\partial \mu_i}{\partial F_j}\bigg|_{F=0}$$

$$\beta_{ijk} = \frac{\partial^2 \mu_i}{\partial F_j \, \partial F_k}\bigg|_{F=0}$$

$$\gamma_{ijkl} = \frac{\partial^3 \mu_i}{\partial F_j \, \partial F_k \, \partial F_l}\bigg|_{F=0} \quad (24)$$

practice, the derivatives could be computed using numerical differentiation strategies,[107-109] but the development of analytic gradient techniques, originally by Pulay[110] and later by a number of other workers,[111-113] has resulted in the development of electronic structure codes that evaluate such energy derivatives analytically. Some nomenclature might be useful in understanding the various papers devoted to using such treatments: analytic derivative methods use the gradient techniques just discussed to compute responses, CPHF methods generally refer to the use of analytical gradients to compute hyperpolarizabilities (or other properties) from a single-determinant (HF) reference; the FF label is usually attached to calculations where the derivatives are actually done numerically. The CPHF method is equivalent to the random phase approximation (RPA)[114,115] or the time-dependent Hartree–Fock approximation (TDHF or TDSCF)[76,116] for static calculations within a given basis.

An analogous formulation for the α, β, γ coefficients can be obtained by examining the molecular energy expansion, rather than dipole expansion, with respect to the field. The molecular dipole moment is the negative field derivative of the energy, and thus β becomes

$$\beta_{ijk} = \frac{\partial^2 \mu_i}{\partial F_j \, \partial F_k} = \frac{\partial^2}{\partial F_j \, \partial F_k}\left(-\frac{\partial E}{\partial F_i}\right) = -\frac{\partial^3 E}{\partial F_i \, \partial F_j \, \partial F_K}\bigg|_{F=0} \quad (25)$$

Formally the hyperpolarizability is defined through eq 7 for arbitrary frequencies, and in fact one or more of the applied fields in NLO measurements must be oscillatory. Note, however, that the simple relationships given in eqs 24 and 25 are only valid for the static field limit in which all frequencies of the (hyper)polarizabilities vanish. Incorporating frequency dependence in coupled Hartree–Fock treatments is a nontrivial extension of the methodology. Thus, the majority of derivative-based NLO response computations have been reported at zero frequency. Comparisons between computations at differing levels of complexity, therefore, have largely been confined to the static limit, while comparisons between theory and experiment were reported only after an estimation of the frequency dependence was obtained. As we shall describe below, recent advances in the CPHF formulation permit the dispersive dependence of (hyper)polarizabilities to be computed.

i. Coupled *ab Initio* Schemes. NLO response computations based on *ab initio* model Hamiltonians

with a FF or CPHF prescription for computing β, augmented by correlation corrections, are currently the ultimate procedure for obtaining numerically accurate responses. As the basis set approaches completeness and the treatment of correlations converges, the exact solution to the electronic Schrödinger equation should be obtained assuming that such effects as relativity, vibronic coupling, and nonadiabatic behavior are unimportant. Accordingly, a number of workers have reported *ab initio* calculations, treating effects of basis set and correlation at various levels of sophistication.

Three program packages account for most of the recent publications in this area; one is the elegant coupled-cluster (CC) and TDSCF procedures of Sekino and Bartlett[117,118] included in the ACES II electronic structure package,[78] the second is the popular CPHF approach of Karna and Dupuis embodied in the HONDO program,[119] and the third is the useful TDHF-based perturbative scheme of Rice, Handy, and co-workers.[120] These procedures include correlation at various levels of rigor. The CC-TDSCF algorithm has been applied to molecules of limited size (CO,[121,122] H_2O,[121,123] HF,[121,124,125] NH_3,[121] H_2S,[121] and fluoromethanes[117]), and the exhaustive correlation and basis sets included in the computations, suggest that the "exact" first hyperpolarizability was approached in the most extensive of these studies. Not surprisingly, the computed responses with this sophisticated method are generally within 10%[121] of the experimentally-determined values in the gas phase. A slightly different formalism for computed first hyperpolarizabilities with extreme accuracy has been introduced by Rice et al.,[120,126] with applications to methyl fluoride,[120] formaldehyde,[120,126] ammonia,[126] HCl,[127] p-nitroaniline,[128] and acetonitrile.[129]

In contrast to CC, CPHF has been applied (using the HONDO program) to molecules of widely varying sizes, albeit at a somewhat lower degree of rigor. HONDO has been employed to study haloforms,[130,131] push/pull benzenes,[132,133] polyenes,[134,135] pyrroles,[136,137] diphenylacetylenes,[138] benzodithiapolyenals,[101,139,140] quinolines,[141] styrenes,[142] and octopolar molecules.[143] As a testimony to its capabilities, the algorithm has been used to calculate the cubic hyperpolarizabilities (γ) for long polyenes ($C_4H_6 \rightarrow C_{22}H_{24}$) at the Hartree–Fock level in 6-31G+PD and 6-31G* basis sets.[111] While most applications of CPHF using HONDO have been used with slightly smaller basis sets and lower levels of correlation relative to CC, this prescription has proven useful in computing accurate values of β for large systems of interest to chemists. It should also be noted that contributions using a FF approach, available in the GAUSSIAN program, are now appearing in the literature.[144]

Applications of *ab initio* methodologies will be presented in section IV. Note, however, that most of the *ab initio* studies reported in the literature deal with formal computational issues such as correlation effects and basis sets, as well as the inclusion of the dispersive behavior (frequency dependence) of β rather than uncovering mechanistic trends for optimizing the response. Reliable predictions of molecular hyperpolarizabilities require several elements: adequate basis sets, sufficient treatment of correlation, and frequency-dependent responses.

Table 5. Basis Set Convergence of the Static First Hyperpolarizability of HCl $[\beta_\| (\hbar\omega = 0.0 \text{ eV})]$ As Computed by an SCF Method^{a,b}

	basis 1^c	basis 2^d	basis 3^e	basis 4^f	basis 5^g
β_{xxz}	−3.60	−3.57	−2.20	−2.20	−2.49
β_{zzz}	13.87	13.87	10.79	10.86	10.69
$\beta_\|$	4.02	4.04	3.83	3.88	3.41

^{a} All NLO data are in atomic units. ^{b} Tabular data taken from ref 127, Table I. ^{c} [5 + 1s4 + 1p2 + 1d/3 + 1s2 + 1p] + (2s2p2d/2s2p). ^{d} [5 + 1s4 + 1p2 + 1d/3 + 1s2 + 1p] + (3s3p3d/3s3p).^{e} [5 + 1s4 + 1p2 + 1d/3 + 1s2 + 1p] + (3s3p3d3f/3s3p3d). ^{f} [5 + 1s4 + 1p2 + 1d1 + 1f/3 + 1s2 + 1p1 + 1d] + (3s3p3d3f2g/3s3p3d). ^{g} [5 + 1 + 1s4 + 1 + 1p2 + 1 + 1d1 + 1f/3 + 1s2 + 1p1 + 1d] + (4s4p4d4f/4s4p4d).

Basis Sets. As the form of eq 11 makes clear, choice of different basis sets is equivalent to choosing different model Hamiltonians.[145] From the previous discussion on the early models of describing β, the model Hamiltonian must be able to describe excited states, their dipolar properties, the mixing of excited and ground states, and the excitation energies. Also, as pointed out by Dykstra, "the electronic polarizability and hyperpolarizability tend to be very sensitive to the electronic distribution in the fringe regions".[146] Therefore, basis sets for computing hyperpolarizabilities must involve both diffuse and polarization functions and are substantially larger than those required for computing ground-state properties such as molecular geometries.

Most calculations use traditional Gaussian basis functions, centered on the atomic nuclei. With such bases, convergence of β is obtained using very large bases, at least for relatively small molecules. For example, Table 5 gives some results for the various static components of the β_{ijk} for HCl, calculated using large extended basis sets.[127] The authors conclude that "a minimum of two sets of diffuse functions are required to demonstrate basis-set convergence and the diffuse f functions are essential in the treatment of Cl". For very accurate (convergence within a few percent) *ab initio* calculations on atoms and small molecules, this sort of basis requirement is common. Inclusion of basis functions not centered on atoms, to describe polarization effects, can result in some reduction in basis requirements.[121] Convergence of the basis expansion can be measured in several ways; one can, for example, examine the extent to which sum rules are satisfied, or can look for the equivalence of dipole length and dipole velocity forms,[75,76] or can compare with numerical basis calculations.[147] Most commonly, one simply expands the basis by adding further functions until apparent convergence is reached.

From a very qualitative point of view, basis functions act to characterize the density of the electronic distribution in the full configuration space of the molecule.[145] As the basis becomes larger, one expects a better description; accordingly, increases in basis size will generally give more accurate results. The difficulty is that, for properties that are not simple ground-state expectation values, the variational principle does not help significantly in the choice of basis functions, particularly of diffuse and polarization type. Additionally, as molecules become larger there is some superposition effect, in which orbitals centered on one atom can help to describe densities that are actually closer to other atoms. While such superposition effects

Table 6. Basis Set Convergence of the Static Quadratic Hyperpolarizability [β_{vec} ($\hbar\omega$ = 0.0 eV)] of p-Nitroaniline Computed with GAUSSIAN-FF[a,b]

$$H_2N-\langle\!\!\!\bigcirc\!\!\!\rangle-NO_2$$

basis set	β_{vec}
STO-3G	1.7
3-21G	2.9
4-31G	3.6
6-31G	3.6
6-31G*	3.1
6-31G**	3.1
6-31+G	4.4

[a] All NLO data are in units of 10^{-30} cm^5 esu^{-1}. [b] Kanis, D. R.; Ratner, M. A.; Marks, T. J. Unpublished data.

Table 7. Static First Hyperpolarizability Data, $\beta_{\parallel}$ ($\hbar\omega$ = 0.0 eV) Computed for HCl with Various Levels of Electron Correlation[a-c]

	SCF	MP2	CCSD	CCSD(T)
β_{xxz}	-2.30	1.11	-0.24	0.47
β_{zzz}	10.79	11.27	10.69	11.11
$\beta_{\parallel}$	3.72	8.09	6.12	7.23

[a] All NLO data are in atomic units. [b] Tabular data taken from ref 127, Table II. [c] Basis set is [5 + 1s4 + 1p2 + 1d1 + 1f/3 + 1s2 + 1p1 + 1d] + (3s3p3d3f/3s3p3d).

can lead to artifacts in calculations of intermolecular interactions, they can also result in slightly less severe basis-set demands in larger systems than in smaller.[111,127] Often, the effective basis sets can be estimated at the Hartree–Fock level, without the necessity for inclusion of electron correlation—that is, to some extent, correlation effects and basis-set effects can be separated in the accurate computation of hyperpolarizability. Both basis and correlation contributions are most demanding for atoms and small molecules, where the change in the charge cloud upon excitation is, proportionally, largest.

The basis set dependence of a somewhat larger system, nitrobenzene, was examined with CPHF by Daniel and Dupuis.[132] They conclude that diffuse functions are required for quantitative adequacy of second-order responses, however, β is not exceptionally sensitive to the size of the diffuse functions. They also find that diffuse basis functions on neighboring atoms help in describing the polarization of the valence electrons.

The dependence of Hartree–Fock level β (static) values for p-nitroaniline is presented in Table 6. The CPHF-derived responses change dramatically from the minimal STO-3G basis set (1.7 × 10^{-30} cm^5 esu^{-1}) to the split-valence 3-21G set (2.9 × 10^{-30} cm^5 esu^{-1}), and when diffuse functions are added to the basis (6-31+G – 4.4 × 10^{-30} cm^5 esu^{-1}). Clearly, diffuse functions play a pivotal role in such computations, and therefore extended basis sets and substantial allocations of computational resources are required for calculating quantitative responses for large molecules at the ab initio level. As pointed out by Davidson and Feller,[145] the basis-set requirements for hyperpolarizability computations "have proven to be discouragingly large".

The requirement for diffuse functions is, in some ways, reminiscent of the requirement for screening in semiempirical models: polarization of the molecule arises both from the direct response of a given electron to the applied field and from the modification of that response caused by the screening due to the other electrons. In ab initio calculations using Gaussian basis sets, no screening is explicitly included, and therefore both polarization and diffuse functions are required to describe the change in shape of the molecular electronic structure.

Treatment of Electron Correlation. Another issue in ab initio computations is the level of ground-state correlation included in the calculation. Ordinarily, one means by "correlation energy", the energy difference between ground-state energy calculated at the Hartree–

Fock level (in a given basis), and the exact electronic energy calculated in the same basis. In the consideration of response properties, including hyperpolarizabilities, a more general notion of correlation is called for, since one is interested in the effects of electron correlation (beyond the Hartree–Fock level)—not in the energy expectation value, but in a dynamical response property. Indeed, simple variational principle arguments no longer give upper or lower limits for the computed response properties.

To overcome the deficiencies of a Hartree–Fock wavefunction, the function may be represented as a linear combination of Slater determinants and is referred to as configuration interaction (CI). Alternatively, most ab initio packages use Rayleigh–Schrödinger many-body perturbation theory (MBPT) as applied to molecular systems following Møller and Plesset[148,149] to account for electron correlation. This treatment, which can be terminated at second (MP2), third (MP3), or fourth order (MP4), accounts for correlation by mixing excitations to virtual orbitals of the SCF wavefunction into the ground-state SCF wavefunction. Coupled cluster (CC) approaches are also popular methods for including electron correlation in electronic structure computations.[150]

Extensive studies have shown, for atoms and small molecules, that correlation effects tend to be most pronounced for smaller systems, and for those components of β that are the smallest in absolute magnitude.[127] The quadratic hyperpolarizability data presented in Table 7 for HCl indicate that computations at the MP2, CCSD, and CCSD(T) levels lead to static $\beta_{\parallel}$ values that are 2–3 times that at the SCF level. Recent MP2 computations on p-nitroaniline[128] suggest that correlation may be important in larger molecules as well for PNA. Specifically, the ab initio MP2-derived static response for PNA (β_0; 8.55 × 10^{-30} cm^5 esu^{-1}) was roughly double that computed at the SCF level with CPHF (β_0; 4.4 × 10^{-30} cm^5 esu^{-1}; see note added in proof). Generally, many-body perturbation theory and coupled cluster techniques can capture nearly all of the effects of electron correlation on the static first hyperpolarizability. On the other hand, simple MP2 calculations, in which the fluctuation between the Hartree–Fock and exact Hamiltonians is treated as a perturbation to second order, again captures the dominant correlation effects, without being too computationally demanding. It appears, on the basis of a number of studies on small molecules,[122,127] that the MP2 treatment is adequate for describing at least 90% of the effects of electron correlation on static hyperpolarizabilities.

To reiterate, it is generally found that contributions from both correlation and basis-set extension are most important for relatively smaller hyperpolarizabilities

Table 8. Theoretical and Experimental First Hyperpolarizability Data, $\beta_\parallel^{SHG}(\omega)$, for Small Molecules with Various Levels of Electron Correlation As Computed with ACES II[a-d]

molecule	MBPT(2)	CCSD	CCSD(T)	EXPT
CO	11.2	11.4	11.7	12.9 ± 1.4^e
HF	−3.3	−3.2	−3.4	-4.70 ± 0.41^f
H_2O	−8.8	−8.2	−9.1	-9.4 ± 0.4^e
NH_3	−20.1	−18.4	−21.2	-20.9 ± 0.5^e
H_2S	−4.4	−2.8	−3.8	-4.3 ± 0.9^e

[a] All NLO data are in units of 10^{-32} cm^5 esu^{-1}. [b] λ_{input} = 694.3 nm. [c] Tabular data taken from ref 121, Table XVI. [d] Basis set employed is that from ref 160 augmented with an additional hydrogen d function and heavy-atom lone-pair functions of s and p types. [e] Reference 161. [f] Reference 162.

and for relatively smaller Cartesian components. Again, this might be qualitatively expected: for large responses, one anticipates that even a simple electronic structure description should capture the tendency of the molecule to exhibit the appropriate polarizability or hyperpolarizability. Smaller responses are more difficult to characterize, and therefore put more severe requirements on treatments of the correlation or basis.

Frequency-Dependent Responses. The frequency-dependent response adds an additional level of complexity. Essentially, the formalism must be extended to treat applied fields of the form

$$F(\omega) = F_o + F_\omega \cos(\omega t) \qquad (26)$$

where ω is the frequency of the applied field. Formally, the frequency-dependent first hyperpolarizability is the response of the system at a frequency $\omega_1 + \omega_2$ to oscillatory applied fields of frequencies ω_1, ω_2. From eq 7, it can be shown[126,127] that the frequency-dependent response can be computed, formally, as a higher derivative of a so-called "pseudo-energy" with respect to the applied field (a simple generalization of eq 25). Here the pseudo-energy is defined as the eigenvalue of the operator $H - i\hbar\ \partial/\partial t$. This approach has been developed[120] and employed[126,127] by Rice, Handy, and their co-workers. A second approach, that generalizes the time-dependent Hartree–Fock (TDHF) or random phase approximation (RPA),[117] has been extensively applied by Bartlett and his collaborators.[121,122,125] Finally, a scheme that begins with a general formulation of the frequency-dependent quadratic response, originally proposed by Dalgaard,[151,152] has been applied to a large number of properties by Jørgensen and collaborators.[153-155] This so-called multiconfiguration response function approach has been used for hyperpolarizability calculations by Jørgensen and co-workers (HF[156] and p-nitroaniline),[157] by Parkinson and Oddershede,[158] and by Aiga and collaborators.[159]

Just as with static hyperpolarizabilities, dynamic hyperpolarizabilities can be calculated using different levels of correlation. Particular choices of correlated states include those based on MP2 perturbation theory, those based on coupled cluster techniques at the singles and doubles; singles, doubles and quadruples; or singles, doubles, triples, and quadruples level; multiconfiguration self-consistent field; and configuration interaction. Particularly in the case of the coupled cluster techniques, satisfactory convergence of the result with increasing levels of correlation has been demonstrated[121] for small molecules as shown in Table 8.
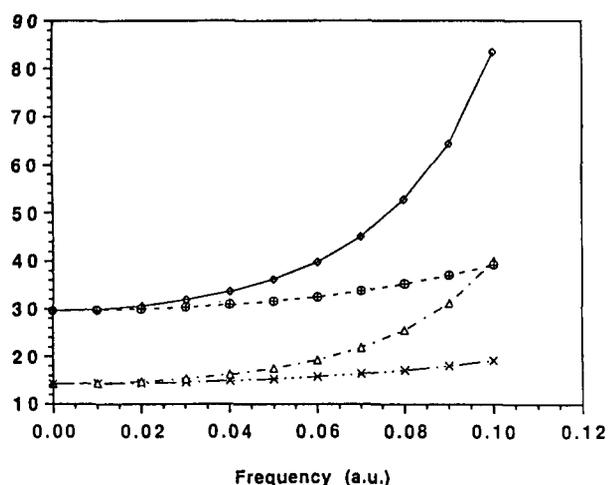

Figure 5. Frequency-dependent first hyperpolarizability (atomic units) as a function of frequency ω (atomic units) for NH_3 as computed at the *ab initio* level. Diamonds correspond to MP2 SHG responses, and circles to MP2 OREC values; triangles represent SCF SHG values, and crosses SCF OREC responses. (Reprinted from ref 126. Copyright 1992 Wiley.)

The effects of frequency dependence (dispersion) and of correlation and basis set can to some extent be separated: that is, one can approximate the frequency-dependent response by

$$\chi_{corr}^n(\text{dynamic}) \cong \left[\frac{\chi_{corr}^n(\text{static})}{\chi_{SCF}^n(\text{static})}\right]\cdot\chi_{SCF}^n(\text{dynamic}) \qquad (27)$$

Here χ^n is the nth order response (polarizability, first, or second hyperpolarizability), and its frequency dependence is separated in terms of the static response multiplied by the ratio of the frequency dependencies that arise using the simple TDHF scheme, where corr and SCF denote correlated and SCF values. This has been used by Bartlett and collaborators,[122] and similar arguments have been made by Rice and co-workers.[126] The fact that eq 27 is not exactly correct follows quite clearly from the spectral representation, or the equivalent sum-over-states form of eq 29, below. For example, in formaldehyde, the frequency-dependent correction using SCF, compared to that using MP2, gives a difference in the hyperpolarizability of only 3% at a frequency of 0.05 Hartree.[126] As resonances are approached, damped singularities will occur in the response functions, and the sensitivity to correlation becomes greater—see Figure 5.[126] By using the general quadratic response formalism, the separation of eq 27 is generally not made, but the frequency dependence can be characterized directly. Starting with the spectral representation, and performing an expansion around zero frequency, one can show[163] that to leading order the hyperpolarizability should go as

$$\beta(-\omega_1-\omega_2;\omega_1,\omega_2) = (A\omega_L^2 + 1)\beta(0;0,0) \qquad (28)$$

where $\omega_L^2 = 2(\omega_1^2 + \omega_2^2 + \omega_1\omega_2)$ and the constant A is unique for each molecule. Jørgensen and collaborators have fitted their computed response for the HF molecule to this form, and it fits their points well at both the correlated and SCF levels of theory as shown in Figure 6.[157] With more complicated molecules, there will be many singularities in the response function, and the simple expansion of eq 28 will hold only up to the lowest frequency of these.
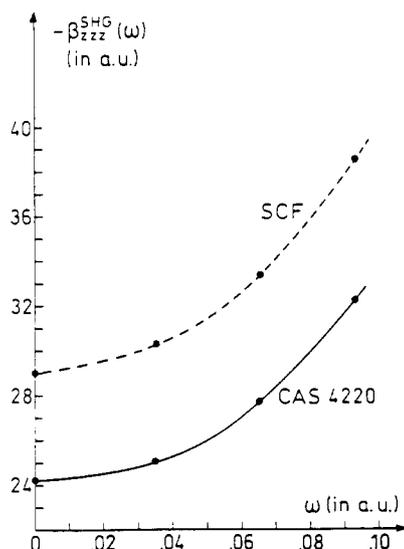
Figure 6. Frequency-dependent response ($\beta_{zzz}^{SHG}(\omega)$) of HF as computed at the *ab initio* SCF and CAS levels. (Reprinted from ref 157. Copyright 1992 Elsevier.)
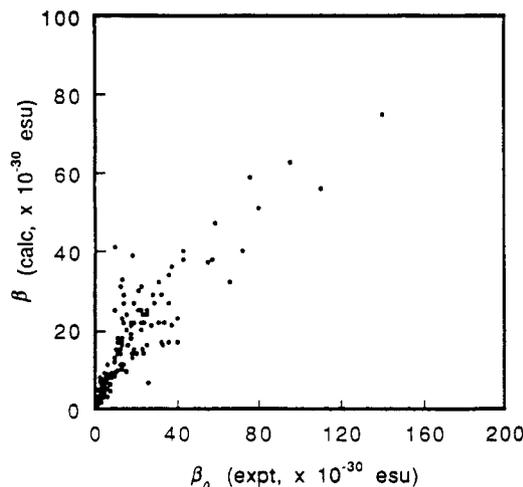

Figure 7. Plot of MOPAC-FF-derived static second-order responses (β_0) and measured responses (β; $\hbar\omega = 0.65$ eV). (Reprinted from ref 177. Copyright 1992 American Chemical Society.)

Often, then, the best way to estimate the accuracy of a theoretical computation is by means of such internal checks as satisfaction of the Reiche–Thomas–Kuhn sum rule, or agreement between calculations in the dipole length or dipole velocity forms. With large basis sets and adequate correlation, some groups have shown that these consistency tests are adequately satisfied by good calculations,[158,163] but that the requirements for the computation of hyperpolarizabilities are more taxing than those appropriate for simple linear optical response. Only a few such calculations have been carried out so far, however, and therefore knowledge of the precise requirements of basis set, levels of correlation, and inclusion of dynamical response are still ill-defined.

Comparison with experiment is, for reasons already cited, sometimes quite difficult. For example, Bartlett and collaborators have studied quite extensively the conceivable sources of difference between their best computation and the experimental result for the HF molecule.[121,125] These corrections include correlation effects, increases in basis-set size, vibrational effects, etc. They nevertheless obtain a disparity from the best experimental value by 20% (Table 8). If one is interested in very precise results, then even the best current calculations differ from experiment: this may be due to missing terms in the theory, in particular to relativistic or nonadiabatic effects, or to difficulties in deducing the isolated molecular response from experiment, particularly when EFISH techniques are used.

ii. Coupled Semiempirical Schemes. Semiempirical Hamiltonians can also be used in conjunction with coupled formalisms. For example, many years ago Schweig[164] applied a π-electron-FF treatment to representative push/pull chromophores, and in 1979 Zyss applied in INDO-FF scheme to monosubstituted benzenes[165] and diphenylpolyenes,[71] and later to urea.[166] More recently, Parkinson and Zerner[167] employed a derivative approach with INDO/S to compute hyperpolarizabilities for molecules of modest size such as fluoromethanes, CO, HF, and H_2O. In addition, a CNDO-FF scheme has been applied to push/pull benzene chromophores,[168] and a PPP-CPHF methodology to push/pull π-systems.[169] Waite and Papa-

dopoulos have published NLO studies using a coupled-CNDO approach augmented with an extended and optimized basis set.[170] Hydrogen 2s and 2p functions were included in the basis set, and the CNDO parameterization scheme modified to reproduce NLO data for a handful of benchmark chromophores. The so-called CHF-PT-EB-CNDO[171] (coupled Hartree–Fock-perturbation theory–extended basis–CNDO) scheme has been used to study nitrogen heterocycles,[172] polyenes,[172,173] and intermolecular interactions.[174] The CHF-PT-EB-CNDO approach is the only example of a semiempirical treatment for hyperpolarizabilities employing more than a minimal basis set. The appropriateness of extending ZDO approximations into the realm of extended basis functions is somewhat controversial.

One semiempirical-coupled scheme in widespread use is that contained in the MOPAC software package. Specifically, a finite field routine can be used to compute α, β, and γ, with either MNDO, AM-1, or PM-3 parameterization schemes.[175] The critical question surrounding such an approximate, as opposed to *ab initio*, algorithm is reliability. An extensive study comparing PM3-FF generated β values with experimental measurements for donor–acceptor chromophores was carried out by Matsuzawa and Dixon,[176,177] and the results are shown in Figure 7. Note that frequency-dependent theory has not as yet been implemented in this algorithm, therefore computed static values (β_0) are being compared with experimental values (β_ω) measured at $\lambda = 1.91~\mu$m. Nevertheless, good linear correlation between theory and experiment is obtained, suggesting that this approach could be used to identify chromophores with potentially-optimal responses from a large database of structures.

The MOPAC-FF approach has been employed in numerous second-order response studies. In addition to the benchmark studies,[176,177] the method has been applied to small molecules (MNDO),[178] monosubstituted benzenes (MNDO, AM1),[175] π-electron polycyclic hydrocarbons, (MNDO, PM3),[179–181] heterocyles (MNDO, AM1, PM3),[182] cyanobiphenyl chromophores (PM3),[183] quinoline derivatives (AM1),[184] and polyeneic structures (AM1),[185–188] and in conformational studies

of donor/acceptor-substituted diarylacetylenes[189] and stilbenes (MNDO).[190]

Consistent with the parameterization scheme, NLO studies using one of the MOPAC-FF routines employ minimal basis sets, and no ground-state electronic correlation is included. These correction factors are assumed to be accounted for in the parameterization. As with *ab initio* coupled schemes, the semiempirical coupled algorithms do not easily lend themselves to interpretation. Another potential shortcoming of this approach when implemented with MOPAC is that the intricate parameterization scheme is chosen to reproduce heat of formation data, rather than properties linked to the NLO response.

b. Uncoupled Treatments. As an alternative to directly coupling the applied field to the molecular Hamiltonian, NLO responses can also be computed using standard time-dependent perturbation theory. In the uncoupled formulation,[191-193] electronic excited states created by the perturbing laser field are treated as an infinite sum over unperturbed particle–hole states, where the individual components of the quadratic hyperpolarizability are given by eq 29. Here ω is the

$$\beta_{ijk}^{SHG} = -\frac{e^3}{8\hbar^2} \sum_n \sum_{n'} \left\{ (r_{gn'}^j r_{n'n}^i r_{gn}^k + r_{gn'}^k r_{n'n}^i r_{gn}^j) \right.$$

$$\left(\frac{1}{(\omega_{n'g} - \omega)(\omega_{ng} + \omega)} + \frac{1}{(\omega_{n'g} + \omega)(\omega_{ng} - \omega)} \right) +$$

$$(r_{gn'}^i r_{n'n}^j r_{gn}^k + r_{gn'}^i r_{n'n}^k r_{gn}^j) \left(\frac{1}{(\omega_{n'g} + 2\omega)(\omega_{ng} + \omega)} + \right.$$

$$\left. \frac{1}{(\omega_{n'g} - 2\omega)(\omega_{ng} - \omega)} \right) + (r_{gn'}^i r_{n'n}^k r_{gn}^i + r_{gn'}^k r_{n'n}^j r_{gn}^i)$$

$$\left. \left(\frac{1}{(\omega_{n'g} - \omega)(\omega_{ng} - 2\omega)} + \frac{1}{(\omega_{n'g} + \omega)(\omega_{ng} + 2\omega)} \right) \right\} \quad (29)$$

frequency of the applied electric field, $r_{n'n}^i = \langle \psi_{n'} | r^i | \psi_n \rangle$ is the matrix element of the displacement operator $r^{(i)}$ along the ith molecular axis between electronic states $\psi_{n'}$ and ψ_n, and $\hbar\omega_{ng}$ is the energy separation between the ground state (denoted by g) and an excited state ψ_n. It is often convenient to transform to a charge-centroid coordinate system as described by Morley and collaborators.[194] In the new coordinate system, g is removed from the summation and the diagonal transition moment matrices are replaced with equation 30.

$$\langle n|r|n \rangle = \langle n|r_{\text{Cartesian}}|n \rangle - \langle g|r_{\text{Cartesian}}|g \rangle \quad (30)$$

If a charge-centroid approximation is applied to eq 29 and the diagonal matrix elements are separated from the off-diagonal elements, the familiar SOS expression for β emerges (eq 31),where $\Delta r_n^i = r_{nn}^i - r_{gg}^i$ is the dipole moment difference between excited state and ground state. The formal divergences at excitation resonances are usually avoided by adding relaxation-based broadening terms to the denominators.[1-3,195]

The sum-over-states perturbation theory expression for the hyperpolarizability (eq 31) indicates that one requires dipole matrix elements between ground and

$$\beta_{ijk}^{SHG} = -\frac{e^3}{8\hbar^2} \left[\sum_{n \neq g} \sum_{\substack{n' \neq g \\ n' \neq n}} \left\{ (r_{gn'}^j r_{n'n}^i r_{gn}^k + r_{gn'}^k r_{n'n}^i r_{gn}^j) \right. \right.$$

$$\left(\frac{1}{(\omega_{n'g} - \omega)(\omega_{ng} + \omega)} + \frac{1}{(\omega_{n'g} + \omega)(\omega_{ng} - \omega)} \right) +$$

$$(r_{gn'}^i r_{n'n}^j r_{gn}^k + r_{gn'}^i r_{n'n}^k r_{gn}^j) \left(\frac{1}{(\omega_{n'g} + 2\omega)(\omega_{ng} + \omega)} + \right.$$

$$\left. \frac{1}{(\omega_{n'g} - 2\omega)(\omega_{ng} - \omega)} \right) + (r_{gn'}^j r_{n'n}^k r_{gn}^i + r_{gn'}^k r_{n'n}^j r_{gn}^i)$$

$$\left. \left(\frac{1}{(\omega_{n'g} - \omega)(\omega_{ng} - 2\omega)} + \frac{1}{(\omega_{n'g} + \omega)(\omega_{ng} + 2\omega)} \right) \right\} +$$

$$4 \sum_{n \neq g} \left\{ [r_{gn}^j r_{gn}^k \Delta r_n^i (\omega_{ng}^2 - 4\omega^2) + r_{gn}^i (r_{gn}^k \Delta r_n^j + r_{gn}^j \Delta r_n^k) \right.$$

$$\left. \left. (\omega_{ng}^2 + 2\omega^2)] \times \frac{1}{(\omega_{ng}^2 - \omega^2)(\omega_{ng}^2 - 4\omega^2)} \right\} \right] \quad (31)$$

excited states, excitation energies, and excited state dipole moments to compute the β response. Since the electric field perturbation $\vec{F}\cdot\vec{\mu}$ is a one electron operator, eq 31 implies that only singly excited states will mix with the ground state, if the ground-state is taken as a single determinant. Thus, the first hyperpolarizability, like the polarizability or the optical excitation spectrum, will formally involve only monoexcited configurations, if the ground state is of single determinant type (*vide infra*).

For calculations based on eq 31, one requires the definition of the dipole moment matrix elements that do not appear directly in the semiempirical model Hamiltonians of eq 11. Ordinarily, but not always, the Pariser approximation (eq 32) is used.[196,197] Here R_λ^i is

$$r_{\kappa\lambda}^i = \delta_{\kappa\lambda} R_\lambda^i \quad (32)$$

the geometric coordinate of the atom on which the λth atomic orbital is found. In the SOS calculations, the molecular orbital coefficients are taken from diagonalizations of the excited states at the monoexcited configuration interaction level, and the energy denominators come from the same diagonalization.

The sum-over-states expansion in eq 31 is, in general, infinite, since the applied optical fields mix the molecular ground state with many excited states. This situation is the same as that for any other frequency-dependent response function, such as conductivity, susceptibility, dielectric constant or chemical shift. As with these other properties, one generally truncates this sum after apparent convergence has been reached, leading to a formally valid criticism of the SOS methodology. For typical organic molecules, this sum involves between dozens and hundreds of singly-excited configurations, where the configurations are generally ordered in terms of energy differences, such that each subsequent configuration involves smaller energy denominators than the previous. A number of researchers have shown that such a truncation is, in fact, justified for β computations. For example, Morley and Pugh
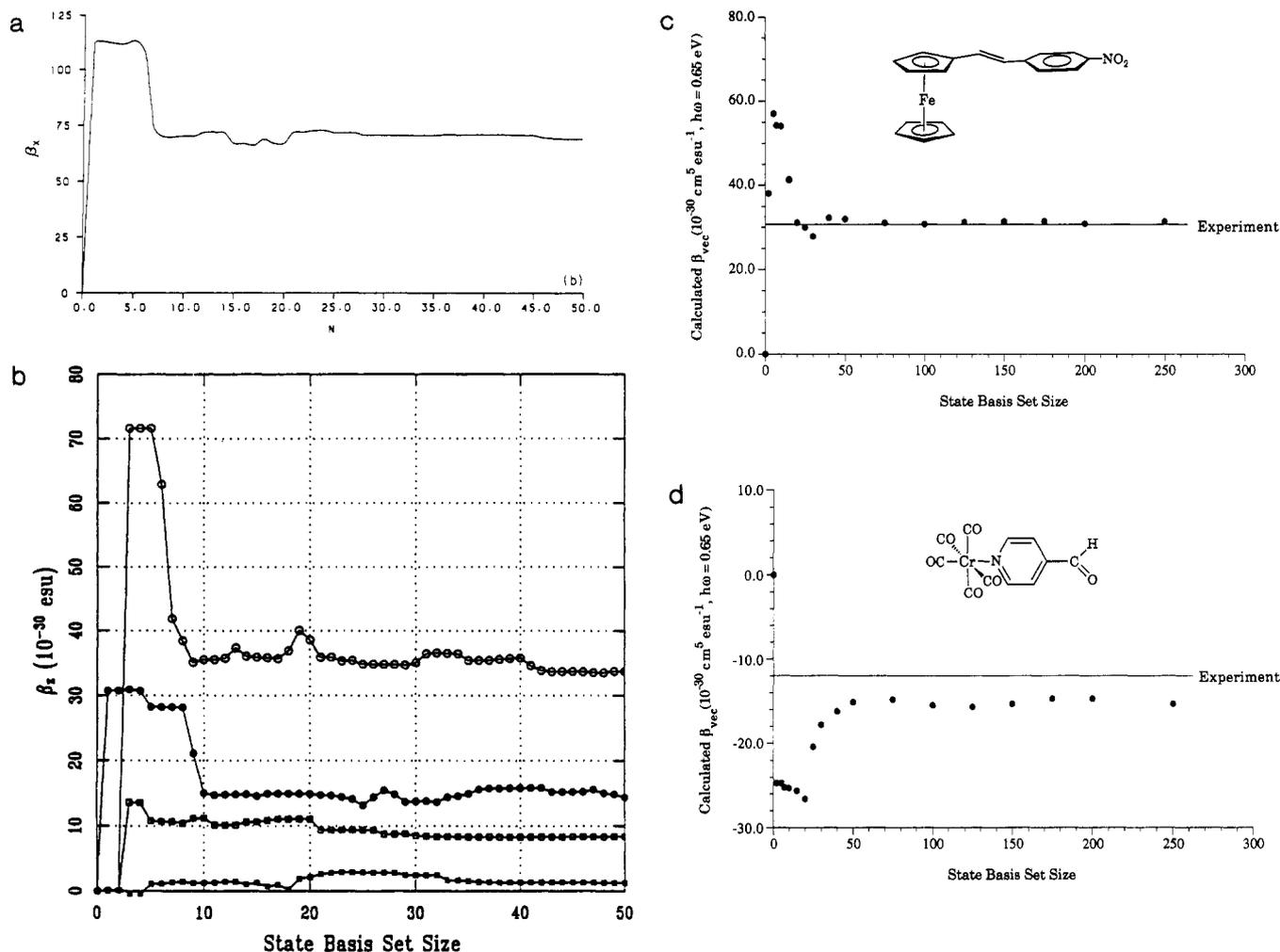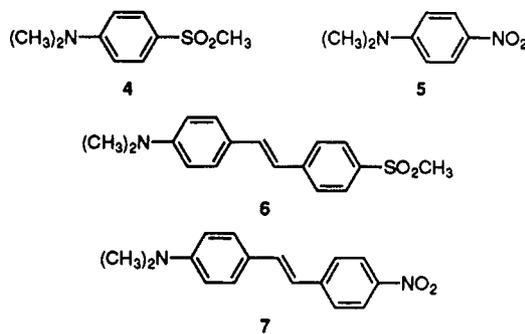
Figure 8. Plots of responses as computed in the SOS formalism as a function of the number of basis set functions included in the SOS expansion for (a) **3** (CNDO-SOS); (b) **4** (■), **5** (□), **6** (●), **7** (O), (INDO-SOS); (c) *trans*-1-ferrocenyl-2-(4-nitrophenyl)-ethylene, (INDO-SOS); and (d) (4-formylpyridine)chromium pentacarbonyl (INDO-SOS). (a: Reprinted from 239. Copyright 1987 Academic Press. b: Reprinted from ref 199. Copyright 1992 American Chemical Society. c and d: Reprinted from ref 200. Copyright 1992 American Chemical Society.)

examined the effect of increasing the number of excited states (N) in a CNDO-SOS computation of β_x (dipolar direction) for 4-amino-4'-nitrostilbene (**3**)at 1064 nm
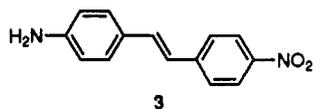
(Figure 8a), and found that the second-order response converges rapidly with number of excited states included. Note that the excited states are ranked in terms of increasing energy. The authors conclude that a set of 50 excited states is sufficiently large to ensure that the comparatively smaller number of states that make a substantial contribution to β are included. A similar conclusion regarding the rapid convergence of the summation was reached by Ulman et al.[199] in their INDO-SOS studies on sulfonyl-containing chromophores, the dependence of β_z (1910 nm, z is the dipolar direction) is plotted for four molecules **4–7** in Figure 8b. Finally, a recent INDO-SOS study on organometallic structures confirmed that the truncation conclusions are equally valid for organometallic molecules.[200] The basis-set plots for *trans* 1-ferrocenyl-2-(4-nitrophenyl) ethylene, and 4-formylpyridinechro-

mium pentacarbonyl are displayed in Figure 8, parts c and d, and demonstrate that the SOS expansion summation converges rapidly even for these complex chromophores.

In principle, *ab initio* electronic structure procedures could be coupled to the SOS prescription, however, these formulations are by and large absent from the literature. Most likely this is due to the perceived "approximate" character of the SOS approach, due to the required truncation of the infinite (though finite for a finite basis) sum in eq 31. Exhaustive *ab initio* electronic structure computations tend to be coupled with the more precise derivative prescriptions.

Table 9. Comparison of PPP-Derived β_{vec} Values and Experimental β_{vec} Values[a-c]

molecule	$\beta_{vec}^{(PPP)}$	$\beta_{vec}^{(exp)}$	$\hbar\omega$, eV
⬡—F	1.02	1.06	1.17
⬡—NH₂	1.84	0.79–2.46	1.17
⬡—NO₂	4.55	1.97–4.6	1.17
H₂N—⬡—NO₂	34.4	16.2–47.7	1.17
CH₃O—⬡—NO₂	11.7	14.3–17.5	0.656
H₂N—⬡—CN	13.26	13.4	0.656
O₂N / H₂N—⬡—NO₂	29.3	21	1.17
H₃C / H₂N—⬡—NO₂	36.3	16–42	1.17
H₂N—⬡—CH=CH—⬡—NO₂	298.1	225–295	1.17
Me₂N—⬡—CH=CH—⬡—NO₂	451.9	450	1.17
H₂N—⬡—CH=CH—NO₂	213.1	180–260	1.17
Me₂N—⬡—CH=CH—CH=CH—NO₂	466.8	470–790	1.17

[a] All NLO data are in units of 10^{-30} cm⁵ esu⁻¹. [b] Tabular data taken from ref 208, Table III. [c] All experimental references are provided in ref 208.

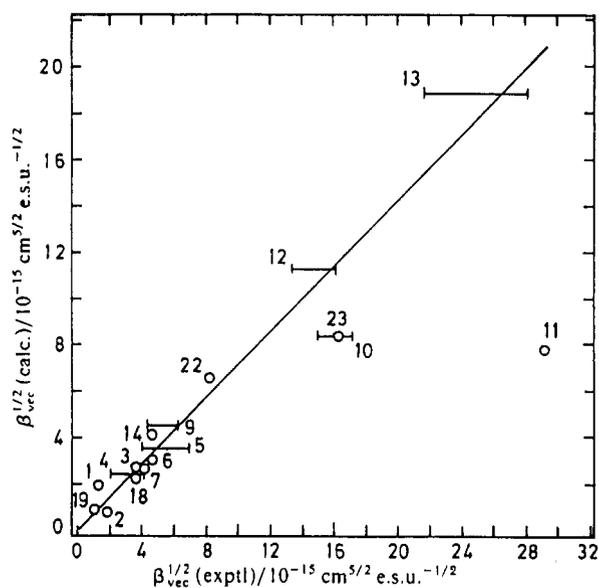**Figure 9.** Plot of 22 π-organic chromophore $\beta_{vec}^{1/2}$ values computed by the CNDOVSB procedure versus experimental $\beta_{vec}^{1/2}$. The second-order response is computed for a given chromophore at the optical energy $\hbar\omega$ that the experimental measurement was performed. Error bars indicate the limits of a wide range of experimental β_{vec} values reported for the same molecule. (Reprinted from ref 238. Copyright 1985 Royal Society of Chemistry.)

Hückel-type models remain important for qualitative understandings, such as the intriguing work by Marder and collaborators,[21,188,201-203] in which it is argued, on the basis of four-site Hückel-type models, that the frequency-doubling response of organic chromophores will show particular trends as functions of polarity differences among substituents at the molecular termini, and excitation energies. For such qualitative arguments, Hückel-type models are extremely useful; for quantitative or semiquantitative analyses within chromophore families, however, electron repulsion effects are simply too important to be ignored.

Since the optical response, the polarizability, and the first hyperpolarizability of conjugated molecules are indeed dominated by π-electron contributions in many high-β chromophores, computations based on the Pariser–Parr–Pople (PPP) model have proven useful and reliable when applied to classes of promising chromophores. For example, in Table 9 PPP-derived and experimentally-determined quadratic hyperpolarizabilities are tabulated for comparative purposes. The correlation between theory and experiment is excellent over the range of β (2.5 orders of magnitude) illustrated in the table. The PPP-SOS model has been applied to traditional push/pull chromophores,[204-212] benzobisthiazoles,[213] phthalocyanines,[207] polyaniline oligomers,[213] push/pull polyenes,[214-217] polymethineimines,[218] phenol/cinnamic acid bound to a surface,[219] hemicyanines/

merocyanines,[220] and octopolar molecules.[221]

In general, however, chromophores useful in nonlinear optical response will contain contributions from the σ-electrons as well as π-electrons; this is particularly important when triple bonds enter, when distortions from molecular planarity must be included, when metal centers are included in the molecules, when the conjugation is broken, or when inductive effects become important. For all of these reasons, semiempirical models of the all-electron type should generally be more useful than π-electron PPP computations.

The CNDO/S model Hamiltonian has enjoyed widespread use in the NLO literature. Albrecht and coworkers first applied the CNDO-SOS technique to the computation of β for p-nitroaniline,[222] and later to urea[223] and β-metaborate.[224] The CNDO-SOS method has also been used to examine the effect of solvent on β[225,226] using a simple solvent cavity model. In addition, Kodaka et al.[227] investigated the effect of attaching a phenyl group to a push/pull 1,3-dithiole chromophore. Lalama and Garito employed a slightly modified version of CNDO/S to examine p-nitroaniline.[228] Specifically, well-known CNDO parameterization schemes[229,230] were systematically adjusted to nitrobenzene and aniline to reproduce spectral and photoemission data. These parameters were then employed to determine the origin of β in p-nitroaniline.[228] This contribution[228,231] is also particularly lucid in explaining the technical details of computing β within the SOS prescription. The parameterization scheme of Lalama and Garito was later used to investigate additional push/pull benzene structures.[232-237]

The most widespread application of a CNDO/S model Hamiltonian is the CNDOVSB method developed by Morley, Pugh, and co-workers.[197,238,239] As in the work of Garito and Lalama, the conventional CNDO/S parameterization scheme is adjusted in CDNOVSB to
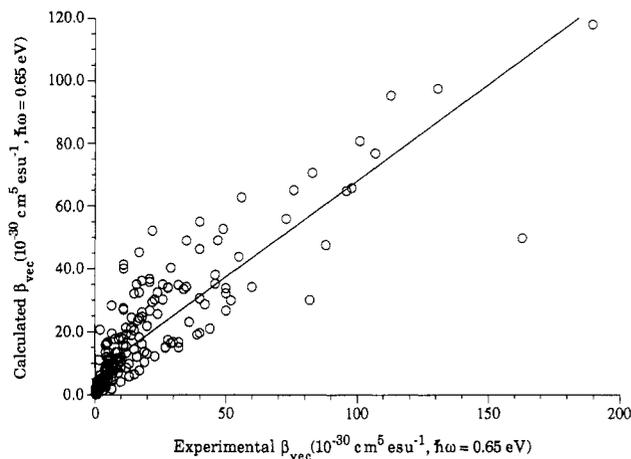
Figure 10. Plot of 203 π-organic chromophore β_{vec} values computed by the ZINDO-SOS procedure versus experimental data from ref 56 and 57. Slope of least-squares fit is 0.8. (Reprinted from ref 257.)

reproduce optical and dipolar data for six molecules with high-β architectures.[198,238,239] The reliability of the CNDOVSB method in computing β for 17 push/pull structures is illustrated in Figure 9. Here, the computed responses are compared with EFISH values and a reasonably good correlation is observed.[198,238,239] Exploratory NLO computations using this approach have been carried out using CNDOVSB.[102,194,240-255] Representative chromophore classes include polyenes,[102] monosubstituted benzenes,[244] sulfur-containing systems,[245] 2-pyrazolines,[246] azulenes,[247,248] hexammine,[249] polyheterocycles,[250] phenylsilanes,[251] polyynes,[254] and dye arichtectures.[252] In addition, a recent CNDO/S-CI study examines second-order NLO effects in disubstituted polyene structures.[256]

The INDO/S electronic structure method has recently gained popularity in second-order response computations. The primary platform for these computations is the ZINDO code developed by Zerner and co-workers.[92-95] This particular method possesses two advantages, namely a unique set of parameters and capabilities for handling transition metal systems. All NLO computations use the parameterization as defined by Zerner and collaborators without specifically reparameterizing to reproduce NLO quadratic hyperpolarizabilities. Semiempirical, all-valence electron calculations of first hyperpolarizabilities have now been performed on hundreds of molecules.[257] For example, Figure 10 shows a comparison between the frequency-doubling response at $\hbar\omega$ = 0.65 eV; notice that, over several orders of magnitude, the comparison is quite satisfactory. The slope of this curve is roughtly 0.8, rather than the unity that would be expected if the computation effectively mirrored the experiment;[258] this probably reflects solvent stabilization of the excited states. The ZINDO-SOS approach has also been applied to inorganic and organometallic chromophores,[200] and a representative correlation with experiment is shown in Figure 11. Even with these more complex structures, the ZINDO-derived responses accurately reflect those observed in the laboratory. The demonstrated accuracy of this approach has spawned several studies. Specifically, the ZINDO-SOS methodology has been used to examine traditional push/pull organic architectures,[100,199,200,259-267] main group element structures,[268,269] organometallic molecules,[200,270,271] and chromophore–chromophore interactions.[272,273] Finally, a MOPAC-SOS paradigm (AM1 Parameterization) has recently been developed and applied to push/pull π-systems.[274]

Note that the laser frequency (ω) is an input parameter in the SOS formulation, therefore computing frequency-dependent responses is trivial in this formalism. An important advantage of the SOS approach is that the dispersive character of the hyperpolarizability can be easily computed. For example, the calculated $\beta(\omega)$ versus the frequency of the incoming laser beam (ω) is plotted for p-nitroaniline and 4-(dimethylamino)-4'-nitrostilbene in Figure 12, parts a and b. Note that β is not defined at both the incident and second-harmonic frequencies. As seen in Figure 12a, Garito and collaborators[228] calculated the frequency dependence of several tensorial components of the hyperpolarizability using a CNDO/S model, however,
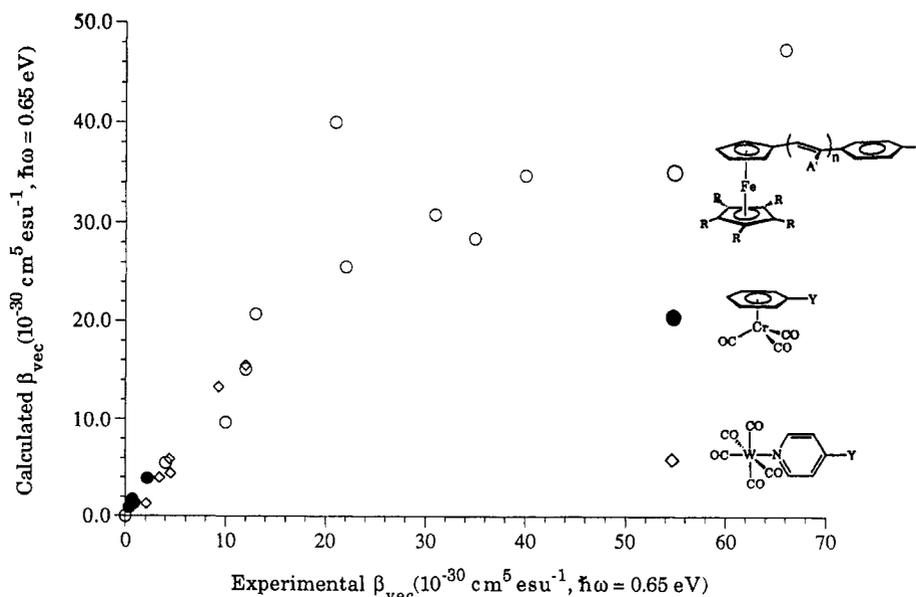

Figure 11. Plot of organometallic chromophore β_{vec} values computed by the ZINDO-SOS procedure versus experimental data. (Reprinted from ref 200. Copyright 1992 American Chemical Society.)
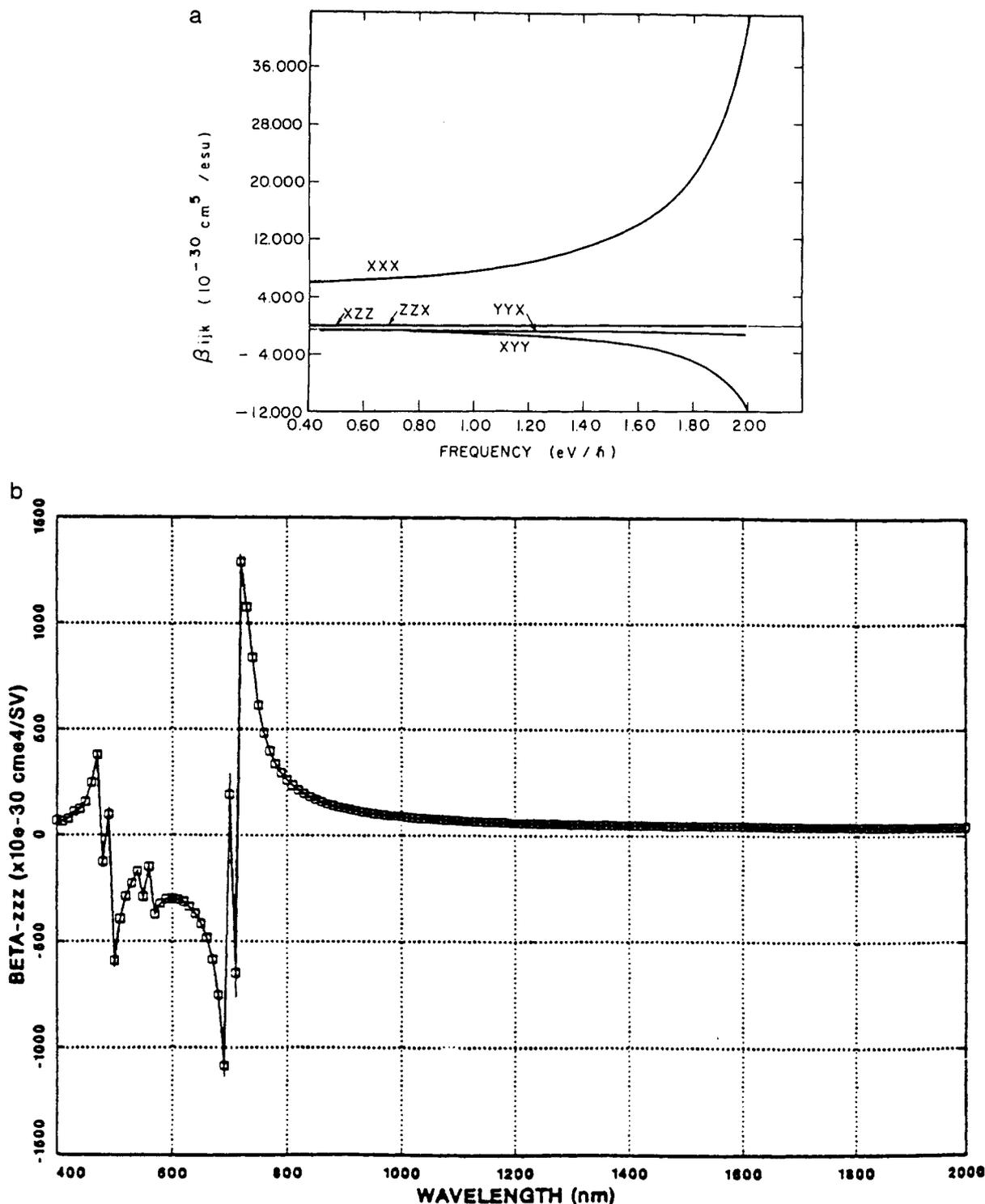
Figure 12. Calculated frequency dependence of (a) various tensors of p-nitroaniline and (b) the β_{zzz} tensor (z is charge-transfer direction) of DANS (7). Note that energy increases to the right in a and to the left in b. (a: Reprinted from ref 228. Copyright 1979 American Institute of Physics. b: Reprinted from ref 259. Copyright 1988 American Chemical Society.)

the predominant component β_{xxx} (x defined as the charge-transfer direction) is of primary interest. Note that this component varies slowly until ω approaches a resonance and then diverges as expected from eq 29 (poles corresponding to zeros in the energy denominators). In Figure 12b, a plot of INDO/S-derived $\Delta\beta_{zzz}$ (z defined as charge transfer direction) is plotted as a function of the laser wavelength for DANS ($\lambda_{max}^{calc} = 396$ nm), with $\Delta\beta_{zzz} = 0$ as $\omega \rightarrow \infty$. Note the resonance at the 2ω frequency. As the frequencies approach resonance, effects due to lifetimes and vibrations

become important and appropriate corrections to eqs 29 and 31 are required. Very large hyperpolarizabilities can be obtained at frequencies close to one-photon or two-photon resonances, however, linear absorption occurs and therefore the utility of the resulting large-β chromophores at near-resonant frequencies is marginal.

In the limiting static situation, the β parameters for all second-order phenomena (LEOE, SHG, and OREC) should converge to one unique value. Figure 13 shows that this is true for various PPP-derived second-order responses of aniline.
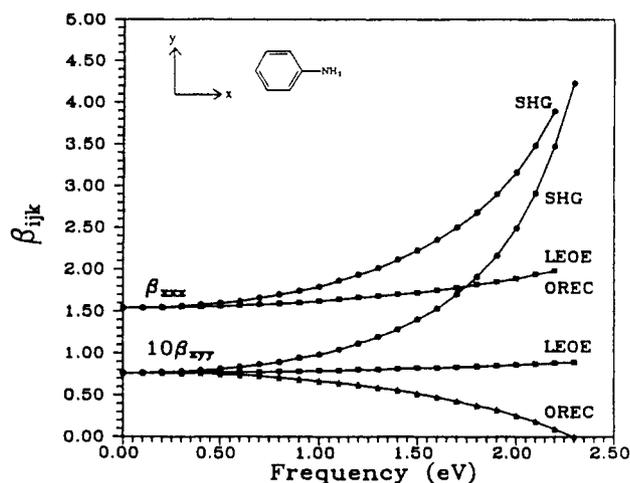
Figure 13. Computed frequency dependence of β_{xxx} and β_{xyy} for various second-order processes in aniline. (Reprinted from ref 208. Copyright 1992 American Chemical Society.)

Table 10. The Sensitivity of PPP-SOS-Derived β_{vec} of p-Nitroaniline with Choice of Carbon and Nitrogen Parameterization

$$H_2N\text{—}\langle\bigcirc\rangle\text{—}NO_2$$

Carbon Parameterization

Vary C_{IP}; $C_{EA} = 0.03$

IP	8.93	10.04	11.16	12.28	
β_{vec}	45.2	39.4	35.9	31.9	

Vary C_{EA}; $C_{IP} = 11.16$

EA	−2.24	−0.43	0.03	0.23	0.53
β_{vec}	45.2	36.6	35.9	35.7	35.8

Nitrogen Parameterization

Vary N_{IP}^{nitro}, N_{IP}^{amino}; $N_{EA} = 8.97$

IP$_{nitro-N}$	20.58	23.16	25.73	28.30	33.88
IP$_{amino-N}$	17.18	19.32	21.47	23.62	25.76
β_{vec}	29.5	33.6	35.9	39.1	51.9

Vary N_{EA}; $N_{IP}^{nitro} = 25.73$, $N_{IP}^{amino} = 21.47$

EA	7.18	8.07	8.97	9.87
β_{vec}	49.8	43.0	35.9	30.8

[a] All NLO data are in units of 10^{-30} cm^5 esu^{-1}; β_{vec} calculated at λ = 1064 nm ($\hbar\omega$ = 1.17 eV). [b] Excerpts of table taken from ref 206, Table III. [c] EA refers to electron affinity (in eV) and IP refers to ionization potential (in eV).

Table 11. Comparison of β Components for Aniline ($C_6H_5NH_2$) at 1064 nm ($\hbar\omega$ = 1.17 eV) As Calculated with PPP (Full CI and MECI) and CNDO (MECI)[a]
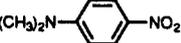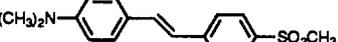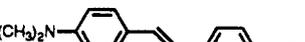
	PPP^{exact} [b]	PPP^{MECI} [c]	CNDO^{MECI} [d]
β_{xxx}	0.46	1.71	1.22
β_{xyy}	0.04	−0.32	0.25
β_{yxy}, β_{yyx}	0.10	−0.27	0.43
β_x	0.54	1.42	1.59

[a] All NLO data are in units of 10^{-30} cm^5 esu^{-1}, λ = 1064 nm ($\hbar\omega$ = 1.17 eV). [b] Reference 205, Table VI. [c] Reference 207, Table III. [d] Reference 228, Table VI.

rameter choice would render the use of semiempirical models problematic.

Another issue that deserves comment is the level of correlation included in semiempirical NLO computations. In coupled *ab initio* schemes, varying levels of correlation are used, from the independent particle model to essentially fully correlated wavefunctions. For semiempirical-SOS computations, most calculations are carried out using a truncated form of CI, specifically correlated wavefunctions including only single excitations. At this level of CI, the ground-state wavefunction is not correlated, however, the excited states are correlated. This level of CI is often referred to as the Tamm-Dancoff approximation, monoexcited configuration interaction (MECI or CIS).[275,276] The inclusion of MECI in computing optical properties is widespread, and therefore spectroscopically-based semiempirical electronic Hamiltonians are parameterized at the MECI level.[277,278] Technically, double excitations could also be included in the electronic structure computation (SDCI or CISD) effectively correlating the ground state as well. Moreover, a fully correlated semiempirical wavefunction could be defined. In fact, the fully correlated second-order response within the PPP model (β^{exact}) has been computed for a series of π-organic chromophores.[205,215-218] Representative β^{exact} values for aniline are compared with PPP-MECI and CNDO-MECI level computations in Table 11. Note that the inclusion of correlation beyond the MECI level can lead to significant changes in the computed responses. Specifically, β_x ($\hbar\omega$ = 1.17 eV) computed with full correlation (62.7 in atomic units) is less than half the singles-only value (164 in atomic units). This result is confirmed when INDO/S-SDCI-SOS (singles and doubles) computed responses are contrasted to INDO/S-SCI-SOS (singles) and experiment (Table 12). For example, for p-nitroaniline, the INDO-SDCI computation of β ($\hbar\omega$ = 0.65 eV) yields 4.2 × 10^{-30} cm^5 esu^{-1} versus SCI (11.3 × 10^{-30} cm^5 esu^{-1}) and experiment (9.2 × 10^{-30} cm^5 esu^{-1}). Such computations show the importance of correlation effects and form a useful complement to extensive studies of correlation effects in an *ab initio* context. There is, however, an important issue of consistency here: the semiempirical model Hamiltonians used in computing β response are based on a parameterization consistent with calculation of optical properties in which the ground state is taken as a single determinant, and the excited states at the MECI level. In this sense, it is not consistent to include electron correlation at higher levels. While such studies are important in indicating that correlation effects can indeed substantially change the computed value of β within a particular model Hamiltonian (semiempirical or *ab initio*), for actual computation of β response using

In an *ab initio* context, one is concerned with how variations in basis set can change the computed nonlinear response. In semiempirical models, the equivalent problem is the sensitivity of the computed response to small changes in the parameterization; that is, in the atomic orbital integrals that enter into eqs 12, 13, and 16. In the case of the PPP model, a number of parameterization schemes exist in the literature. Table 10 shows the results of PPP-type calculations on p-nitroaniline employing various atomic parameters; note that over reasonable variations of the C, N, and O parameter set, the PPP-SOS derived β properties do not exhibit any abrupt variation. Specifically, by choosing ionization potentials (IP) over a 10-eV range and electron affinities (EA) over some 3 eV, enormous parameter fluctuations, β ($\hbar\omega$ = 1.17 eV) only varies from 30 × 10^{-30} cm^5 esu^{-1} to 50 × 10^{-30} cm^5 esu^{-1}. This result is important, since extreme sensitivity to pa-

Table 12. Second-Order Hyperpolarizabilities [β_{vec} ($\hbar\omega$ = 0.65 eV)] As Calculated by ZINDO-SOS Using Singles and Singles/Doubles Versus Experiment[a]

chromophore	SOS-SCI[b]	SOS-SDCI[b]	expt[c]
H_2N—〈benzene〉—NO_2	11.3	4.2	9.2
$(CH_3)_2N$—〈benzene〉—NO_2	11.6	5.6	12
$(CH_3)_2N$—〈benzene〉—CH=CH—〈benzene〉—SO_2CH_3	13.4	12.3	
$(CH_3)_2N$—〈benzene〉—CH=CH—〈benzene〉—NO_2	42.5	15.7	73
$(CH_3)_2N$—〈benzene〉—N=N—〈benzene〉—NO_2	41.8	19.8	

[a] All NLO data are in units of 10^{-30} cm^5 esu^{-1} at 1064 nm ($\hbar\omega$ = 1.17 eV). [b] Calculated values from ref 199, Table I. [c] Experimental values from ref 56, Tables II and III.

semiempirical models, it is probably more appropriate to be consistent, and to do the calculations using standard parameterization, with the sum-over-states form of eq 31, the ground state limited to a single determinant, and the excited states treated at the monoexcited CI level.

It is important to note that SOS methods can be, and recently have been, used in conjunction with *ab initio* model Hamiltonians. Tomonari and collaborators[279] employed a simplified SOS treatment to extract β from an SCF wavefunction (with an extended basis set) for conventional push/pull benzene structures. The authors find good agreement between the modified-SOS approach and a first principles CPHF treatment. Also, Stanton and Bartlett[280] have developed an SOS method to extract α from a CCSD wavefunction.

4. Summary of Computational Methods

To summarize this section, *ab initio*-CPHF computations are numerically more accurate and precise, however the results are not easily amenable to chemical interpretation and require substantial allocations of computational resources. Compared to *ab initio* methods, the semiempirical-CPHF methodologies offer computational economic advantages at some expense of accuracy and can therefore be applied to large systems. However, since they are based upon derivative rather than SOS formalism, the interpretation of the computed responses is difficult. All of the semiempirical-SOS procedures discussed here provide second-order responses in reasonable agreement with experiment. Moreover, they permit a basic understanding of origin of the NLO response in a chemical sense, by identifying the molecular excited states primarily responsible for an NLO response within the SOS formalism, as will be discussed in section III of this review.

While formally there are differences between the coupled and uncoupled schemes, and the derivations and implementations are substantially different, the essential notion (computation of the hyperpolarizability as the response to frequency-dependent fields) is similar. Indeed, Parkinson and Oddershede[158] demonstrate that spectral representation of the quadratic

response function can be obtained by inserting complete sets of stationary state eigenfunctions and that, when this is carried out, the resulting expression (eq 11 of their paper) is essentially identical to form of eq 31, used in the sum-over-states perturbation theoretic analysis. The differences arise from the forms taken for the ground-state wavefunction, the values of the matrix elements, the nature of the excited states, and the values of the energy denominators. In the *ab initio* calculations, all of these are effectively replaced by properly calculated values arising from a choice of model Hamiltonian (definition of basis set) and a particular level of correlation for ground and excited states (in fact, the sums are not calculated directly, but are replaced by solutions to equations of motion in frequency space, as is done for simple TDHF). The coupled and uncoupled approaches, which at first glance appear very different, are really very similar.

III. Gaining Chemical Insight through Computational Studies

From a chemical perspective probably the most important feature of the NLO response calculations is the insight they provide into how architectural and electronic structural properties of particular molecular chromophores lead to frequency-doubling behaviors. The reliability of various computational procedures was demonstrated in the previous section. If such computational models are indeed reproducing experiment, researchers should be able to pinpoint the electronic features that lead to enhanced responses, and therefore more effectively target a few key molecular morphologies. Various levels of understanding the origin of β can be gained from such computations via four distinct models; these will be discussed in increasing level of complexity.

A. Qualitative Electronic Asymmetry Model

The importance of electronic asymmetry in enhancing β is well established.[16-34] In this particular model, either computed or measured responses for prototypical donor/acceptor π-organic chromophores are rationalized on the basis of dissimilarities in electron-donating and electron-withdrawing abilities of the appended substituents. The Hammett free-energy relationship provides what is probably the most broadly applicable measure of such acentricity in simple π-organic systems. These empirical parameters have been compiled for hundreds of substituent moieties through experimental measurements of ionization constants for organic acids in solution.[281-284] Specifically, the general relationship defines the Hammett parameter (σ_x)
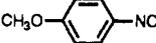
$$\sigma_x = \log K_X - \log K_H \tag{33}$$

where K_H is the ionization constant for benzoic acid at 25 °C, and K_X is the corresponding constant for a *meta* (m) or *para* (p) substituted benzoic acid.[281-284] The electronic asymmetry ($\Sigma\sigma_p$) for a *para*-derivatized donor/acceptor chromophore can be expressed as

$$\sum \sigma_p = \sigma_{p,acceptor} - \sigma_{p,donor} \tag{34}$$

where the acceptor Hammett constants are positive (NO_2 = 0.78) and the donor constants are negative (NH_2 = −0.66).

Table 13. Molecular Hyperpolarizabilities [β_{vec} ($\hbar\omega$ = 0.65 eV)] Computed by ZINDO-SOS Versus Experimental Values for Representative para-Disubstituted Benzenes[a]

chromophore	$\beta_{vec}^{calc\ b}$	$\beta_{vec}^{expt\ c}$
H_2N—⟨⟩—NO_2	10.7	9.2
H_2N—⟨⟩—CN	3.28	3.1
CH_3O—⟨⟩—NO_2	6.21	5.1

[a] All NLO data are in units of 10^{-30} cm^5 esu^{-1}. [b] Calculated data from ref 100, Table V. [c] Experimental data from ref 56, Table II.
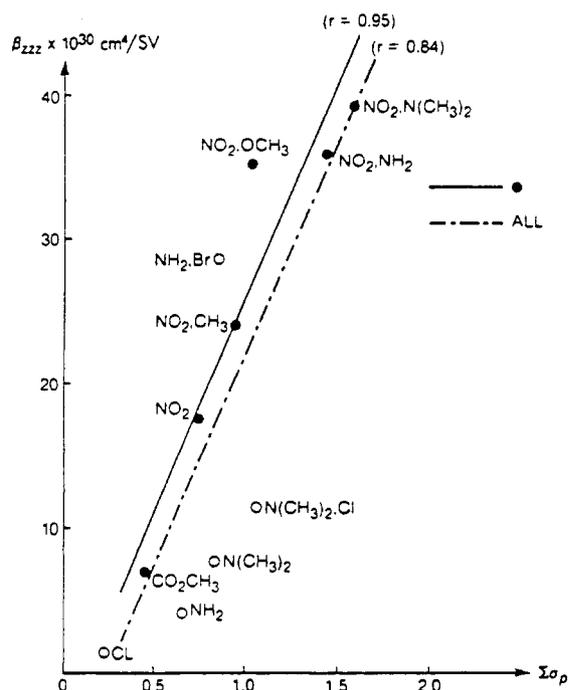
Figure 14. Calculated β_{zzz} ($\hbar\omega$ = 0.65 eV) for mono- and disubstituted stilbenes as a function of the electronic asymmetry as calculated from Hammett parameters. (Reprinted from ref 259. Copyright 1988 American Chemical Society.)

Table 13 provides some evidence as to the applicability of this interpretation. The quadratic hyperpolarizabilities for the benchmark p-nitroaniline chromophore (β_{vec}^{expt} = 9.2 × 10^{-30} cm^5 esu^{-1}; β_{vec}^{calc} = 10.7 × 10^{-30} cm^5 esu^{-1}) decreases with the substitution of less potent electronic acceptors such as -CN (β_{vec}^{calc} = 3.28 × 10^{-30} cm^5 esu^{-1}) or less potent donors such as -OCH$_3$ (β_{vec}^{calc} = 6.21 × 10^{-30} cm^5 esu^{-1}) in complete agreement with experiment. The second-order responses for a series of mono- and disubstituted stilbene chromophores are plotted as a function of the Hammett electronic asymmetry ($\Sigma\sigma_p$) in Figure 14. Ulman,[259] using the ZINDO/S-SOS method in this thorough study, obtains a remarkably linear relationship (R = 0.95) between electronic asymmetry and β—an important result. It assures the synthetic chemist that π-asymmetry is indeed a relevant criterion for predicting second-order NLO responses. While this simplistic model works well for classical π-donors linked through classical polyene-like bridges to classical π-donors, it encounters severe difficulties if exotic bridge architectures are investigated, additional substituents are

appended to the chromophore, or metal fragments are incorporated into the molecule. For these, a more detailed interpretation is needed.

B. Qualitative Two-Level Picture

The connection between the linear optical properties of a chromophore and quadratic hyperpolarizability is widely recognized.[16-34] As discussed earlier in this review, Oudar and Chemla[65,66] established a link between β and the details of a low-lying charge-transfer transition though the two-level model. The two-level formula (eq 10) can be obtained from the full quantal expression for β_{ijk} (eq 29) by restricting the "summation" to one excited state (n) and assuming that one tensorial component (β_{iii}) dominates the response (this assumes that the charge-transfer transition is unidirectional). The complicated expression of eq 29 reduces to the simplified proportionality

$$\beta_{vec} \approx \beta_i \approx \beta_{iii} \propto \frac{(\hbar\omega_{gn})^2\,(r_{gn}^i)^2\,\Delta\mu_{gn}^i}{[(\hbar\omega_{gn})^2-(2\hbar\omega)^2][(\hbar\omega_{gn})^2-(\hbar\omega)^2]}$$ (35)

where $\Delta\mu_{gn}$, r_{gn}, and ω_{gn} (= $E_{gn}/\hbar$, $2\pi c/\lambda_{gn}$) become the crucial two-level parameters in chromophore design. The oscillator strength (f_{gn}), which is proportional to $r_{gn}^2 E_{gn}$, can be incorporated into eq 35 to yield eq 36

$$\beta_{vec} \approx \beta_i \approx \beta_{iii} \propto \frac{(\hbar\omega_{gn})\,f_{gn}\,\Delta\mu_{gn}^i}{[(\hbar\omega_{gn})^2-(2\hbar\omega)^2][(\hbar\omega_{gn})^2-(\hbar\omega)^2]}$$ (36)

which is in the form of eq 10. The oscillator strength, a classical spectroscopic term, can be related to the more familiar molecular absorptivity (ϵ_{max}).[285]

Often the details of the above equations are omitted, the static case ($\hbar\omega$ = 0.0 eV) is assumed, and the following two-level expressions are found in the literature:

$$\beta \propto \frac{r_{gn}^2\,\Delta\mu_{gn}}{E_{gn}^2}$$

$$\beta \propto \frac{f_{gn}\,\Delta\mu_{gn}}{E_{gn}^3}$$ (37)

$$\beta \propto (\mu_{ee}-\mu_{gg})\frac{\mu_{ge}^2}{E_{ge}^2}$$

The two-level expressions imply that frequency doubling will be enhanced near resonance either of the single photon or the two photon type, or by increasing the "allowedness" or charge-transfer character of the important transition.

The validity of the two-level approximation is best illustrated by analyzing the relationship between measured values of β and λ_{max} ($1/\Delta E_{gn}$)[56,286] as shown in Figure 15. From the para-substituted benzene and 4,4'-disubstituted stilbene data included in Figure 15, lower energy transition energies directly correlate with enhanced second-order responses. Unfortunately, many applications of high-$\chi^{(2)}$ materials (such as optical storage),[287,288] require visible transparency and have led
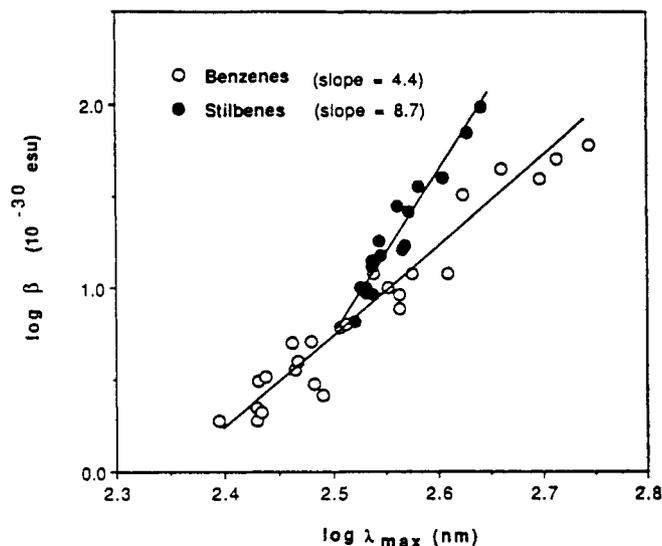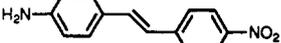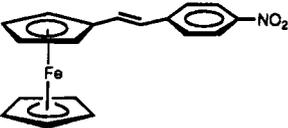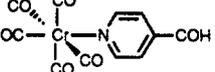
Figure 15. Logarithmic plot of β versus λ_{max} for *para*-substituted benzenes (1) and 4,4'-disubstituted stilbenes 2. (Reprinted from ref 56. Copyright 1991 American Chemical Society.)

Table 14. Comparison of ZINDO-Derived Two-Level Parameters for four Representative Chromophores[a]

chromophore	β_{vec}	λ_{max} (nm)	$\Delta\mu$ (D)	f
H₂N—⟨⟩—NO₂	10.7	317	11.9	0.48
H₂N—⟨⟩—CH=CH—⟨⟩—NO₂	46.4	375	14.9	1.19
(ferrocenyl)—CH=CH—⟨⟩—NO₂	30.8	354	14.2	0.90
OC—Cr(CO)₄—N⟨⟩—COH	−15.5	401	−17.3	0.21

[a] All NLO data are in units of 10^{-30} cm⁵ esu⁻¹ and were calculated at 1910 nm ($\hbar\omega = 0.65$ eV).

to a hitherto unsuccessful search for high-β chromophores that do not absorb in the visible range.

The two-level model has proven valuable for analyzing responses calculated within the SOS formalism. The virtues and shortcomings (in an NLO sense) of hypothetical structures can be assessed by identifying the crucial charge-transfer transition, analyzing it in detail, and comparing it to analogous excitations in molecules displaying optimal response characteristics. For example, the relevant two-level parameters of p-nitroaniline and 4-amino-4'-nitrostilbene as computed by ZINDO-SOS are provided in Table 14. Note that all three of the crucial variables of the charge-transfer transition ($\Delta\mu$, f, λ) are substantially greater in the stilbene relative to the phenylene chromophore, thus it is not surprising that the second-order response is much greater for the stilbene (46.4×10^{-30} cm⁵ esu⁻¹ versus 10.7×10^{-30} cm⁵ esu⁻¹). It was precisely this sort of analysis that allowed Kanis, Ratner, and Marks[200] to conclude that the modest $\Delta\mu$ and f parameters associated with most organometallic chromophores results in small β values for many transition metal
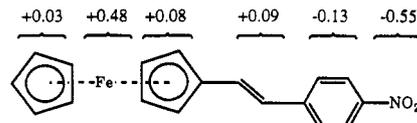

Figure 16. The differences in electronic populations between ground state and crucial excited state for *trans*-1-ferrocenyl-2-(4-nitrophenyl)ethylene (8) as determined by ZINDO calculations. A negative population reflects an increase in electron density in the charge-transfer process. (Reprinted from ref 200. Copyright 1992 American Chemical Society.)

containing structures.[200]

Another instructive analysis of the NLO-dictating charge-transfer transition can be performed by probing the change in charge density from ground state to excited state. For example, the computed ZINDO-SOS second-order response for *trans*-1-ferrocenyl-2-(4-nitrophenyl)ethylene (8) (30.8×10^{-30} cm⁵ esu⁻¹) compares favorably with experiment (31×10^{-30} cm⁵ esu⁻¹); a low-lying MLCT transition dominates the SOS expansion for β.[200] In Figure 16, the details of the important charge-

8
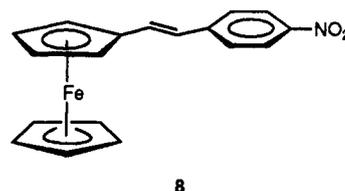
transfer excitation in 8 are illustrated through the change in electron density between the ground and excited states. Note that the predominant source of electrons in the charge-transfer process is the ferrocene group and the electron sink is the NO₂ acceptor, thus the dominating transition is labeled MLCT. Using this sort of analysis, Kanis and collaborators[200] confirmed that a ferrocenyl moiety is essentially identical in its nonlinear optical influence to a methoxyphenyl group.

The simplified two-level picture can be used to understand the sign of β. The first hyperpolarizability is usually measured and computed to be positive; however, a few important examples of negative responses are known. If the two-level picture holds for negative β-chromophores, only the $\Delta\mu(\mu_e - \mu_g)$ term can afford a negative value. The relationship between the computed ground state and excited state dipole moments and the measured responses for three representative chromophores is shown in Figure 17. For the prototypical $+\beta$ molecule (7, 4-(dimethylamino)-4'-nitrostilbene), the excited-state dipole moment is greater than and aligned in the same direction as the ground-state dipole moment. This reflects the relative stability of aromatic conjugation (ground state) relative to quinoidal structures (excited state). The electron density in the ground state is weakly biased toward the π-acceptor ($\mu_g = +9.85$ D), but heavily localized on the acceptor in the excited state ($\mu_e = +23.5$ D) resulting in a *positive* $\Delta\mu$ (13.6 D).

In special molecules, such as 4-[2-(1-methyl-4-1H-pyridinylidene)ethylidene]-2,5-cyclohexadiene-1-one (9), the nonpolar (merocyanine) architecture is found to be the ground state in apolar solvents.[289,290] However, in polar media the aromatic resonance structure (10) can be stabilized relative to the quinoidal structure.[289–291] The hypsochromic shift of the predominant $\pi \rightarrow \pi^*$

$$\mu_g \xrightarrow{+9.85\,D} \qquad \mu_g \xrightarrow{+22.6\,D} \qquad \mu_g \xleftarrow{+7.84\,D}$$

$$\mu_e \xrightarrow{+23.5\,D} \qquad \mu_e \xrightarrow{+13.7\,D} \qquad \mu_e \xleftarrow{-10.5\,D}$$

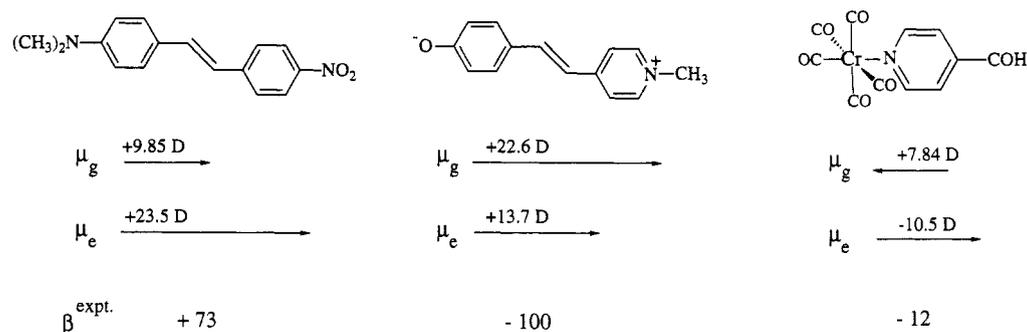$$\beta^{\text{expt.}} \qquad +73 \qquad\qquad -100 \qquad\qquad -12$$

Figure 17. Schematic diagram of three prototypical chromophores representing the conventional two-level situation (positive second-order response), and two atypical mechanisms that result in negative second-order responses. The experimentally-derived sign of β can be understood by analyzing the relative sign and magnitude of the ground- and excited-state dipole moment vectors. The dipole moment data is that computed with ZINDO, the β numbers are literature values in units of 10^{-30} cm^5 esu^{-1}. Note that β^{expt} of the organometallic chromophore was measured on the tungsten analogue.

excitation (negative solvatochromism) observed for the merocyanine chromophore pictured (in polar solvents) provides strong evidence that the zwitterionic resonance structure accurately describes the molecular ground state in highly polar solvents.[289] Obviously such a polar ground state possesses a greater dipole moment (μ_g = +22.6 D), relative to the neutral excited state (μ_e = +13.7 D), giving a *negative* $\Delta\mu$ (−8.9 D). If the contribution from this particular excitation over-whelmed all other contributions in the SOS formalism, the two-level model would predict that a negative second-order response would be measured. As shown in Figure 17, a negative β-value (−100 × 10^{-30} cm^5 esu^{-1}) is measured in methanol,[292] in accordance with pre-dictions of the two-level model.
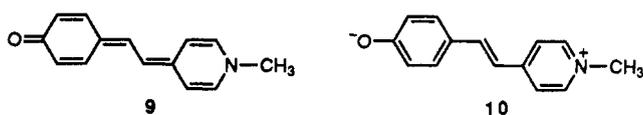
Negative solvatochromic behavior,[293] as well as neg-ative β-NLO responses[294] are also observed for orga-nometallic chromophores of substituted (pyridine)W-(CO)$_5$. As displayed in Figure 17, for example, the EFISH-derived β_{vec} value of (4-formylpyridine)W(CO)$_5$ is −12 × 10^{-30} cm^5 esu^{-1}. The two-level model also provides insight into the negative response of this structure. In contrast to the first two chromophores in Figure 17, the ground-state dipole moment of the inorganic compound is dominated by the σ-framework, specifically, the donation of lone pair of σ electrons from the pyridinyl nitrogen into a vacant metal d orbital.[271] The β-determining MLCT is described as a metal d$_\pi \rightarrow$ pyridine ligand excitation process, where the excited state is localized on the aldehyde acceptor moiety. Clearly then, the dipole vectors of the ground state and excited state are antiparallel, resulting in the negative solvatochromic behavior of the MLCT and the negative second-order susceptibility. This fasci-nating correlation between characteristic solvatochro-mic behavior and the second-order susceptibility is further evidence supporting the qualitative two-level model. In fact, some researchers choose solvatochromic experiments of CT transitions over labor-intensive EFISH measurements to screen large numbers of potential chromophores for NLO activity.[287,295]

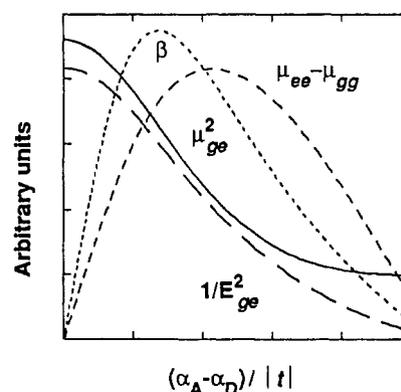Several research groups have tried to identify mol-ecules with potentially optimal nonlinearities through

$$(\alpha_A - \alpha_D) / |t|$$

Figure 18. The dependence of two-level parameters (μ_{ee} − μ_{gg}, μ_{ge}^2, and $1/E_{ge}^2$) and β versus $(\alpha_A - \alpha_D)/|t|$ as derived from a four-site Hückel model (donor, acceptor, two bridge orbitals). The coupling between the bridge and atoms is t and coupling between the bridge and end atoms is $0.8t$. The definition of the strength of the acceptor (α_A) and the donor (α_D) in this model is given in ref 21. Physically, strong donors/acceptors are on the left, weak donors/acceptors are on the right. (Reprinted from ref 21. Copyright 1992 American Association for the Advancement of Science.)

the two-level model. For example, Marder et al.[21,201-203] used a four-site Hückel model to examine how each of the two-level parameters varies with the electron-donating and electron-accepting abilities of appended substituents (Figure 18). The β responses derived from this model were not optimized with maximal electronic asymmetry, but with some asymmetry unique to a given bridge structure. The maximum was due to the behavior of $\Delta\mu$. Their conclusion from this work is that tuning the amount of quinoidal character in a largely aromatic ground state should permit one to find an optimal $(\alpha_A - \alpha_D)/t$ value that optimizes β.

In a similar vein, Yoshimura[185-187] has examined the spatial requirements of ground- and excited-state wavefunctions required to amplify the numerator of the two-level contribution ($r_{gn}^2\Delta r$). As shown sche-matically in Figure 19, β is optimized not when the two states are fully delocalized or localized, but at some intermediate point where there is nonnegligible overlap between the two states. In accord with the work of Marder et al.,[21,201-203] Yoshimura concludes that com-plete charge separation (i.e. wavefunction localization) will not lead to optimal responses. Further analysis of molecular orbitals near the Fermi surface (presumably as representations for ground → excited state transi-

$$\beta \ \propto \ r_{gn}^{2} \ \Delta r$$

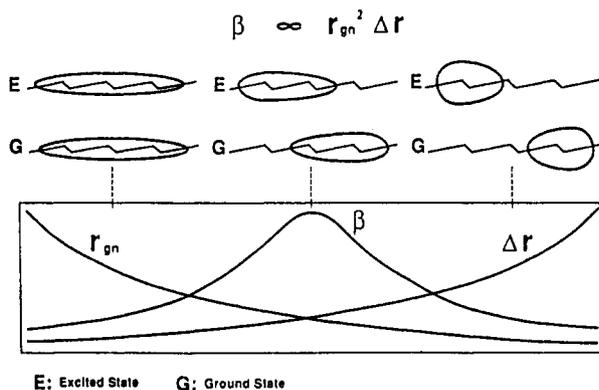E: Excited State   G: Ground State

Figure 19. A phenomenological diagram describing the charge separation necessary for obtaining optimal second-order responses. (Reprinted from ref 186. Copyright 1989 American Institute of Physics.)

tions) reveals that overlap between the molecular HOMO and LUMO in the bridging region is necessary for obtaining very large second-order responses in push/pull polyenic architectures.[187]

Related two-state models have also been described in the literature.[296,297] A conclusion from one of these studies[296] is particularly relevant to our discussion, namely, that for conventional polyene chromophores, simply changing the donor/acceptor substituents will never allow one to satisfy the high-β, high-visible transparency requirements of these materials.

C. Quantitative Two-Level Picture

The quantitative two-level picture differs from its qualitative counterpart in that the computed response is partitioned into specific contributions, rather than simply assuming one particular state is responsible for the calculated value of β. While the qualitative two-level picture has proven to be extremely useful in searching for new chromophores and interpreting NLO response computations, the convergence plots in Figure 8, parts a–d, suggest that the two-level model cannot be quantitatively correct within the context of NLO SOS computations. Specifically, the curves generally possess a distinctive maximum arising from a single state (two-level state) followed by a steep decline to approximately half the maximum value at convergence. These characteristic features are not unique to these molecules; in fact they are representative of all but a handful of chromophores examined in our laboratories. As pointed out in an earlier contribution, the computed response typically declines through so-called three-level mechanisms.[200,298,299]

Formally, the terms in eq 31 include three-level-type terms (enclosed in first braces of eq 31) in addition to the two-level contributions (enclosed in second braces of eq 31) described above. Each two-level component in the sum for $\beta_{ijk,2}$ contains only two states, the ground state, g, and one excited state, n. As shown by the diagrammatic representation of the two-level process (Figure 20), the first photon couples n with the ground state through r_{gn}, the second photon mixes n with itself via Δr_n, and the third couples n with g through r_{gn}. If one of these terms dominates the other two-level contributions, the two-level summation collapses into eq 10.

The three-level contributions in eq 31 involve a ground state and two excited states, n and n'. The first
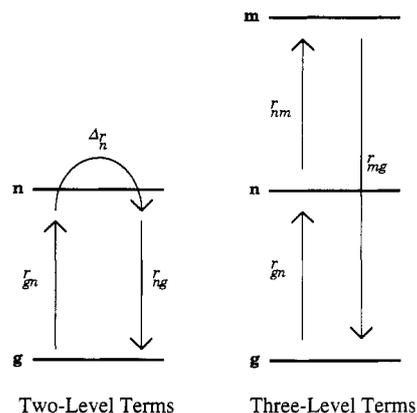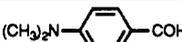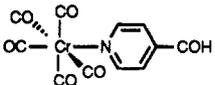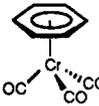

Two-Level Terms   Three-Level Terms

Figure 20. Diagrammatic representations of the two-level and three-level contributions to the second-order susceptibility. (Reprinted from ref 200. Copyright 1992 American Chemical Society.)

photon couples g with n through r_{gn}, the second photon magnitude mixes n with n' through $r_{nn'}$, and the third connects n' with g via $r_{n'g}$ (Figure 20). Since detailed information on excited state-to-excited state transitions ($r_{nn'}$) is not currently available for most chemical systems, a qualitative, chem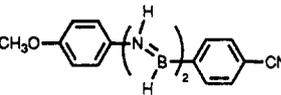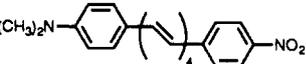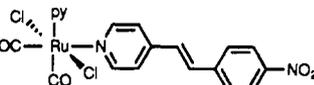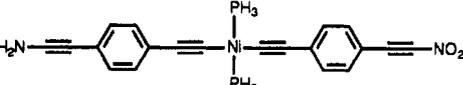ically-oriented description of these three-level expressions is not immediately evident. However, one might naively assume that the magnitude of $\beta_{vec,3}$ is significantly less than that of $\beta_{vec,2}$. Most chromophoric structures possess only one highly-allowed electronic transition in the visible or near-UV spectral region; that is, if r_{gn} is large, $r_{gn'}$ must necessarily be small. The product of $r_{gn}r_{nn'}r_{n'g}$ (generic three-level expression) should then be significantly less than $r_{gn}\Delta r_n r_{ng}$ (generic two-level expression) for most non-linear chromophoric structures. However, a ZINDO-SOS analysis[299] reveals that many n' states can efficiently couple to a given n through large $r_{nn'}$ integrals. Characteristically, the three-level contributions sum to roughly 50% as much as the two-level contributions and are of opposite sign as shown in Table 15 for several representative organic and organometallic molecular structures. The ratio of $\beta_{vec,2}/\beta_{vec,3}$ for these 14 structures ranges from -1.3 to -3.2, a fairly consistent trend. As displayed in Table 15, this empirical relationship holds for both positive and negative β molecules. The data presented in Table 15 also suggest that for most molecules, the two-level contribution is largely derived from one excited state in the SOS expansion, for complex molecules this percentage may be as low as 65%, for less intricate structures can approach 90%. Thus, the characteristic steep incline in basis set plots (Figure 8, parts a–d) can be universally described as follows: the maxima in the plots can be attributed to a two-level contribution from one charge-transfer state and the decline of computed β due to three-level contributions. Simple arguments based on Hückel-type, three-site models can be used to justify this behavior, but it also serves as an empirical criterion for the convergence properties of sum-over-states calculations.[299]

Since the three-level terms are nonnegligible in these β_{vec} results and there is no chemically-oriented model available to rationalize the $\beta_{vec,3}$ contributions, how then can we rationalize the β_{vec} values in familiar chemical terms? The empirical answer lies in the relative magnitudes of the three-level versus two-level contri-

Table 15. Relative Contributions of Two-Level ($\beta_{vec,2}$) and Three-Level Terms ($\beta_{vec,3}$) to the Quadratic Hyperpolarizability (β_{vec}) for a Variety of Molecular Chromophoric Units as Calculated by ZINDO-SOS (Also Included Is the Percentage (State %) of $\beta_{vec,2}$ Comprised of One Dominant Excitation and the Predominant CI Mixing Coefficient (C_{CI}) for One Filled Orbital → Empty Orbital Excitation)[a,b]

chromophore	β_{vec}	$\beta_{vec,2}$	$\beta_{vec,3}$	$\beta_{vec,2}/\beta_{vec,3}$	state %	C_{CI}
$(CH_3)_2N$—C$_6$H$_4$—COH	6.7	9.6	-2.9	-3.3	100	0.96
Cr(CO)$_5$—pyridine—COH	-11.4	-24.0	12.6	-1.9	73	0.97
(arene)Cr(CO)$_3$	-1.3	-2.4	1.1	-2.2	60	0.77
H_2N—anthracene—CN	11.8	31.6	-19.8	-1.6	86	0.90
CH_3O—fluorene—NO_2	14.6	34.6	-20.0	-1.7	81	0.92
CH_3O—C$_6$H$_4$—CH=CH—C$_6$H$_4$—CN	8.8	19.4	-10.6	-1.8	84	0.98
H_2N—C$_6$H$_4$—N=N—C$_6$H$_4$—NO_2	31.4	67.7	-36.3	-1.9	88	0.87
H_2N-pyrrole-pyrrole-NO_2	40.3	69.0	-28.7	-2.4	93	0.95
$(CH_3)_2N$—C$_6$H$_4$—C≡C—C$_6$H$_4$—NO_2	30.4	77.9	-47.5	-1.6	80	0.80
ferrocenyl—CH=CH—C$_6$H$_4$—NO_2	30.8	71.8	-41.0	-1.8	76	0.77
CH_3O—C$_6$H$_4$—(N=B)$_2$—C$_6$H$_4$—CN	4.7	8.3	-3.6	-2.3	61	0.71
$(CH_3)_2N$—C$_6$H$_4$—(CH=CH)$_4$—C$_6$H$_4$—NO_2	81.2	232	151	-1.5	86	0.77
Ru(CO)(py)(Cl)$_2$—pyridine—CH=CH—C$_6$H$_4$—NO_2	-12.4	-24.0	11.6	-2.1	65	0.85
H_2N—C≡C—C$_6$H$_4$—C≡C—Ni(PH$_3$)$_2$—C≡C—C$_6$H$_4$—C≡C—NO_2	26.2	128	-102	-1.3	75	0.74

[a] All NLO data are in units of 10^{-30} cm^5 esu^{-1} and were calculated at 1910 nm ($\hbar\omega$ = 0.65 eV). [b] Unpublished data.

butions. The *sum of the three-level terms is found to scale approximately as the sum of the two-level terms in nearly all organic and organometallic molecules examined to date*, as shown in Table 15 for several prototypical chromophoric units. It has been proposed,[200] therefore, that a qualitative description of the nonlinear optical response can be gleaned from analyzing the charge-transfer states contributing to two-level terms of the quadratic hyperpolarizability, even though the $\beta_{vec,3}$ contributions are nonnegligible. Perhaps a key question in the future concerns the nature of the relative contributions of the two- and three-level contributions. Is it generally correct or merely fortuitous? If the latter is true, one wonders if the high-β,

visible transparency dilemma could be circumvented by identifying molecular units with very large $\beta_{vec,3}$ contributions and somewhat less-than-optimal $\beta_{vec,2}$ values. This concept is currently under investigation.

To put this issue in further perspective, we focus on the 4-methoxy-4'-nitrostilbene chromophore (11). The

CH_3O—C$_6$H$_4$—CH=CH—C$_6$H$_4$—NO_2
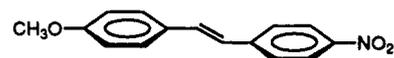
11

ZINDO-SOS computed response of 34.2 × 10^{-30} cm^5 esu^{-1} is in excellent agreement with the experimental values[56] of 28.0 × 10^{-30} cm^5 esu^{-1} in p-dioxane and 34.0

+0.07 +0.36 +0.18 -0.07 -0.54
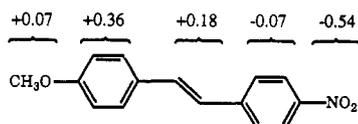
CH₃O—⟨phenyl⟩—CH=CH—⟨phenyl⟩—NO₂

Figure 21. The difference in electronic populations between ground state and crucial excited state for 4-methoxy-4'-nitrostilbene (11) as determined by ZINDO calculations. A negative population is indicative of a increase in electron density in the charge-transfer process. (Reprinted from ref 200. Copyright 1992 American Chemical Society.)

Scheme 1. Analysis of β for Molecule 11

two-level contribution ($\beta_{vec,2}$)	84.4
three-level contribution ($\beta_{vec,3}$)	-50.2
total ($\hbar\omega = 0.65$ eV)	34.2

(β_{vec} in units of 10^{-30} cm⁵ esu⁻¹)

Assumption 1. Three-level terms scale as two-level terms. Therefore, understanding two-level terms will provide qualitative understanding of β.

86% of the total two-level contribution comes from one two-level term involving a transition at 363 nm with an oscillator strength of 1.17.

Assumption 2. Two-level contribution is dominated by one excited state. Therefore, understanding this excited state will provide qualitative understanding of β.

$\Psi_{excited\ state} = 0.91\ \Phi_{4a \to 5a}$

where 4a is a filled orbital

and 5a is an unfilled orbital.

Assumption 3. The β-determining excited-state transition is dominated by one transition between molecular orbital configurations as dictated by the ZINDO CI coefficients. A description of this transition will lead to a chemical interpretation of β.

× 10^{-30} cm⁵ esu⁻¹ in chloroform. Note that the ZINDO-derived ratio of $\beta_{vec,2}$ to $\beta_{vec,3}$ is -1.7 (Scheme 1) for this molecule, in accord with the findings of other computations (Table 15). From the data in Scheme 1, one low-lying charge-transfer excitation is primarily responsible (86%) for the two-level contribution (λ^{calc} = 363 nm; λ^{expt} (dioxane) = 364 nm, λ^{expt} (chloroform) = 370 nm),[56] and the electronic details of this state can be appreciated from Figure 21. According to the $\Delta\rho_{ge}$ populations listed in Figure 21, the phenyl group adjacent to the methoxy moiety is the principal source of electrons in the charge-transfer transition, the nitro group serves as the primary accepting group.

D. Molecular Orbital Picture

In the detailed quantum mechanical computations employed in frequency-doubling studies, the significant excitation can be traced to prominent orbital-to-orbital transitions via configuration interaction mixing coefficients (C_{CI}).[266] Referring again to the 14 representative architectures in Table 15 and the tabulated C_{CI} coefficients, note that one transition between orbital configurations accurately ($C_{CI}^2 > 0.70$) represents the crucial state-to-state transition in most of these molecules. For π-organic chromophores, this typically involves a π bonding → π^* antibonding orbital. Thus, we have simplified the complex SOS expansion to understanding the details of one excited state, and then further reduced the problem to analyzing an occupied and unoccupied orbital. In the case of the prototypical

Table 16. ZINDO-Derived Nonlinear Optical and Linear Optical Data for Seven Representative π-Organic Chromophores (Molecules Ranked in Order of Increasing β_{vec})[a]

(CH₃)₂N—⟨phenyl⟩—CH=CH—⟨phenyl⟩—X

X	β_{vec}[b]	$D_{vec,2}$[c]	λ_{max}[d]	f[d]	$\Delta\mu$[d]	C_{CI}[e]	ϵ[f]
SO₂CH₃	15.2	0.98	347	1.3	7.0	0.94	-0.79
PCl₂	15.9	0.81	341	1.3	6.0	0.97	-0.44
SO₂F	22.9	0.95	351	1.3	9.6	0.95	-0.97
BCl₂	45.6	0.87	367	1.4	12.2	0.90	-1.39
NO₂	54.8	0.84	382	1.2	15.7	0.86	-1.39
NO	73.0	0.91	398	1.5	14.0	0.92	-1.65
N₂⁺	680	0.85	582	1.2	14.1	0.93	-5.12

[a] Excerpts of table taken from ref 266, Table III. [b] All NLO data are in units of 10^{-30} cm⁵ esu⁻¹; β_{vec} calculated at $\lambda = 1.91\ \mu m$ ($\hbar\omega = 0.65$ eV). [c] $D_{vec,2}$ is the fraction of $\beta_{vec,2}$ from one dominant excited state. [d] Calculated linear optical properties of the dominant excited state. Energy data in nanometers, dipole data in debyes. [e] The CI mixing coefficient for the dominant filled orbital → unfilled orbital transition in the dominant excited state. [f] SCF orbital energy (in eV) of the lowest unoccupied orbital in the acceptor moiety.

chromophore 11 described in Scheme 1, the principal excited state is primarily composed of a HOMO → LUMO excitation. The simplified molecular diagram of the chromophore (Figure 22) permits a detailed understanding of these important orbitals. The HOMO is largely centered on the phenyl ring adjacent to the methoxy donor, and not on the donor group itself. This is a direct consequence of the bridge HOMO being higher in energy than the π-lone pair on the OCH₃ group, as shown in Figure 22. Also note that the molecular LUMO is localized on the nitro acceptor; thus, the molecular orbital description is in complete agreement with the charge-transfer pattern of the important excited state sketched in Figure 21.

The molecular orbital picture can also be used to predict the trends in β with varying substitution patterns. Since the HOMO in most chromophores largely dictates the source of charge-transfer, and the details of the molecular LUMO govern the acceptor portion of the excitation, one can tailor the asymmetry of the electron density by tuning the energetics (SCF energies) of the appended substituents. For example, a generic molecular orbital diagram for 4-(dimethylamino)-4'-acceptor stilbene is shown in Figure 23. The energetics of the HOMO (donor end of the chromophore) remain relatively unchanged with exchange of acceptor substituents. In contrast, the LUMO is greatly affected by the accepting substituent. The more potent withdrawing substituents (NO, NO₂) possess much lower SCF energies than the weaker acceptors (SO₂CH₃, PCl₂). In Table 16 the correlation between β_{vec}^{calc}, λ_{max}^{calc}, and $\epsilon_{SCF,acceptor}$ is presented for several acceptor-derivatized stilbenes. The configuration interaction coefficients (C_{CI}) are all close to unity for these chromophores, suggesting that the molecular orbital picture is appropriate for these structures. Note that the SCF energy (ϵ_{SCF}) of the accepting fragment LUMO correlates very well with the computed responses.

The essential aim of the more complex analysis procedures is to pinpoint exactly the source of the second-order NLO response. Since the number of
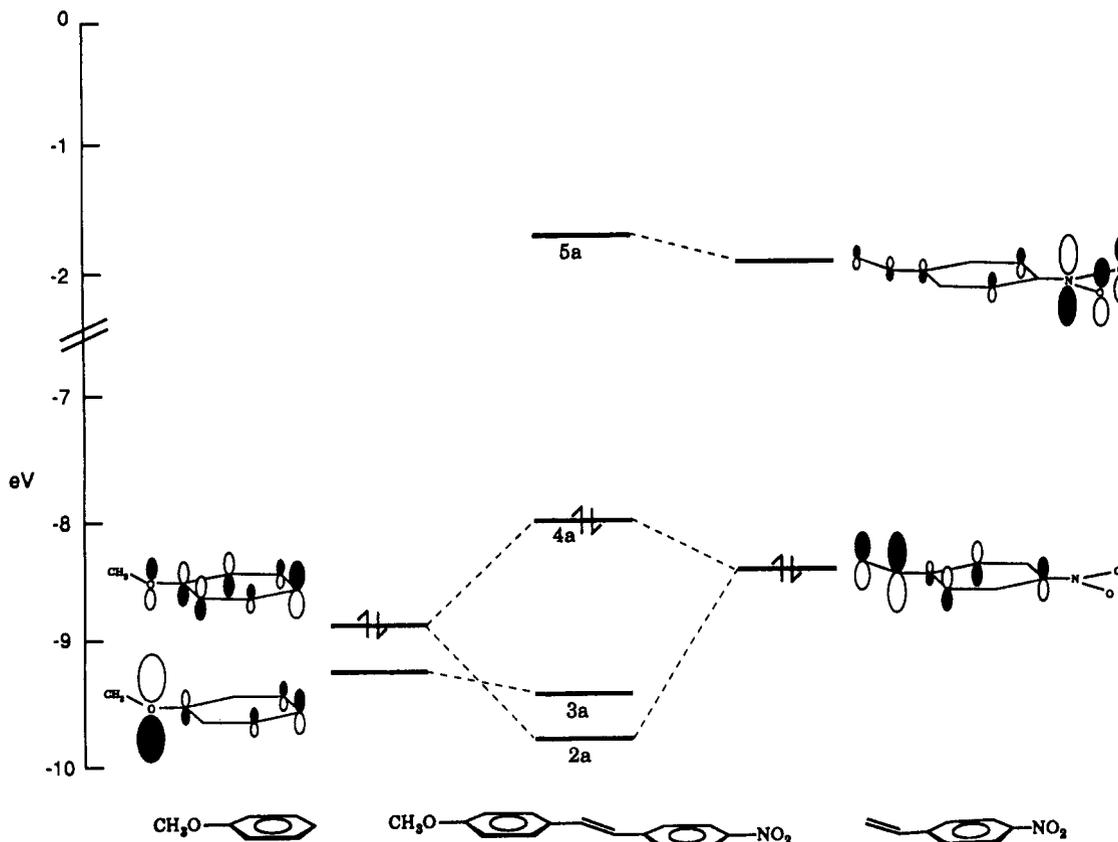
Figure 22. Molecular orbital diagram for 4-methoxy-4'-nitrostilbene (11). (Reprinted from ref 200. Copyright 1992 American Chemical Society.)
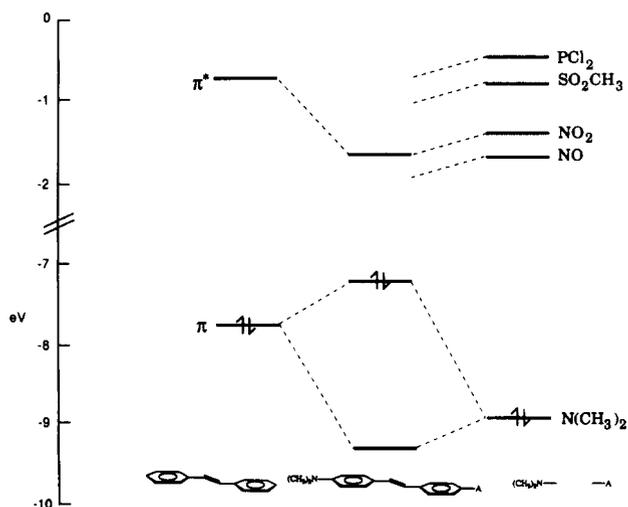

Figure 23. Generic molecular orbital diagram for 4-(dimethylamino)-4'-acceptor stilbene. Note that the donor and acceptor fragments are on the right side of the diagram, and the stilbene backbone is on the left side. Neither the stilbene nor the $N(CH_3)_2$ fragment is appreciably altered by changing the acceptor group. (Reprinted from ref 266.)

relevant states and relevant molecular orbitals is small (the valence basis is minimal), one can interpret specific excitations that enter into the sums of eq 31 and therefore suggest how modifications in the structure, based on modifications in these molecular orbitals, will affect the NLO response. Thus, these models can be effective tools that experimentalists can use to understand the responses observed, and to predict new structures with potentially optimal optical properties.

As will be stressed in the next section, *ab initio* methods differ from semiempirical ones in that extensive basis sets can be used to characterize very accurately the response of the molecular electronic charge distribution in the applied fields. For extended molecules with large β responses dominated by charge transfer, semiempirical methods should (and do) work quite well; for small species with small β values, like H_2O, CO, HF, or CH_2O, conversely the semiempirical models are very seriously in error—their use of minimal bases sets simply makes it impossible for them to describe the nonlinear response of these small electronic structures.

IV. Applications of ab Initio and Density Functional Methodologies

Ab initio calculations, generally at the Hartree–Fock CPHF level, are beginning to be used to interpret, as well as to predict, second-order NLO responses. For example, recent work by Tsunekawa and Yamaguchi[134,135] examines the origin of β in nitrogen-containing π-conjugated push/pull polyenes of the form
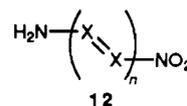
where X = CH or N and n is between 1 and 3. The computed static hyperpolarizability and dipole moment data for the $n = 1$ chromophores are displayed in Table 17. The CPHF-derived responses for the all-carbon backbones provide the largest hyperpolarizability of the four model structures **13–16**, and the response is

Table 17. *Ab Initio*-CPHF Nonlinear Optical and Orbital Energy Data for $O_2N-X=X-NH_2$ Structures[a]

	π-system	$\mu^{b,c}$	$\beta_{vec}^{b,d}$	$\epsilon(HOMO)^e$	$\epsilon(LUMO)^e$	$\Delta\epsilon^e$
13	$-C=C-$	8.13	2.06	-10.01	1.33	11.34
14	$-C=N-$	7.47	1.53	-11.02	0.91	11.93
15	$-N=C-$	7.97	0.84	-11.56	1.14	12.70
16	$-N=N-$	7.23	0.47	-12.32	0.68	13.00

[a] Excerpts of table taken from ref 135, Tables II and IV. [b] Computed with HONDO-CPHF in a 6-31G+ basis set. [c] μ is the molecular dipole moment in debyes. [d] β is the static quadratic hyperpolarizability ($\hbar\omega$ = 0.0 eV) in units of 10^{-30} cm^5 esu^{-1}. [e] Orbital energies in units of electron volts.
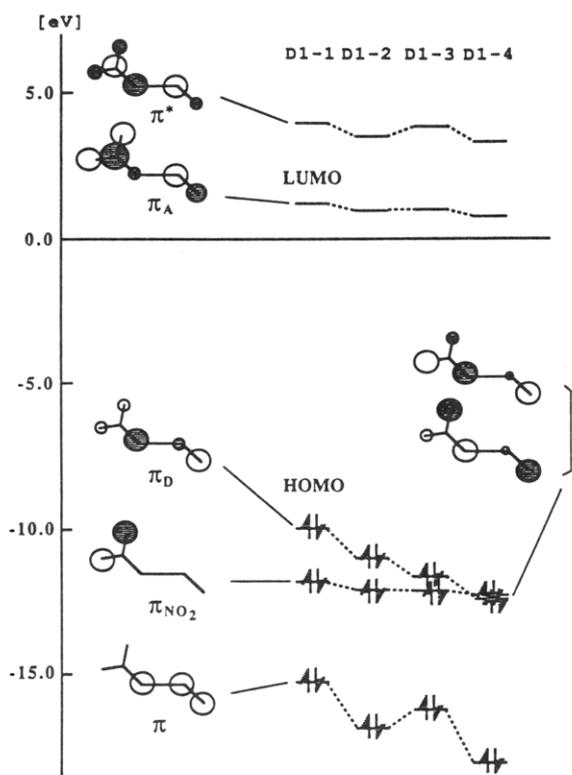

Figure 24. Changes in the energy levels (in eV) of the frontier π-orbitals of molecules **13** (D1-1), **14** (D1-2), **15** (D1-3), and **16** (D1-4). The details of this figure depict the results of *ab initio*-CPHF computations using 6-31G+1p basis sets. (Reprinted from ref 135. Copyright 1992 American Chemical Society.)

systematically lowered with each sequential substitution of a C–H unit with a nitrogen atom. Note that β decreases from 2.06×10^{-30} cm^5 esu^{-1} in the ethylene chromophore **13** to 0.47×10^{-30} cm^5 esu^{-1} in the N=N analogue **16**, and similar trends hold for the n = 2 and n = 3 structures. To understand this phenomenon in the context of a molecular orbital picture, the authors examined the molecular HOMOs (presumably the π_{donor}) and molecular LUMOs (presumably the $\pi_{acceptor}$) generated via HONDO. The results for ethylene analogues are tabulated in Table 17 and are summarized graphically in Figure 24. As shown in Figure 24, heteroatom substitution drastically lowers the energy of the molecular HOMO, while leaving the LUMO energy essentially unchanged (slight decrease in energy). Thus, the energy gap ($\Delta\epsilon$) increases with the number of nitrogen atoms in the backbone and produces a smaller β through the two-level model (eq 10). Then in a way reminiscent of an SOS-centered study, the molecules were further analyzed by calculating the three

Table 18. Optical Properties for Charge-Transfer Transition for Four Polyenic Chromophores of the Type $O_2N-X=X-NH_2$ As Computed by an RHF/6-31G/CIS Calculation[a]

	π-system	λ^b	% contribution[c]	f	$\Delta\mu^d$
13	$-C=C-$	207	92.7	0.58	4.39
14	$-C=N-$	189	86.0	0.51	4.98
15	$-N=C-$	182	72.9	0.41	3.06
16	$-N=N-$	177	84.2	0.26	1.37

[a] Excerpts of table taken from ref 135, Table V. [b] λ is the transition energy in nanometers. [c] The contribution of a single-electron excitation from HOMO to LUMO to the important charge-transfer state. The values are the square of the CI coefficients $\times$ 100. [d] The difference in molecular dipole moments (in debyes) between the ground state and charge-transfer state.

crucial two-level properties (f, $\Delta\mu_{ge}$, λ_{max}) of the lowest lying optical transition (*assumed* to be responsible for the computed response) with a RHF/CIS-level treatment. Results for the n = 1 class of chromophores are presented in Table 18. These subsequent computations confirm that the HOMO $\rightarrow$ LUMO excitation dominates the primary charge-transfer excitation (>70%) and suggests there is a direct relationship between β_{vec} and λ_{max} for not only the n = 1 frameworks, but also the n = 2 and n = 3 backbones. This contribution also demonstrates that the correlation between the ground-state dipole moment (μ) and β_{vec} is somewhat different for heteroatom versus pure carbon backbones. Specifically, high-β heterocycles have somewhat lower dipole moments than polyene chromophores of similar SHG magnitude. The authors suggest that the heterocycle chromophores, possessing smaller dipole moments, could reduce chromophore–chromophore interactions in macroscopic assemblies relative to more conventional polyenic architectures, and may, therefore, be more useful in NLO materials.

Meyers, Brédas, and Zyss[101,139,140] have reported *ab initio*-CPHF computations on a series of benzodithia **17** and dithiolene **18** polyenals, recently synthesized by Lehn's group[300,301] and exhibiting large experimental $\vec{\mu}\cdot\vec{\beta}$ values. Not surprisingly, the authors conclude that the aldehyde group serves as the electron acceptor, and the sulfur ring groups as the electron donors in all molecules examined in this study.
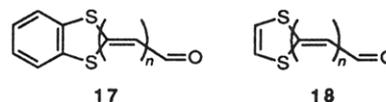
Two interesting results emerging from these calculations are the substantial changes in the directionality of β_{vec} and μ with different substitutions and the rapid rise in the predicted hyperpolarizability, compared to polarizability and dipole moment, with an increase in bond length for the dithiolene polyenals as shown in Figure 25 ($\mu\cdot\beta^{calc}$ evolves as $n^{2.9}$). The authors also point out that an EFISH measurement may not provide direct information on the first hyperpolarizability in these structures and that as the angle between the dipole moment and the vector part of β changes, it is quite dangerous to deduce a "β" value directly from EFISH—Figure 26 shows this quite directly. As this figure demonstrates, the primary charge-transfer direction (denoted by $\vec{\beta}$) is not necessarily parallel to the μ vector and therefore β_{vec} does not necessarily contain
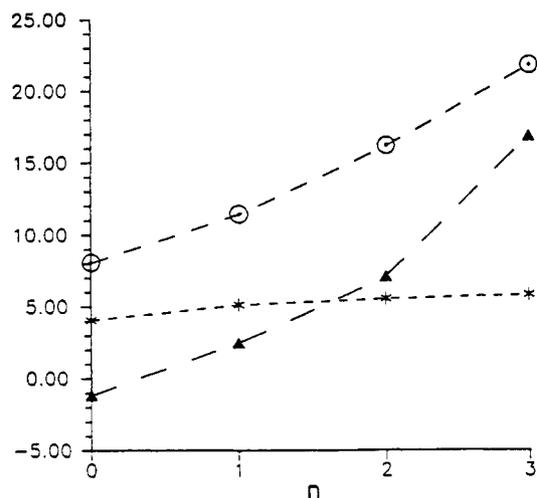
Figure 25. Evolution of CPHF-derived quantities for the dithiolene polyenals (18) with the number of ethylenic units in the polyenic segment. The dipole moment μ (debyes) is denoted by *, the average first-order polarizabilities $\langle\alpha\rangle$ (Å^3) denoted by O, and the second-order polarizabilities β_{vec} (10^{-30} $\text{cm}^5\text{esu}^{-1}$) denoted by ▲. (Reprinted from ref 101. Copyright 1992 American Chemical Society.)
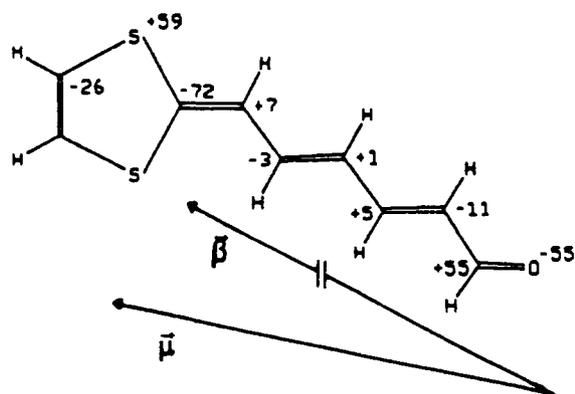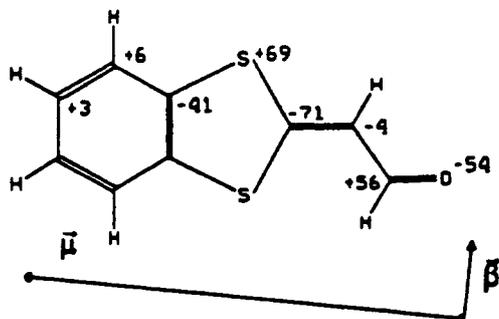

Figure 26. Atomic charges (10^{-2} e units) of two representative chromophores, with sketches of the relative orientations of the ground-state dipole moment $\vec{\mu}$ and $\vec{\beta}_{vec}$ vectors. (Reprinted from ref 101. Copyright 1992 American Chemical Society.)

the large components of the second-order tensor. This is particularly true for the benzodithia polyenal shown in Figure 26.[101] This situation is reflected in the somewhat unpredictable β_{vec} values listed in Table 19 for representative molecules. Notice in Table 19 that for the dimensionally shortest molecules, the β value is negative—this is due to charge transfer toward the donor group extremity in these small molecules. As

Table 19. Static Quadratic Hyperpolarizabilities (β_{vec} and β_{tot}) As Computed with HONDO-CPHF in a 3-21G Basis Set for a Series of Sulfur-Containing Polyenes[a,b]

n	β_{vec}	$\beta_{tot}{}^c$
Benzodithia Polyenals 17		
0	-1.57	1.57
1	0.05	1.11
Dithiolene Polyenals 18		
0	-1.19	1.19
1	0.82	1.14
2	7.06	7.52
3	16.9	17.6
Benzodithia Polyenes[d]		
1	-1.38	1.38
Dithiolene Polyenes[d]		
1	-0.12	0.12
2	1.58	1.67

[a] All NLO data are in units of 10^{-30} cm^5 esu^{-1}. [b] Tabular data taken from ref 101, Table IV. [c] Note that β_{tot} is a positive number by definition, see ref 46. [d] In the polyene chromophores, the =O functionality is replaced with a =CH_2 moiety.

the polyene path extends, the charge transfer goes in the opposite direction, and β both changes in sign and increases substantially in magnitude.

The qualitative details of the one-electron charge-transfer transition were examined through computing the energetics of the highest occupied and lowest unoccupied molecular orbitals for chromophores of various dimensions. The nature of the charge-transfer transition (presumably responsible for the second-order response) in each molecule was examined in detail using the nonempirical valence effective Hamiltonian (VEH)[302] and was confirmed with INDO/CIS computations. The authors conclude that their work "clearly illustrates the necessity to complement EFISH measurements by theoretical computations in order to reach the modulus of tensor β".

It is interesting that both the work of Meyers et al. and that of Tsunekawa and Yamaguchi used *ab initio* calculations at various degrees of rigor, but that the original insights were based upon one-electron transitions from the ground state, very similar to the SOS approach. It is therefore appropriate, in trying to understand the behavior of particular molecules or molecular series, to use both of these techniques; generally, the SOS approach used with semiempirical models permits understanding of precisely which excited states mix and how, whereas the *ab initio* models are excellent for understanding geometrical changes, dipole moment results, and quantitatively estimating the β response.

Density functional theory has become a popular alternative to more traditional *ab initio* electronic structure methods in calculating molecular properties such as ground-state geometries and force constants, molecular energies, ionization potentials, and optical transitions.[303,304] For optical response computations, the application density functional paradigms to compute molecular *polarizabilities* (α) of numerous small molecules has been reported,[305-307] however, the application of such theories to compute *hyperpolarizabilities* (β) have only recently been described.[308-311] Westin and Rosén,[308] for example, have used a sum-over-states formalism equivalent to eq 31 in concert with local density approximation (LDA) calculations

to compute the frequency-doubling response for the ionic crystals BaF_2 and CaF_2. Dixon and callaborators[309] have used LDA methods to examine both β and λ for a series of push/pull benzenes. The first extensive applications of density functional methods in NLO calculations have recently been presented by Gaun et al. (on CO, HF, H_2O, and NH_3)[310] and by Colwell and collaborators (on CH_2O and CH_3CN).[311] It is found that, sufficiently large basis sets, the density functional results are more reliable (compared with experiment) than are simple Hartree–Fock calculations with comparable basis sets. This is as expected, since density functional models incorporate correlation effects into the model Hamiltonian, whereas in standard Hartree–Fock models correlation effects must be specifically added (MP, MCSCF, CI, etc.).

V. Applications of Semiempirical Methodologies

Extensive calculations using semiempirical models have now been reported for many varieties of molecular architectures. Many of these calculations have not only determined numerical values for nonlinear response, but have also dealt with interpretation issues, specifically identifying features of the molecular geometry and the electronic structure that are responsible for the nonlinear response. Accordingly, we selectively review several illustrative studies that are representative of what can be learned from semiempirical calculations.

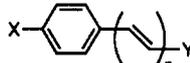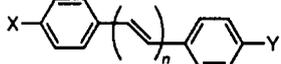## A. Dependence of Hyperpolarizability on Chain Length

An noted earlier, one anticipates an enhancement in the second-order response with an increase in π-conjugation length (L) between an electronic donor and electronic acceptor. A logarithmic relationship between L and β (or γ) is usually assumed in both experimental and theoretical studies, where the power law expression (eq 38) defines the exponential factor η and κ is a

$$\beta = \kappa L^{\eta} \qquad (38)$$

constant. Previous experimental studies on π-electron polyenic systems estimated η to be 2.1,[63] 2.4,[312] and 3.4.[313] Matsuzama and Dixon,[176] in a comprehensive FF study using the PM3 model, compared the computed values of η to observed values for a series of 4,ω-disubstituted α-phenylpolyenes and 4-4'-disubstituted α,ω-diphenylpolyenes (Table 20). Note that theory and experiment are in reasonable agreement ($1.5 < \eta_{calc} < 2.0$; $1.9 < \eta_{expt} < 3.2$), however theory consistently predicts a lower power law exponent than is determined via experiment.

A dramatic red-shift in λ_{max} is observed as additional conjugation units are added to the π-backbone.[313] However, it is generally acknowledged that the band gap in π-electron chains (long) approaches a limiting value as the chain is increased.[314,315] Within the two-level model, such a saturation in ΔE_{gn} should be reflected in a characteristic saturation of the second-order response. To date, such a saturation length has not been detected with EFISH in traditional systems such as α,ω-diphenylpolyenes (i.e. β continues to

Table 20. Coefficient of the Power Law for 4,ω-Disubstituted α-Phenylpolyenes and 4-4'-Disubstituted α,ω-Diphenylpolyenes As Computed with PM3-FF. Experimental Values Included for Purposes of Comparison[a,b]

X	Y	$\eta^{expt\ a}$	$\eta^{calc\ a}$
OCH_3	COH	3.2	2.0
$N(CH_3)_2$	COH	2.7	1.7
$N(CH_3)_2$	$C_2H(CN)_2$	2.1	1.7

X	Y	η^{expt}	η^{calc}
Br	NO_2		2.0
SCH_3	NO_2		1.5
OCH_3	CN	2.3	1.7
OCH_3	NO_2	2.0	1.9
$N(CH_3)_2$	NO_2	1.9	1.5

[a] The conjugation length L was defined as the number of ethylene units in the chromophore. [b] Tabular data taken from ref 176, Table III.

exponentially increase with L).

While enlarging the π-backbone will usually enhance the second-order response, Morley[198] has suggested that large β_{vec} values are not necessarily the parameters researchers should be seeking to optimize. Rather, the relative efficiency parameter in assessing potential NLO building blocks should be the hyperpolarizability "density" ($\rho = \beta_{vec}$/molecular volume). Obviously, molecules with large geometric dimensions must possess equally large NLO properties relative to much smaller structures if they are to be the microscopic units of choice in macroscopic NLO materials. Figure 27 shows the dependence of CNDOVSB-derived ρ on conjugation length for α-(dimethylamino)-ω-nitropolyphenylenic (19) and α-(dimethylamino)-ω-nitropolyenic (20) n-mers. This work predicts that β_{vec} will reach an optimum value in the ethylenic chromophores near $n = 20$, well beyond current synthetic capabilities. The same study predicts that the polyphenic architecture saturates in ρ at very short conjugation lengths ($n = 3$).[198]

19

20
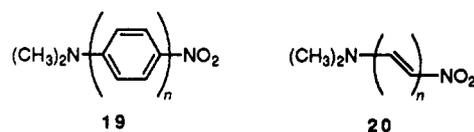
B. Double-Bonded versus Triple-Bonded Architectures

Polyyne structures, such as 21 and 22, are obvious extensions of the widely investigated polyene chromophores discussed above. ZINDO-SOS derived re-

21

22
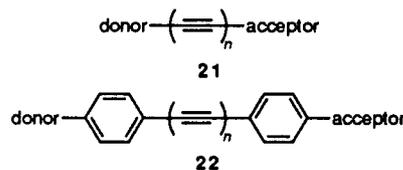
sponses for representative push/pull α,ω-diphenylpoly-

a

b

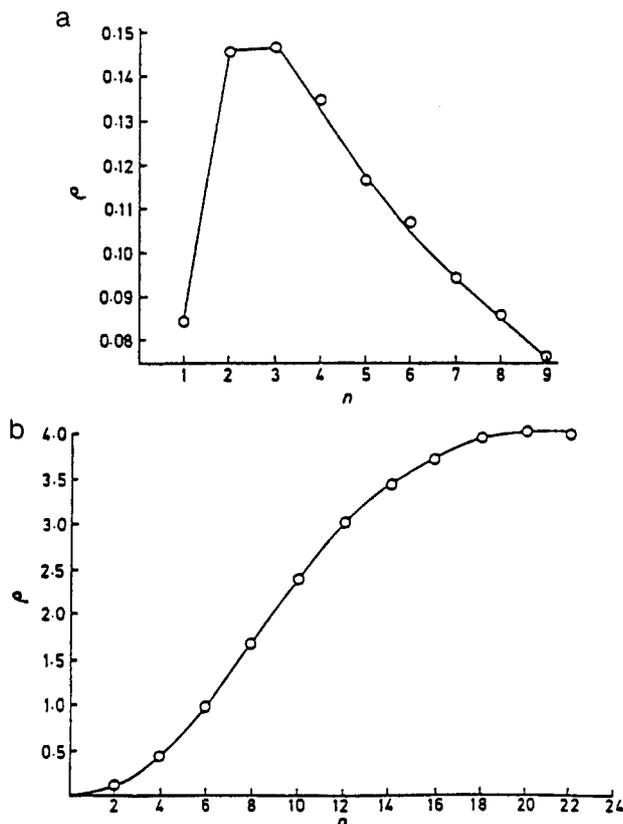**Figure 27.** Dependence of the "hyperpolarizability density" $\rho = \beta_{vec}/$(molecular volume), calculated using CNDOVSB, for the polyphenylenic structures (**19**, a) and the polyene structures (**20**, b). (Reprinted from ref 198. Copyright 1989 Royal Society of Chemistry.)

ene and analogous α,ω-diphenylpolyyne structures are displayed in Figure 28.[316] These data suggest that a single acetyleneic bridging unit yields NLO responses comparable to, or greater than, a single ethylenic unit, however, the increase in β with conjugation length (n) is much diminished relative to the corresponding ethylenic structures. It appears that α,ω-diphenylpolyyne response is in the asymptotic region after

only one bridging unit. Moreover, these results are in accord with the conclusions of other computational studies. For example, Matsuzawa and Dixon[176] computed a power law exponent (eq 38) $\eta = 0.03$–0.04 for molecules of the **22** type. Morley[254] reported that β_{vec} for push/pull polyynes (**21**; donor = $N(CH_3)_2$, acceptor = NO_2) and the corresponding polyenes (**20**) were nearly identical for $n = 1$ structures, but the responses for polyenes were three times greater for 6-mers, and 1 order of magnitude larger for 12-mers. When frequency dependence was incorporated into the computations, the differences became even more pronounced.

Recent EFISH studies provide evidence that the NLO response in polyyne architecture does indeed saturate at very short conjugation lengths. Measurements by Stiegman et al.[317] have shown that the second-order response is nearly identical for α,ω-diphenylpolyyne structures containing one- and two-bridging triple bond units. For example, β_{vec} increases from 24×10^{-30} cm^5 esu^{-1} in **23** ($n = 1$) to 28×10^{-30} cm^5 esu^{-1} in **24** ($n = 2$), far less than the relative increase observed for α,ω-diphenylpolyenes.

23

24
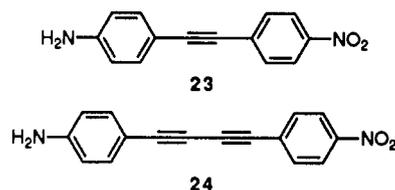
In typical polyene geometries, a single charge-transfer transition dictates the second-order response. Morley,[254] using a qualitative two-level model and a molecular orbital model, recently proposed that the early saturation of β observed in polyynes is due to additional π-electron contributions opposing (in sign) the usual charge-transfer contribution. These extra components of opposite sign are a direct consequence of having two π-electron planes in electronic bridges in diaryl acetylenes. Jain and Chandrasekhar[274] conclude that the early saturation of β in push/pull polyynes is due to configuration mixing of $\pi \rightarrow \pi^*$ transitions. Dehu,
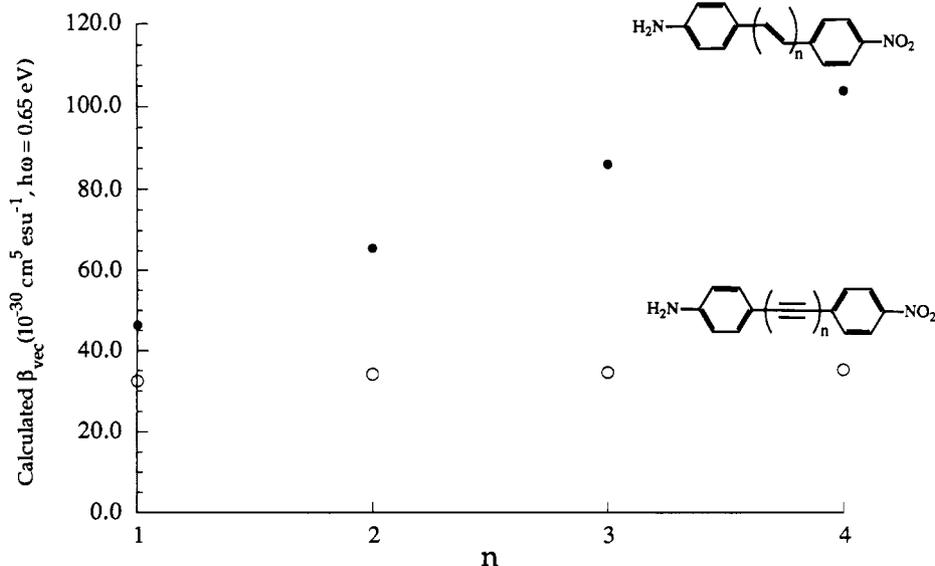

Figure 28. Computed β_{vec} (using ZINDO/SOS) for a series of polyynes (**22**, open circles) and analogous polyenes (filled circles). Note that the polyyne β does not grow with chain length. (Reprinted from ref 316).

Meyers, and Brédas[318] attribute the saturation to a breakdown in the two-level approximation as the conjugation length is increased.

The chosen input geometry is an important issue in these chromophores. Specifically, the distortion from an all-planar conformation is much more likely in a polyyne than a polyene; therefore another possible explanation for the unexpected saturation level is that a partial breaking of the charge-transfer plane is occurring as proposed by Barzoukas et al.[189] These authors conclude that a Boltzmann weighting of all possible conformations is required to adequately treat polyyne chromophores. While it is certainly true that highly-accurate NLO responses must include thermally-weighted averages of conformational geometries, approximate computations employing all-planar morphologies have been shown to provide reasonably-accurate second-order responses for this class of molecules.[198,254,316] For instance, in a MOPAC study, β as a function of torsion angle (θ) was examined and found to be a rather minor correction factor in determining the overall response.[198] Finally, crystallographic data on four polyyne structures definitively shows that chromophores such as **22** are essentially planar.[319]

C. Second-Order Response of Charged Chromophores

The widely-used β-determining measurement (EFISH) is essentially inoperable for measuring the second-order response of charged molecules. This is unfortunate, since many of the most potent electron-withdrawing substituents are cationic while many of the best donors are anionic. For example, a ZINDO-SOS study shows that the (presumably highly reactive) chromophore 4-(dimethylamino)stilbene-4'-diazonium (**25**) is calculated to possess a very large second-order response of 680×10^{-30} cm^5 esu^{-1} at 1.91 μm.[266] Theory,

25
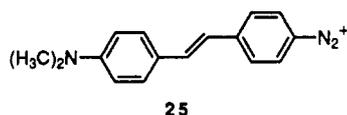
then, plays crucial role in testing and proposing potential microscopic anionic or cationic units.

One of the recent novel applications of charged chromophores is in self-assembled superlattices.[320-323] ZINDO-SOS NLO computations on molecular structures representing the active components in these materials are shown in Table 21. The ability of ZINDO to accurately compute λ_{max} for the stilbene-based (calculated, 479 nm; measured, 509 nm) and tolan-based (calculated, 466 nm; measured, 472 nm) chromophores is encouraging and supports confidence in ZINDO-level formalisms to accurately compute NLO susceptibilities for these structures. The data listed in Table 21 suggest that the inclusion of an additional ethylenic unit will nearly double the second-order susceptibility. Also of interest, the rodlike molecule containing a triple bond is computed to possess nearly the same response as the analogue with a double bond.

D. Inductive Acceptors

To date, most highly nonlinear optical second-order chromophores have been constructed by following the

Table 21. ZINDO-Derived Nonlinear Optical ($\hbar\omega$ = 0.65 eV) and Linear Optical Data for Chromophoric Superlattice Building Blocks[a-c]

β_{vec}	178	343	171
λ_{max}^{calc}	479	526	466
λ_{max}^{expt}	509		472

[a] All NLO data are in units of 10^{-30} cm^5 esu^{-1}; linear optical data in nanometers. [b] Kanis, D. R.; Ratner, M. A.; Marks, T. J. Unpublished data. [c] Experimental λ_{max} data for iodide salts in CH$_2$Cl$_2$ solution.

"π-donor linked to π-acceptor through a π-backbone" prescription. An intriguing question, however, centers around the possibility of using modifications in the "NLO-inactive" σ-framework to indirectly affect the "NLO-active" π-system. Electronegative fluorine substituents, which are weak π-donors and strong σ-acceptors, could serve as such prototypical moieties. ZINDO-SOS results strongly suggest that so-called inductive acceptors can be used to produce highly-efficient chromophores. For example, the NLO responses for 4-amino-4'-fluorostilbene (**26**) and 4-amino-2',3',4',5',6'-pentafluorostilbene (**27**) were calculated to be 7.2×10^{-30} cm^5 esu^{-1} and 23.3×10^{-30} cm^5 esu^{-1}, respectively. For comparative purposes, the ZINDO-

26   **27**
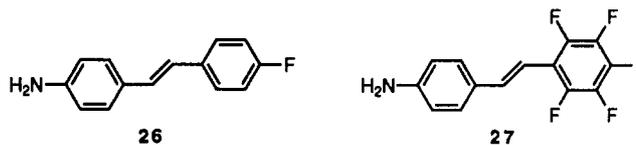
SOS β_{vec} response for 4-aminostilbene is 7.9×10^{-30} cm^5 esu^{-1}, while that containing the potent NO$_2$ acceptor 4-amino-4'-nitrostilbene (**3**) is 46.4×10^{-30} cm^5 esu^{-1}. Thus, replacing one hydrogen atom by a σ-accepting, π-donating fluorine atom has little effect upon β, however, replacing all five hydrogen atoms by fluorine atoms dramatically enhances the NLO response. One can conclude from these data that in a qualitative sense, the pentafluorophenyl acceptor group is approximately half as potent as a 4-nitro substituent, or approximately as strong as a 4-cyano acceptor. It thus appears that a multiplicity of inductive acceptors is required to strongly influence the π-framework. We should note however, that there is no experimental evidence to date supporting these conclusions.

E. Chromophores Containing Main Group Elements

Main group inorganic chromophores offer an intriguing alternative to the more conventional organic-based chromophores. One possibility is to exploit the π-acidity of inorganic group 13 fragments to serve as

Table 22. ZINDO-Derived Nonlinear Optical and Linear Optical Data for Representative Group-13 Substituted Stilbene Chromophores at 1.91 μm ($\hbar\omega$ = 0.65 eV)^{a,b}


$(CH_3)_2N$—⟨benzene⟩—CH=CH—⟨benzene⟩—A
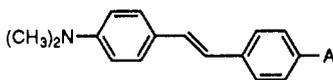
A	β_{vec}	λ_{max}
Al(CH₃)₂	25	342
BF₂	26	346
BH₂	31	351
AlCl₂	44	359
BCl₂	45	365

^{a} All NLO data are in units of 10^{-30} cm⁵ esu⁻¹; linear optical data in nanometers. ^{b} Tabular data taken from ref 268, Table II.

strong electron-withdrawing groups. In Table 22 are shown results for a series of stilbene chromophores in which the NO₂ group in high-β chromophore 7 (β_{vec} = 53.3 × 10^{-30} cm⁵ esu⁻¹) has been replaced by various group 13 Lewis acid/π-acceptor moieties. It can be seen that the substituents expected to have the greatest Lewis acidity afford predicted β_{vec} values nearly as great as for NO₂.[268]

As a second alternative, inorganic structures offer a variety of novel conjugation pathways, and Table 23 explores several. The B=N unit forms the basis for numerous π-electron structures with similarities to organic π-systems.[324,325] However, the ZINDO-derived quadratic hyperpolarizabilities for planar borazine chromophores 28 and 29 are significantly lower than

28   29
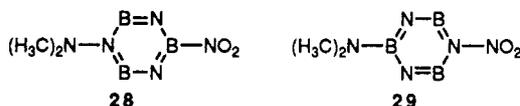
for the isoelectronic p-(dimethylamino)nitrobenzene (5). In comparing the two borazine derivatives, the larger optical nonlinearity is predicted for 28, in which the dimethylamino donor group is attached to an electron-rich nitrogen atom and the nitro acceptor group is attached to the electron-deficient boron atom. Our analysis suggests that the β_{vec}-determining transannular charge-transfer excitation in the borazine derivatives is not as strong nor as energetically accessible as the same transition in 5. Essentially, nitrogen and boron atoms in the heterocyclic ring act as localized donor and acceptor centers, respectively, thus reducing the net electron density redistributed through the ring. In contrast, the β_{vec} values for conventional organic chromophores reflect the ability of an aromatic ring or polyene backbone to act as an effective linkage between electron-rich and electron-deficient groups. In the same vein, calculations on chromophores 30–32 suggest that

30   31   32
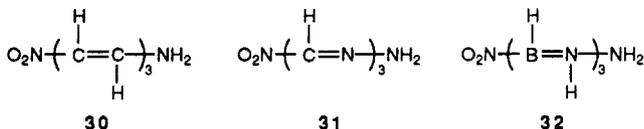
the C=N unit can also function as an efficient pathway between donor and acceptor groups, yet the isoelectronic B=N unit again displays poor delocalization characteristics as demonstrated by the predicted β_{vec} and λ_{max} values.

Table 23. ZINDO-Derived Nonlinear Optical and Linear Optical Data for Representative Inorganic Chromophores at 1.91 μm ($\hbar\omega$ = 0.65 eV)^{a,b}

	molecule	β_{vec}	λ_{max}
28		5.4	341
29		3.2	319
30		53	417
31		75	471
32		3.5	232
33		−0.4	218
34		−1.6	241
35		−1.0	197
36		−1.5	213
37		−10	287

^{a} All NLO data are in units of 10^{-30} cm⁵ esu⁻¹; linear optical data in nanometers. ^{b} Table taken from ref 268, Table III.

Calculations on chromophores 33–37 explore the possibility of using electronically saturated linkages in chromophoric structures (Table 23). The calculated β_{vec}

33   34   35

36   37
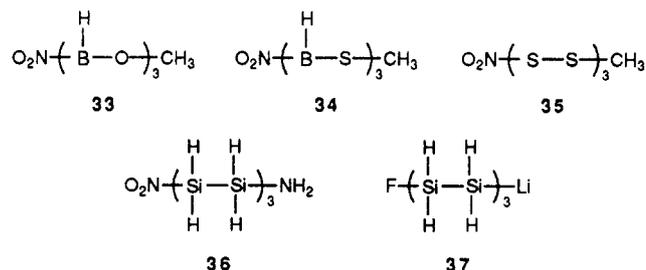
values and optical absorption wavelengths for molecules 33–35 are in accord with the low degree of electron delocalization which such structures exhibit.[326,327] In contrast, saturated polysilanes exhibit significant degrees of σ-bond electronic delocalization[328–331] and substantial nonresonant third-order optical nonlinearities.[332] Since the predominant intramolecular charge-transfer transitions in polysilanes are σ-based rather than π-based, optimal second-order nonlinearities should be obtained through σ-donor/acceptor substitution. This is confirmed by the ZINDO-derived β_{vec}

values for two all-*trans* planar polysilanes **36** and **37**, where the computed frequency-doubling efficiency for a polysilane containing π "push/pull" susbstitution (**36**) is 1 order of magnitude lower than that of a σ-donor/acceptor polysilane (**37**).

F. Organometallic Chromophores

Organometallic structures are intringuing candidates for study as NLO chromophores by virtue of their low energy, yet sometimes intense, electronic transitions.[333,334] As discussed in section III of this review, such *linear* optical characteristics are suggestive "two-level" signatures of molecules exhibiting significant *nonlinear* optical response. One can envision four generic classes of transition metal organometallic architectures which could, in principle, yield enhanced second-order nonlinear optical responses. They are (1) structures possessing spectroscopically intense metal-to-ligand charge-transfer (MLCT) or (2) ligand-to-metal charge-transfer (LMCT) excitations, (3) organometallic or classic Werner-type complexes where the metal atom-(s) act as an intermediary between an electron-donor and an electron-acceptor moiety, and (4) bimetallic compounds exhibiting a low-lying intervalence charge transfer excitation (IT band). Within classes 1 and 2, the π-ligand can be strongly coupled (type A) or weakly coupled (type B) to the metal center, leading to very different optical and nonlinear optical characteristics. Recent computational studies have examined class 1A chromophores (ferrocenyl, arene), and class 1B chromophores (group 6-pyridine, group 6-stilbazole). These contributions will be reviewed and comments on classes 2, 3, and 4 will follow.

In the late 1980s, *trans*-1-ferrocenyl-2-(*N*-methylpyridinium-4-yl)ethylene iodide[335] (**38**) and *trans*-1-ferrocenyl-2-(4-nitrophenyl)ethylene[336] (**8**) were reported to possess rather large second-harmonic generation efficiencies (220 and 62 × urea, respectively), motivating many inorganic chemists to enter this field. As a result, several contributions reporting second-order susceptibilities for organotransition metal systems have appeared in the recent literature. Such diverse architectures as metal-containing polymers,[337,338] octopolar structures,[339] classical coordination compounds,[340-363] and metallocene structures[363-378] have been investigated, and two articles have reviewed this field.[379,380] (Note that most of the NLO measurements sample $\chi^{(2)}$; however, some contributions quote β values for transition metal containing structures.[339-341,356,363,364,369,374,375]) Despite these intense research efforts, none of the measured NLO responses for metal-containing molecules have been found to surpass those observed for common π-organic push/pull topologies of comparable molecular dimensions, with the exception of a recently reported NLO response (resonant-enhanced) for a mixed-valence compound (*vide infra*).[340]

The ZINDO-SOS method has been the computational technique of choice for researchers investigating organometallic structure–NLO property relationships.[200,270,271] Hyperpolarizabilities computed with this procedure are in reasonable agreement with experiment as demonstrated for a variety of organometallic species in Figure 11.[200,270]

The electronic origin of β for two representative groups of class 1A chromophores (MLCT-based, strong-

Table 24. Comparison of Experimental and ZINDO-Derived Molecular Hyperpolarizabilities along the Dipole Moment Direction (β_{vec}) and the ZINDO-Derived Total Intrinsic Hyperpolarizability (β_{tot}) at 1.91 μm ($\hbar\omega$ = 0.65 eV) for a Series of Ferrocenyl Derivatives[a,b]
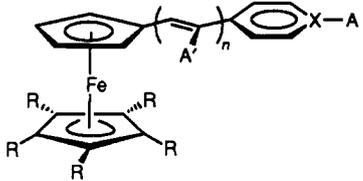
	X–A	R	A'	n	isomer	$\beta_{vec}^{expt\ c}$	$\beta_{vec}^{expt\ c}$	β_{tot}^{calc}
8	C–NO$_2$	H	H	1	E	31	30.8	30.8
39	C–NO$_2$	H	H	1	Z	13	20.7	21.0
40	C–NO$_2$	CH$_3$	H	1	E	40	34.7	34.7
41	C–CN	H	H	1	Z	4.0	5.49	5.92
42	C–CN	H	H	1	E	10	9.72	9.76
43	C–CHO	H	H	1	E	12	15.1	17.2
44	C–NO$_2$	H	H	2	E,E	66	47.4	47.5
45	C–NO$_2$	H	H	3	E,E,E		66.6	66.8
46	C–NO$_2$	H	CN	1	E	21	25.6	29.0
47	C–NO$_2$	CH$_3$	CN	1	E	35	28.4	31.9
48	C-2,4-(NO$_2$)$_2$	H	H	1	E	23	40.0	44.8

[a] All NLO data are in units of 10^{-30} cm^5 esu^{-1}. [b] Tabular data taken from ref 200, Table I. [c] NLO data for molecules 8 and 39–44 from ref 363 and for 46–48 from ref 375.

ly coupled π-systems) have been examined with theoretical techniques.[200,270] It is apparent from the ZINDO-SOS results given in Table 24 that traditional qualitative arguments (sections III.a and b) for enhancing second-order nonlinear optical responses in organic molecules are applicable to the ferrocenyl chromophores.[200] For instance, the greater the electronic asymmetry between donor (ferrocenyl) and acceptor (A) groups,[284] the larger the measured and calculated β responses. As the strength of electronic donor is increased by permethylating the cyclopentadienyl ring, an increase in both computed and observed optical nonlinearity occurs. This is illustrated by comparing a ferrocenyl derivative (**8**, 30.8 × 10^{-30} cm^5 esu^{-1}) with the corresponding permethylated analogue (**40**, 34.7 × 10^{-30} cm^5 esu^{-1}). Also, the susceptibilities of ferrocenyl derivatives are largest for molecules containing the strongest electronic acceptors, nitro (**8**) > aldehyde (**43**) $\approx$ cyano (**42**).[284] In accord with traditional organic chromophore design rules, greater electron delocalization in the ferrocenyl structures leads to enhanced second-order NLO responses. For example, as the number of connecting ethyleneic units in the organic ligand is increased from 1 (**8**) to 2 (**44**) to 3 (**45**), the calculated response increases rather dramatically from 30.8 × 10^{-30} to 47.4 × 10^{-30} to 66.6 × 10^{-30} cm^5 esu^{-1}. Lastly, the calculated response for the prototypical *cis* structure (**39**, 20.7 × 10^{-30} cm^5 esu^{-1}) is somewhat lower than that for the analogous *trans* derivative (**8**, 30.8 × 10^{-30} cm^5 esu^{-1}) in accord with conventional chromophore design wisdom. In summary, the ZINDO-derived quadratic hyperpolarizabilities confirm, in a quantitative fashion, that the ferrocenyl derivatives follow qualitative design rules that have evolved for π-electron organic chromophores. An additional electronic structural conclusion from the ZINDO-derived NLO efficiency results is that the computed inherent quadratic hyperpolarizability (β_{tot}) is essentially equal to the computed NLO response along the ground-state dipole moment direction (β_{vec}), for this

Scheme 2. Analysis of β for Molecule 8

two-level contribution ($\beta_{vec,2}$)	71.8
three-level contribution ($\beta_{vec,3}$)	-41.0
total ($\hbar\omega = 0.65$ eV)	30.8

(β_{vec} in units of 10^{-30} cm^5 esu^{-1})

Assumption 1. Three-level terms scale as two-level terms. Therefore, understanding two-level terms will provide qualitative understanding of β.

76% of the total two-level contribution comes from one two-level term involving a MLCT at 354 nm with an oscillator strength of 0.91.

Assumption 2. The two-level contribution is dominated by one excited state. Therefore, understanding this excited state will provide qualitative understanding of β.

$$\Psi_{excited\ state} = 0.50\ \Phi_{2a \to 5a} + 0.77\ \Phi_{4a \to 5a}$$

where 2a and 4a are filled orbitals

and 5a is an unfilled orbital

Assumption 3. The β-determining excited-state transition is dominated by two transitions between molecular orbital configurations as dictated by the ZINDO CI coefficients. A description of these transitions will lead to a chemical interpretation of β.

class of chromophores, and therefore β_{vec} is a good measure of the chromophore's intrinsic ability to frequency-double light.

The assumptions necessary to unravel the electronic origins of the NLO response within ZINDO-SOS for a prototypical ferrocenyl molecule (*trans*-1-ferrocenyl-2-(4-nitrophenyl) ethylene (8)) through the quantitative two-level model are shown in Scheme 2. Note that $\beta_{vec,3}$ for this molecule (-41.0×10^{-30} cm^5 esu^{-1}) is of opposite sign and approximately half the magnitude of $\beta_{vec,2}$ (71.8

$\times$ 10^{-30} cm^5 esu^{-1}) in accord with two-level model mentioned earlier. The ZINDO results indicate that one optical transition at 354 nm is primarily responsible for the two-level contribution. The calculated redistribution of electron density associated with this transition (Figure 16) suggests that the NLO-determining excitation is MLCT in nature. In the molecular orbital picture, the NLO-dominating transition is composed predominantly of 4a $\to$ LUMO and 2a $\to$ LUMO excitations, and as shown in Figure 29, the HOMO is primarily ferrocene-based and the LUMO/5a primarily acceptor-based.[200]

The ZINDO-derived mechanism for β in these structures differs only in some details with an explanation proposed by Marder, Cheng, et al.,[375] where analysis of an extended-Hückel calculation suggests that two optical transitions are responsible for the second-order response in ferrocenyl chromophores. If in fact, one excited state is primarily responsible for the observed second-order susceptibility, the ferrocene derivatives should bear strong resemblances to classic two-level systems, such as the push/pull polyenes. In Table 25, the ferrocenyl group in selected chromophores is replaced with a methoxyphenyl ($CH_3OC_6H_5$) moiety. From the results of this numerical study, it is immediately obvious that this structural transition *leaves the computed second-order response essentially unchanged*.[200] For example, the ratio of β_{vec} of the methoxyphenyl chromophores relative to their ferrocenyl analogues is 19.8/20.7 for **39**, 50.5/47.4 for **44**, and 42.7/40.0 for the dinitro derivative **48**. *Conclusion: The similarity observed in the computational studies strongly suggests a common electronic origin of the*
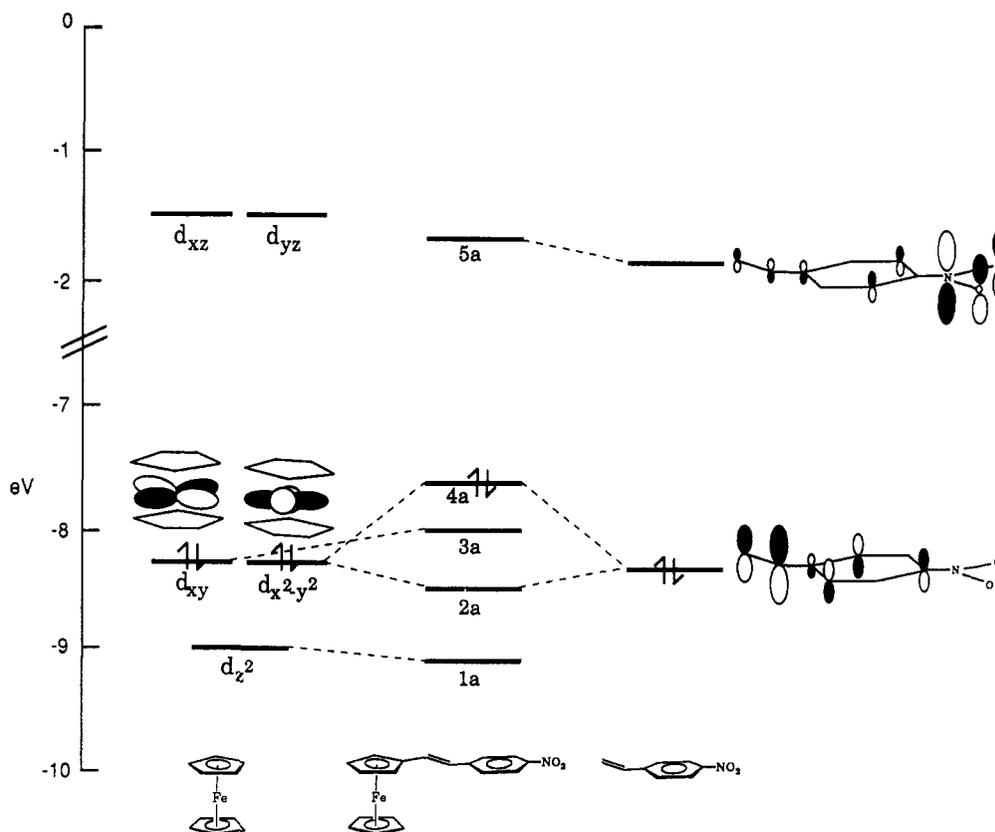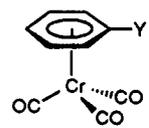

Figure 29. Molecular orbital diagram for *trans*-1-ferrocenyl-2-(4-nitrophenyl)ethylene (8). (Reprinted from ref 200. Copyright 1992 American Chemical Society.)

Table 25. Comparison of ZINDO-Derived β_{vec} Values for Ferrocenyl Derivatives and Their Methoxyphenyl Analogues[a,b]

$$X-\left(\underset{A'}{\overbrace{}}\right)_n-\left(\bigcirc\right)-NO_2$$

			β_{vec}	
A'	n	isomer	X = FeCp(C$_5$H$_4$)	X = CH$_3$OC$_6$H$_5$
H	1	Z	20.7 (39)	19.8
H	1	E	30.8 (8)	34.2
H	2	E,E	47.4 (44)	50.5
H	3	E,E,E	66.6 (45)	68.0
CN	1	E	25.6 (46)	26.8
H	1	(2,4-dinitro species)	40.0 (48)	42.7

[a] All NLO data are in units of 10^{-30} cm^5 esu^{-1} at $\hbar\omega = 0.65$ eV. [b] Tabular data taken from ref 200, Table III.

Table 26. Comparison of Experimental and ZINDO-Derived Molecular Hyperpolarizabilities along the Dipole Moment Direction (β_{vec}) and the ZINDO-Derived Total Intrinsic Hyperpolarizability (β_{tot}) at 1.91 μm ($\hbar\omega = 0.65$ eV) for Various Chromium Arene Derivatives[a,b]

$$\left(\bigcirc\right)-Y$$
$$OC\underset{CO}{\overset{Cr}{\cdots}}CO$$

	Y	$\beta_{vec}^{expt\ c}$	β_{vec}^{calc}	β_{tot}^{calc}
49	H	-0.8	-1.30	1.30
50	OCH$_3$	-0.9	-1.36	1.50
51	NH$_2$	-0.6	-1.27	1.42
52	N(CH$_3$)$_2$	-0.4	-0.91	1.12
53	COOCH$_3$	-0.7	-1.79	4.28
54	trans-styrenyl	-2.2	-3.93	4.80

[a] All NLO data are in units of 10^{-30} cm^5 esu^{-1}. [b] Tabular data taken from ref 200, Table IV. [c] Experimental data from ref 363.

nonlinear optical response in these two classes of chromophores and that the ferrocenyl group is essentially interchangeable with a methoxyphenyl donor group. The exact role (and nature) of weaker, energetically lower-lying ferrocenyl transitions in influencing β remains an open question at present.[200]

(η^6-C$_6$H$_6$)Cr(CO)$_3$-based (arene) architectures (49–54, Table 26) have also been examined with ZINDO-SOS.[200] These classic organometallic structures are symbolic of a broad range of transition metal species containing low-valent metal centers. As shown in Table 26, the ZINDO-derived susceptibilities are in excellent agreement with EFISH results. Note that the magnitude of β_{vec} for these structures is 1 order of magnitude smaller than the aforementioned ferrocenyl derivatives and 2 orders of magnitude less than the most efficient organic chromophores. As shown in Scheme 3, the two-level contributions in the arene prototype **49** are approximately twice the three-level contributions and of opposite sign in accord with observations for most chromophores. As indicated in this scheme, two transitions dictate the NLO response of **49** within the framework of the SOS formalism. The lower energy "ligand field" transition ($\lambda = 292$ nm, $f = 0.13$) comprises 20% (-0.5 × 10^{-30} cm^5 esu^{-1}) of the total two-level contribution, while a higher-energy "MLCT" excitation ($\lambda = 225$ nm, $f = 0.60$) is responsible for 60% (-1.5 × 10^{-30} cm^5 esu^{-1}) of the two-level contribution to β_{vec}.[200]
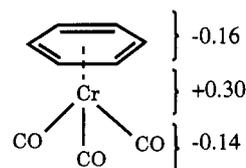
Figure 30. The difference in electronic populations between ground state and crucial excited state for C$_6$H$_6$Cr(CO)$_3$ as calculated by ZINDO. A negative population reflects an increase in electron density for the charge-transfer process. (Reprinted from ref 200. Copyright 1992 American Chemical Society.)

Scheme 3. Analysis of β for Molecule 49

two-level contribution ($\beta_{vec,2}$)	-2.4
three-level contribution ($\beta_{vec,3}$)	1.1
total ($\hbar\omega = 0.65$ eV)	-1.3

(β_{vec} in units of 10^{-30} cm^5 esu^{-1})

Assumption 1. Three-level terms scale as two-level terms. Therefore, understanding two-level terms will provide qualitative understanding of β.

60% of the total two-level contribution comes from one two-level term involving a MLCT at 225 nm with an oscillator strength of 0.60.

20% of the total two-level contribution comes from another two-level term involving a ligand–field–like transition at 292 nm with an oscillator strength of 0.13.

Assumption 2. The two-level contribution is dominated by two excited states. Therefore, understanding these excited states will provide a qualitative understanding of β.

The MLCT contribution to $\beta_{vec,2}$ in the arene is significantly less than that for the representative ferrocenyl chromophore (**49**, -1.5 × 10^{-30} cm^5 esu^{-1}; **8**, 54.5 × 10^{-30} cm^5 esu^{-1}) due to the disparity in the change in dipole moments computed for the respective MLCT transitions (**8**, 14.1 D; **49**, 1.9 D). As shown in Figure 30, significant electron density (0.30 electrons) is transferred to the π-ligands in the MLCT transition in **49**. However, the charge-transfer electron density is nearly equally divided between the carbonyl and arene ligands. As a consequence, only a modest $\Delta\mu$ is associated with this d$_\pi \rightarrow$ ligand π^* transition, and this ultimately limits the quadratic hyperpolarizability of **49**.[200]

If the pseudocentrosymmetry about the metal is removed by increasing the π-conjugation length in the organic arene ligand (**55, 57**), the microscopic response is slightly enhanced relative to chromophores **49–54**. However the susceptibilities are still significantly less than those computed for the analogous "metal-free" ligands (**56, 58**) as shown in Table 27.[200] For example, the computed β_{tot} for the $n = 3$ metal-free arene (**58**, 57.9 × 10^{-30} cm^5 esu^{-1}) is significantly enhanced relative to the Cr(CO)$_3$-coordinated chromophore (**57**, 34.5 × 10^{-30} cm^5 esu^{-1}). From detailed analyses of these representative structures, it is clear that the inherent responses (β_{tot}) in Cr(CO)$_3$-substituted organic structures are lower than their metal-free organic analogues by virtue of the modest $\Delta\mu$ values associated with the dominant charge-transfer excitation. Essentially, the CO ligands are π acceptors which reduce the donating strength of the d$_\pi$ orbitals in the chromium arene chromophores. Therefore, even very asymmetric metal–arene structures are not nearly as asymmetric as conventional organic structures.[200] In addition, the

Table 27. ZINDO-Derived Dipole Moments, Molecular Hyperpolarizabilities along the Dipole Moment Direction (β_{vec}), and ZINDO-Derived Total Intrinsic Hyperpolarizabilities (β_{tot}) at 1.91 μm ($\hbar\omega = 0.65$ eV) for Hypothetical Chromium Arene Derivatives and the Corresponding Free Ligands^{a-c}
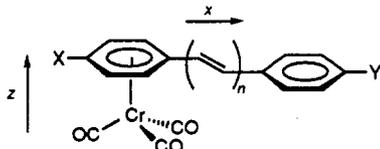
|	X	Y	n		β_{vec}^{calc}	β_{tot}^{calc}	μ_x^{calc}	μ_z^{calc}
55	H	NO$_2$	1	Cr	8.3	23.5	−6.6	8.4
56	H	NO$_2$	1		27.5	27.5	−7.5	0.0
57	H	NO$_2$	3	Cr	15.6	34.5	−6.8	8.6
58	H	NO$_2$	3		57.6	57.9	−8.1	0.0

^{a} All NLO data are in units of 10^{-30} cm^5 esu^{-1}; all dipole moment data in units of debyes. ^{b} A "Cr" designation indicates that the chromophore contains a Cr(CO)$_3$ moiety in the indicated position, no designation is indicative of a metal-free ligand. ^{c} Tabular data taken from ref 200, Table VI.

noncoincidence between the ground-state dipole moment (x,z components) and the charge-transfer (x component only) directions dictates that significant portions of the modest second-order responses (i.e. β_{vec} $\ll$ β_{tot} values) will not be sampled with EFISH nor will conventional poling techniques achieve optimum $\chi^{(2)}$ values for polymer matrices containing these chromophores.[200]

Until recently there existed no experimental evidence supporting the claim that coordinating a Cr(CO)$_3$ fragment will actually decrease the response relative to the isolated π-ligand. Recent work by Gilbert and collaborators[381] measured β_{vec} of **55** (10.5 × 10^{-30} cm^5 esu^{-1} versus a computed response of 8.3 × 10^{-30} cm^5 esu^{-1}) and measured the second-order response of an X = N(CH$_3$)$_2$ derivative to be 10.5 × 10^{-30} cm^5 esu^{-1} in excellent agreement with the previously published response for the related X = NH$_2$ species of 10.7 × 10^{-30} cm^5 esu^{-1}.[200] Kanis, Ratner, and Marks[200] conclude that the small $\Delta\mu$ values associated with the MLCT excitations should be representative of many organometallic chromophores where the metal is strongly coupled to the organic ligand (class 1A). This can be seen by noting that the ligands surrounding a metal center usually reflect the electronic characteristics of the metal center. Hard ligands (NH$_3$, H$_2$O, oxides) are preferentially coordinated to highly-oxidized metal centers, while soft ligands (CO, CN, C$_6$H$_6$) prefer reduced centers. In a low-valent environment, for example, the degree of π-basicity can be varied to create a somewhat asymmetric environment; however, substituting one soft base for another will only lead to small $\Delta\mu$ values and modest NLO responses. To truly destroy the electronic pseudosymmetry about a metal center, hard ligands must be coordinated opposite soft ligands about the metal.

To test this hypothesis, ZINDO-SOS computations were carried out on chromophores **59** and **60**, two structures that should possess very acentric metal centers. In **60** the three labile amine ligands present in **59** are replaced with a tridentate amine ligand. While both of these structures are strictly hypothetical, they illustrate the point: the ZINDO-derived hyperpolarizability responses ($\hbar\omega = 0.65$ eV) are 780 × 10^{-30} cm^5

Table 28. Comparison of Experimental and ZINDO-Derived Molecular Hyperpolarizabilities (β_{vec}), Two-Level Contributions to the Response ($\beta_{vec,2}$), and Three-Level Contributions ($\beta_{vec,3}$) to the Response at 1.91 μm ($\hbar\omega = 0.65$ eV) for a Series of Group 6 Pyridine Derivatives^{a-c}
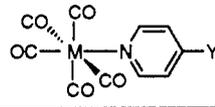

	Y	$\beta_{vec}^{expt\ d}$	β_{vec}^{calc}	$\beta_{vec,2}^{calc}$	$\beta_{vec,3}^{calc}$
61	NO$_2$		−31.8	−50.8	19.0
62	COH	−12	−15.5	−29.2	13.7
63	COCH$_3$	−9.3	−13.3	−25.1	11.8
64	C$_6$H$_5$	−4.5	−4.49	−9.35	4.86
65	H	−4.4	−5.91	−10.4	4.51
66	C$_4$H$_9$	−3.4	−3.98	−12.7	8.74
67	NH$_2$	−2.1	−1.32	−3.24	1.92

^{a} All NLO data are in units of 10^{-30} cm^5 esu^{-1}. ^{b} Note that M = Cr for all computed responses and M = W for all EFISH values. ^{c} Tabular data taken from ref 271. ^{d} Experimental data for transition metal chromophores from ref 356 and 363.

esu^{-1} and 543 × 10^{-30} cm^5 esu^{-1} for **59** and **60**, respectively; both are very large values for β. The Cr(NH$_3$)$_3$ deriva-
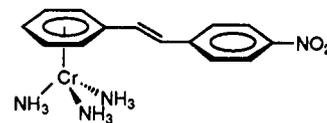
59
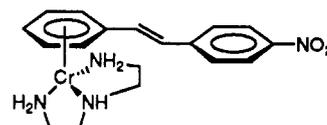
60

tization *significantly* enhances the NLO properties of an arene fragment, while a coordinated Cr(CO)$_3$ moiety acts as a detriment. The Cr(NH)$_3$-appended chromophore fits the qualitative two-level model, and the MLCT transition is truly unidirectional for this species.[200] *Conclusion: In systems with strong coupling between the metal fragment and the electron acceptor, the metal fragment must induce extreme asymmetry in order to observe reasonable NLO responses at the molecular level. Thus, slightly asymmetric environments (most common) will result in only modest responses.*

The group 6–pyridine molecules represent a class of chromophores displaying weak coupling between donor and acceptor. From the MO diagram (Figure 31) of a prototypical class 1B molecule [**62**, (4-formylpyridine)Cr(CO)$_5$] the primary molecular interaction involves the formation of a σ-linkage (coordinate covalent bond) between a nitrogen lone pair (σ) on the ligand and an empty d$_{x^2}$ metal-based orbital.[271] The most striking feature of the MO diagram is the apparent lack of strong π-electron interactions between the two fragments (weak coupling).

Results from ZINDO-SOS second-order response computations on eight pentacarbonylpyridinechromium(0) derivatives [(4-Y-C$_5$H$_5$N)M(CO)$_5$ **61–67**] are compared with experiment in Table 28 and are found to be in excellent agreement. For Y = acceptor, the coordination of the metallic moiety greatly enhances
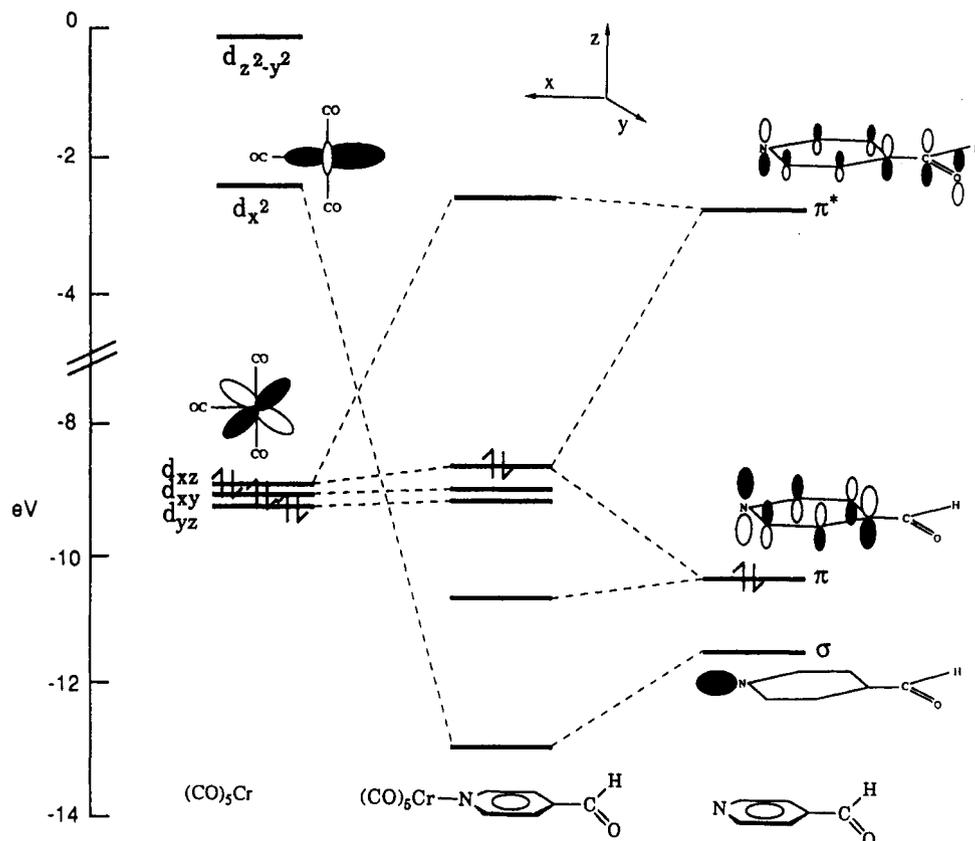
Figure 31. Molecular orbital diagram for (4-formylpyridine)Cr(CO)₅ (62). (Reprinted from ref 271.)

Table 29. Comparison of Experimental and ZINDO-Derived Molecular Hyperpolarizabilities (β_{vec}), Two-Level Contributions to the Response ($\beta_{vec,2}$), and Three-Level Contributions ($\beta_{vec,3}$) to the Response at 1.91 μm ($\hbar\omega$ = 0.65 eV) for a Series of Group 6 Stilbazole Derivatives[a-c]

	Y	$\beta_{vec}^{expt\ d}$	β_{vec}^{calc}	$\beta_{vec,2}^{calc}$	$\beta_{vec,3}^{calc}$	$\beta_{vec}^{calc,corr}$
68	NO₂	−20	−22.8	−99.4	76.6	−50
69	COH	−17	3.54	−44.7	48.2	−22
70	H	−5.7	7.91	−34.2	42.1	−17
71	N(CH₃)₂[e]		34.7	28.4	6.3	14
71	N(CH₃)₂[f]	60	65.5	39.6	25.9	20

[a] All NLO data are in units of 10⁻³⁰ cm⁵ esu⁻¹. [b] Note that M = Cr for all computed responses and M = W for tabulated EFISH values. [c] Tabular data taken from ref 271. [d] EFISH data for transition metal chromophores 68–70 from ref 356, and for chromophore 71 from ref 271. [e] Computed response at 1.91 μm ($\hbar\omega$ = 0.65 eV). [f] Computed response at 1.064 μm ($\hbar\omega$ = 1.17 eV) for purposes of comparison with experimental value.

the response; while for Y = donor, the hyperpolarizability is not greatly affected by the inclusion of the metal fragment. The metal–pyridine chromophores are found to obey the classical two-level model, with a MLCT (represented by a HOMO → LUMO excitation) dictating the second-order response.²⁷¹

The ZINDO-SOS-derived quadratic hyperpolarizability data for four (4-Y-styrylpyridine)M(CO)₅ complexes is tabulated in Table 29. In direct contrast with nearly all molecules examined previously, the $\beta_{vec,3}$ contributions for these particular chromophores rival and in some cases even surpass the $\beta_{vec,2}$ contributions

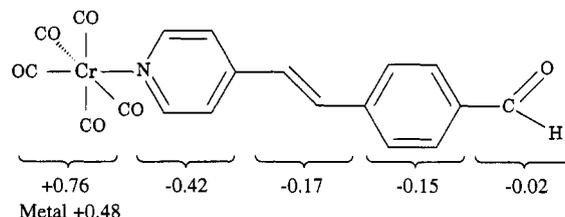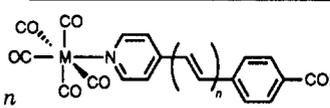+0.76   −0.42   −0.17   −0.15   −0.02
Metal +0.48

Figure 32. The difference in electronic populations between ground state and crucial excited state for (4-formyl-4′-stilbazole)Cr(CO)₅ as calculated by ZINDO. A negative population reflects an increase in electron density for the charge-transfer process. (Reprinted from ref 271.)

as shown in the table. As a consequence, an empirical parameter is defined for these chromophores ($\beta_{vec}^{calc,corr}$) which is defined to be exactly one-half the computed $\beta_{vec,2}$ for a particular molecule in accordance with the quantitative two-level model discussed earlier.²⁷¹ As shown in the table, corrected β_{vec} values for chromophores 68–71 are in reasonable agreement with the EFISH-derived responses, both in sign and in magnitude. For example, $\beta_{vec}^{calc,corr}$ = −22 × 10⁻³⁰ cm⁵ esu⁻¹ for the prototype chromophore 69, compared with the measured β_{vec} of −17 × 10⁻³⁰ cm⁵ esu⁻¹ at $\hbar\omega$ = 0.65 eV. The calculated redistribution of electron density associated with the NLO-dictating transition is found in Figure 32. Unexpectedly, the aromatic ring adjacent to the metal center serves as the primary acceptor of electron density and not the acceptor group itself.²⁷¹ In the case of the 4-formylstyrylpyridine chromophore, 0.42 of the 0.76 electrons involved in the charge transfer migrate to the NC₅H₄ ring, and only 0.17 to the formyl group and the interposed arene π-system. Analysis of the molecular orbitals involved in the charge-transfer transition confirms that the metal pentacarbonyl frag-

Table 30. Comparison of ZINDO-Derived Two-Level Contributions to the Molecular Hyperpolarizability ($\beta_{vec,2}$) for Formyl-Substituted Pyridine-Based Chromium Coordination Complexes and NH$_2$/NO$_2$ Derivatized α,ω-Diphenylene Polyene Molecules of Similar Dimensions at 1.91 μm ($\hbar\omega$ = 0.65 eV)^{a,b}
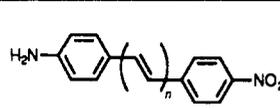

n	$\beta_{vec,2}^{calc}$	
0^c	−29.2	17.2
1	−44.6	105
2	−29.4	155
3	−22.1	221

^{a} All NLO data are in units of 10^{-30} cm^5 esu^{-1}. ^{b} Tabular data taken from ref 271. ^{c} n = 0 refers to (NC$_5$H$_4$–COH)Cr(CO)$_5$ and H$_2$N–C$_6$H$_4$–NO$_2$.

ment acts as σ-acceptor, forcing the adjacent pyridine ring to become the molecular LUMO. As a consequence, the seemingly innocent pyridine ring becomes a primary charge acceptor in these structures, regardless of derivatization or conjugation length.

Perhaps the most striking counterintuitive effect discovered in the group 6–stilbazole studies is evidenced by comparative $\beta_{vec,2}$ data for push/pull α,ω-diphenylene polyenes and (η^1-nitrogen ligand)Cr(CO)$_5$ structures of similar conjugation length as shown in Table 30. As anticipated, the $\beta_{vec,2}$ values for the amino/nitro push/pull derivatives dramatically increase as the π-bridge is lengthened (105 × 10^{-30} cm^5 esu^{-1} for n = 1, 155 × 10^{-30} cm^5 esu^{-1} for n = 2, and 221 × 10^{-30} cm^5 esu^{-1} for n = 3) in accord with common nonlinear optiphore design guidelines. However, note that the corresponding responses for the chromium pentacarbonyl derivatives *do not* display a dramatic increase with conjugation length. In fact, the computations predict that the response actually decreases slightly with longer chain length.[271]

The notion of a metal fragment acting as an inductive acceptor suggests the following unconventional mechanism for enhancing β in metal-containing chromophores.[271] As pictured in **72**, a metal fragment could


72
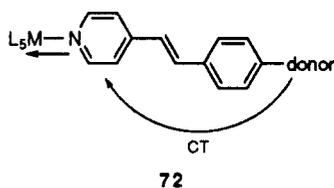
be employed to enhance ligand-to-ligand charge-transfer excitations by increasing the accepting ability of an appended π-ligand. Such a prescription is illustrated by the chromophore [4-(dimethylamino)-4′-stilbazole]W(CO)$_5$ (**71**), a model chromophore that was synthesized on the basis of theoretical computations and the NLO response of which is found to be much larger than one might presume on the basis of π-cloud arguments (Table 29).[271]

Computational studies on the other classes of organometallic architectures have yet to be reported in the literature. Preliminary results, however, suggest that identifying molecules with optimal β characteristics by virtue of low-lying LMCT transitions (class 2) may prove
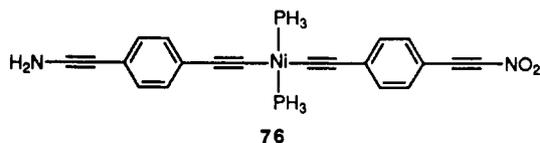
equally elusive as locating large-β molecules containing MLCT transitions.[299] In the LMCT-based chromophores, the metal fragment serves as the π-acceptor, in contrast to the π-donor function they serve in the MLCT structures. Again, however, the environment around the metal center must be highly acentric for the metal fragment to be comparable in accepting strength to an NO$_2$ group, for example.

Conjugated one-dimensional inorganic polymers (class 3) are metal-based analogues of the high-β polyene and polyyne chromophores and should therefore possess large SHG responses. Hopkins and co-workers[337] investigated a class of polymers of the type [N≡M-(OR)$_3$]$_n$ (M = Mo, W) and found them to possess negligible $\chi^{(2)}$ responses. Time-resolved spectroscopic analyses suggest that the NLO-dictating excited state in these metal–nitrido polymers is not extensively delocalized, and therefore only modest responses are observed.[337] ZINDO-SOS computations on a myriad of related polymeric architectures suggest the modest delocalization length observed in the metal–nitrido polymers is a common phenomena in inorganic polymers.[299] The origin of this shortcoming can be demonstrated through the analysis of three isoelectronic chromophores with main group linkages: **73–75**.

73

74

75
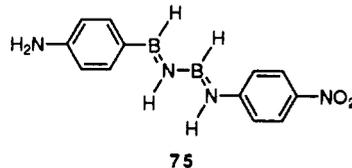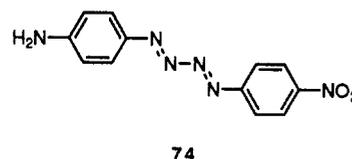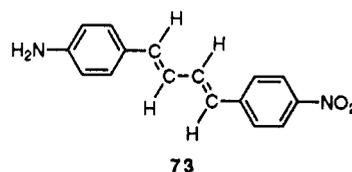
The computed responses for chromophores containing ethylenic and diazo linkages are similar (**73**, 65.7 × 10^{-30} cm^5 esu^{-1}; **74**, 64.0 × 10^{-30} cm^5 esu^{-1}); however, a precipitous drop in β is observed for the molecule containing a —(BH=NH)$_2$— linkage (**75**, 16.3 × 10^{-30} cm^5 esu^{-1}). A detailed analysis of the computed hyperpolarizability suggests that the electron-deficient boron serves to hamper charge transfer in this molecule, thereby limiting β.[299] The implication of this model study is that delocalization lengths in main group polymers or metal-based polymers will be short (and β modest) unless metal fragments along the backbone are tuned to abolish electron sinks between donor and acceptor. As example of such a species, **76** possesses an electron-rich NiL$_2$ connecting group. The computed second-order susceptibility of 26.2 × 10^{-30} cm^5 esu^{-1} is rather large for chromophores in this class.

A recent contribution by Laidlaw et al.[340] reports large second-order nonlinearities from organometallic structures possessing intervalence charge-transfer transitions. The largest response measured for this class

$$H_2N—\equiv\!\!\!=\!\!\!\equiv—\langle\bigcirc\rangle—\equiv\!\!\!=\!\!\!\equiv—Ni—\equiv\!\!\!=\!\!\!\equiv—\langle\bigcirc\rangle—\equiv\!\!\!=\!\!\!\equiv—NO_2$$

with PH_3 above and PH_3 below the Ni.

76

of molecules (via hyper-Raleigh scattering techniques at 1064 nm) was $1440 \times 10^{-30}\,\mathrm{cm^5\,esu^{-1}}$ for the bimetallic ion **77**, an exceptionally large hyperpolarizability. The

77
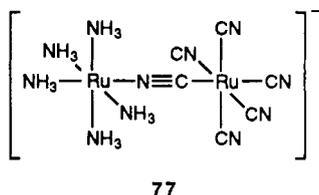
authors attribute the large β values to a low-lying IVCT excited state (a class 4 chromophore in our labeling scheme) and by the near-resonant enhancement of the response. Structure–property relations for this novel class of chromophores are sorely needed, however, the odd-electron count (open-shell) of many mixed-valence species will impede theoretical investigations.

Theory has, and will continue to play, a crucial role in understanding the electronic origin of β, and in the identification of metal-containing molecular motifs displaying optimal NLO characteristics.

G. Relating the Second-Order Response to Superexchange

The two-level model can be simply correlated with a two-site model, involving donor and acceptor ends of a molecule. The effective mixing between these can then be understood in the same sense (molecular superexchange) that one mixes donors and acceptors in discussing intramolecular electron-transfer processes. The parallels between superexchange and NLO response are in fact useful and suggest that perhaps measurements of hyperpolarizabilities can be used to estimate superexchange mixing in extended molecular systems. While the actual mechanism of superexchange is substantially more complex than simple one-electron models might indicate[382,383] and the actual "pathways" by which superexchange occurs remain the subject of controversy, nevertheless, the presence of intervening orbitals between donor and acceptor is critical, both for facilitated intramolecular charge transfer and for frequency doubling. For example, Michl[384] has shown that orbital mixing in silane-bridged chromophores requires both first- and second-neighbor interactions of local bond lobes and therefore cannot be described by a simple tight-binding model.

H. Octopolar Architectures

While classical dipolar prescriptions and two-level models are useful for interpreting the NLO response of most chromophoric systems, there are a number of important and interesting systems for which they fail. Perhaps the most intriguing examples are the chromophores of octopolar symmetry recently investigated by Zyss and his collaborators.[339,385,386] Expansion of

Table 31. Finite-Field AM1, CPHF 3-21G, and INDO/SDCI Computational Results on PNA and TATB[a-c]

	AM1		3-21G		INDO/SDCI	
	PNA	TATB	PNA	TATB	PNA	TATB
$\mu_z(\mathrm{D})$	-7.64	0.0	-7.79	0.0	-8.34	0.0
$\langle\alpha\rangle$ ($\mathrm{\AA}^3$)	11.60	18.90	10.50	16.62		
β_{zzz} (10^{-30} esu)	-11.67	-11.08	-9.55	-8.01	-8.53	-7.68
β_{zyy} (10^{-30} esu)	1.93	11.08	1.66	8.01	0.06	7.68
β_{zxx} (10^{-30} esu)	0.0	0.0	0.0	0.0	0.0	0.0
β_z (10^{-30} esu)	-9.74	0.0	-7.89	0.0	-8.47	0.0
$\|\beta\|$ (10^{-30} esu)	12.14	22.16	9.97	16.02	8.53	15.36

[a] Ground-state dipole moment, μ; average first-order polarizability, $\langle\alpha\rangle$; components of the second-order polarizability tensor; z component of the vectorial part of the β tensor, β_z; modulus of the β tensor, $\|\beta\|$. Note that β_z is equal to $\Sigma_i\beta_{zii}$ and $\|\beta\|^2 = \Sigma_{i,j,k}\beta_{ijk}^2$. The y and z axes define the molecular plane with z corresponding to the NH_2-NO_2 vector in PNA. PNA = p-nitroaniline, TATB = 1,3,5-triamino-2,4,6-trinitrobenzene. [b] All NLO data in units of $10^{-30}\,\mathrm{cm^5\,esu^{-1}}$. [c] Tabular data taken from ref 143, Table I.
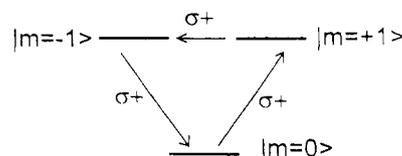

Figure 33. Three-level model used to account for the second-order nonlinearities of an octopolar molecule. The arrows represent the three separate transitions contributing to β. (Reprinted from ref 221. Copyright 1992 American Institute of Physics.)

the β tensor into irreducible components shows that some chromophores contain an *octopolar* contribution in addition to the usual *dipolar* terms.[385,386] It has been proposed that π-electron chromophores of trigonal symmetry (D_{3h}) symmetry such as 1,3,5-triamino-2,4,6-trinitrobenzene (78, TATB) would possess zero dipolar

78
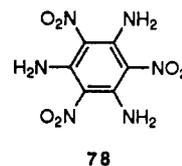
contributions through the two-level model ($\Delta\mu = 0$), but should possess a nonzero octopolar β contribution.[385] Using CPHF, INDO-SOS, and AM1-FF, it has been demonstrated by Brédas, et al.[143] that the total intrinsic hyperpolarizability ($\Sigma\beta_{ijk}^2$) of **78** is 1.6–1.8 times greater than that of p-nitroaniline (Table 31).

The definition of β_{oct} in planar aromatic systems is given as

$$\beta_{\mathrm{oct}} = \beta_{zzz} - 3\beta_{zyy} - 3\beta_{zxx} \tag{39}$$

Joffre et al.[221] have described the electronic origins of β_{oct} in model octopolar systems using semiempirical-SOS techniques. In a nutshell, three doubly-degenerate excited states are responsible for the octopolar response in the SOS formalism, and a modified three-level model (Figure 33) can describe the octopolar contributions to the quadratic hyperpolarizability. To first order, the octopolar molecule is a linear superposition of three dipolar molecules, in which the dipolar components add destructively while the octopolar components add constructively. The authors also report the SDCI is necessary to properly treated β_{oct}.[221]

Table 32. Predicted $\chi^{(2)}$ Values from Madelung Calculations in Two-Dimensional Chromophoric Langmuir–Blodgett Films[a,b]

θ (deg)	$\chi^{(2)}_{xxz}$	$\chi^{(2)}_{zzz}$
0	11.8	-49.8
20	0.6	-44.1
40	-21.0	-19.1

[a] The angle θ is the chromophore orientation angle with respect to the layer normal; the z axis is normal to the layer, and xz is the tilt plane. [b] Tabular data taken from ref 390.

Recently, the hyperpolarizability β_{xxx} ($\hbar\omega = 1.17$ eV) of the potassium salt of the tricyanomethanide ion $[C(CN)_3]^-$ (an octopolar molecule) was measured using the hyper-Raleigh scattering technique developed by Persoons and co-workers[387] to be approximately 7×10^{-30} cm^5 esu^{-1},[388] approximately half that of the prototypical p-nitroaniline chromophore. This value is in quantitative agreement with MOPAC-FF and INDO/SCI-SOS computations on the radical anion.[388] Further theoretical and experimental studies are needed to develop general guidelines for optimizing these unconventional tensorial components of the second-order susceptibility.

I. Intermolecular Effects

Calculations beyond the isolated chromophore level are still not very common. As already stated, intermolecular interactions can substantially affect the hyperpolarizability, as is reflected in the solvatochromism of most high-β chromophores. Computational studies of this effect normally fall into three categories: first, calculations have been done with the full periodicity of a two-dimensional film or a three-dimensional crystal.[389,390] For such calculations, the input data are the geometry of the repeat units and the charge distribution and hyperpolarizability of the individual molecule. Second, calculations of the finite field-type have been carried out, in which the finite local field is comprised both of the applied field and of local field variations arising either from the solvent molecule or from other chromophores.[166,226] Third, supermolecule, or molecular cluster, calculations have been reported in which an electronic structure calculation is carried out for a finite cluster (dimer, trimer, etc.) of chromophores.[174,272,273,391–393]

Most of these calculations have been completed using semiempirical methods, although an important earlier study of Zyss and Berthier[166] studied crystalline urea using *ab initio* techniques. Munn has reported extensive calculations on periodic structures, using the full long-range Madelung sum to compete the local variation in potential.[389,390] Typical results are shown in Table 32, which describes a calculation on a model Langmuir–Blodgett film. In this calculation, molecules were stacked in a tilt plane, and the hyperpolarizability of the structure was calculated along the various axes for different values of the tilt angle. As Table 32 shows, there is substantial sensitivity to the tilt angle, with some components of $\chi^{(2)}$ actually changing in sign for different angles. While these calculations are for a model chromophore, Munn has also reported work on actual molecular crystals. He finds, in general, that the crystal effects on $\chi^{(2)}$ (the local field factors in the relationship between $\chi^{(2)}$ and β) are less dramatic than

might be expected, and that, for a broad class of molecules, the agreement between calculated and experimental $\chi^{(2)}$ is good.

In Munn's calculations, the computed effects can be interpreted not in terms of intermolecular interactions, but simply in terms of a molecule interacting with a local field (that field is simply set up by the other molecules). Analogous arguments, using different local fields, can be used to describe both intermolecular effects[166] and the effects of solvent. Several calculations have used this local field to study the effects of intermolecular attractions on optical properties of molecules,[394] and some reports have discussed how hyperpolarizabilities change due to local fields. In liquids, as opposed to the crystals studied by Munn, there is substantial arbitrariness involved in defining these local fields, and ignoring dynamical aspects of the response of the solvent makes it difficult to obtain quantitative information from such local field calculations (see note added in proof).

Finally, there have been a number of studies based on "supermolecule" calculations and examining how pairs, trimers, or clusters of molecules vary in their β-property from the individual molecules. Several of these calculations concern themselves with urea, since the urea crystal was one of the early standard materials for nonlinear response. Urea is unfortunately a difficult case since there is extensive hydrogen bonding in the crystal structure, and the actual hyperpolarizability is quite small. Calculations on water clusters and on HF clusters have shown the importance of intermolecular charge transfer, and the substantial increases in β for linear clusters (comparable to the expected growth in β for linear polyenes discussed earlier).[166,392] Dirk et al.[204] studied a dimer of 2-amino-5-nitropyridine in a monoclinic unit cell. They found that including intermolecular interaction reduces the average β-value by nearly 50% and discussed this result in terms of electrostatic interactions. DiBella et al.[272,273] studied cofacial dimers and trimers and of organic π-electron chromophores using ZINDO techniques. In homodimers, they found that the dimeric β was sensitive to orientational and distance effects between the monomers; the dimer β-response scaled properly with the sum of the individual components for large internuclear distances, but changed considerably with angle and translation when the pairs are placed at intermolecular distances typical of crystal structures. For example, Figure 34 shows the sensitivity of the computed hyperpolarizability of a coplanar pair of p-nitroaniline molecules, as a function of slip distance. The maximum in the response occurs when the positive end of one molecular dipole is directly over the negative end of the other molecular dipole, and DeBella et al. argue that this should lead to the largest red-shifts, and therefore (following the two-level model) the greatest enhancement of β by intermolecular attraction.

Also interesting is the situation in which a donor–acceptor pair is studied.[273] For example, when coplanar 1,2,4,5-tetramethylbenzene and TCNE molecules are stacked center over center, the resulting charge-transfer complex exhibits computed a β_{zzz} of 69×10^{-30} cm^5 esu^{-1} which is comparable to that of 4-(dimethylamino)-4'-nitrostilbene. The large β response arises, as the two-level model suggests, from a strongly allowed transition,
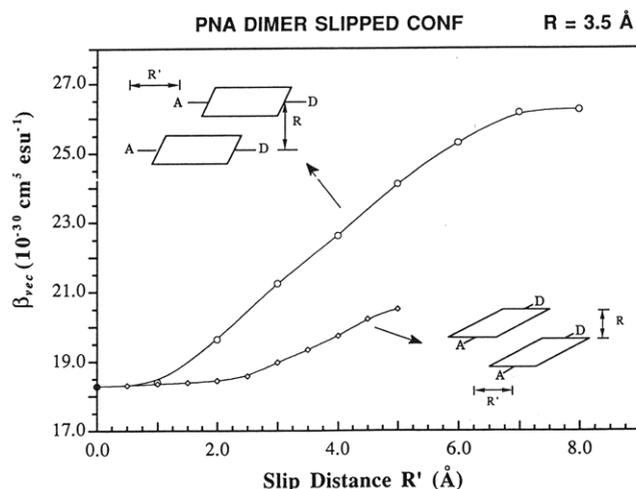
PNA DIMER SLIPPED CONF   R = 3.5 Å

Figure 34. Variation of ZINDO-derived β_{vec} ($\hbar\omega = 0.65$ eV) with slip distance (R') along the x and y axes in a p-nitroaniline dimer ($R = 3.5$ Å). (Reprinted from ref 273. Copyright 1992 American Chemical Society.)

(a)   (b)
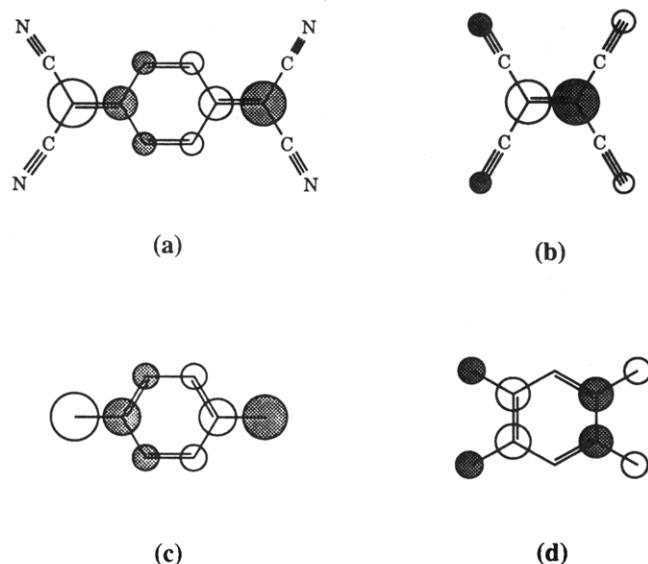

(c)   (d)

Figure 35. Frontier orbitals of selected electron donor/acceptor complexes: LUMO of TCNQ (a) and TCNE (b) complexes, HOMO of TCNQ-N,N,N',N'-tetramethyl-p-phenylenediamine (c), and TCNE-1,2,4,5-tetraminobenzene (d) complexes. (Reprinted from ref 272. Copyright 1993 American Chemical Society.)

at relatively low excitation frequency, and a substantial change in dipole moment. DiBella and collaborators suggest that, in fact, the supermolecular LUMO is almost independent of the donor molecule, whereas the HOMO is strongly modulated by substituents on the aromatic. Then, as Figure 35 shows, the overlap of donor and acceptor nodal properties is nearly optimal, and one expects an extremely large oscillator strength. The change in dipole moment is essentially fixed by geometry, and is much less sensitive to the nature of the donor or the acceptor than is the oscillator strength. Table 33 shows results, calculated using the ZINDO-SOS method, on a number of co-facial donor–acceptor complexes; note that the value of β is well-described by the two-level model, that it is sensitive to the exact nature of the donor and acceptor groups (particularly the donor group), and that the absolute magnitudes in favorable cases can be as large as those reported for

Table 33. ZINDO-Derived Dipole Moment, Linear Optical Spectroscopic, and Molecular Hyperpolarizability $\beta(-2\omega;\omega,\omega)$ Data[a] (10^{-30} cm^5 esu^{-1}; $\hbar\omega$ = 0.65 eV) for Cofacial 1:1 Electronic Donor–Acceptor Complexes involving Various Electron-Acceptor Molecules (A)

donor[b] (D)	μ (D)[c]	$\hbar\omega_{ge}$(eV)[c,d]	f[c]	$\Delta\mu_{ge}$ (D)[c]	β_{zzz}[c]	$\beta_{ct,zzz}$[e]
A = TCNQ						
TMDP	1.07	2.04	0.14	14.43	68.36	69.96
PD	1.04	2.33	0.14	14.46	39.04	38.50
DMB	0.40	3.02	0.08	14.29	8.39	7.77
PX	0.60	3.27	0.11	13.75	9.08	8.04
HMB	0.68	3.03	0.11	14.04	11.06	10.23
A = TCNE						
TTAB	1.33	2.04	0.14	14.54	68.51	69.08
PD	0.83	2.45	0.10	14.94	23.22	22.78
DMB	0.54	3.25	0.09	14.98	8.23	7.79
PX	0.62	3.48	0.11	14.95	7.28	6.97
HMB	0.59	3.37	0.12	15.65	9.34	8.95
A = TNB						
TAB	0.59	2.29	0.06	14.46	21.95	18.97
TRIAZ	0.36	3.00	0.06	15.03	11.18	7.10

[a] Tabular data taken from ref 272, Table II. [b] TMPD = N,N,N',N'-tetramethyl-p-phenylenediamine; PD = p-phenylenediamine; DMB = 1,4-dimethoxybenzene; PX = p-xylene; HMB = hexamethylbenzene; TTAB = 1,2,4,5-tetraaminobenzene; TAB = 1,3,5-triaminobenzene; TRIAZ = 2,4,6-tris(dimethylamino)-1,3,5-triazine. [c] Calculated using the INDO/S SOS formalism. [d] Lowest energy CT transition. [e] Calculated using the simple two-level model of eq 10.

strong donor–acceptor, push/pull stilbene-type chromophores.

VI. Concluding Remarks

In the past decade, theoretical techniques have become a primary tool for finding and understanding molecules with optimal second-order NLO responses. These methodologies have proven to be reliable and essential in guiding synthetic chemical efforts. The traditional push/pull π-organic templates so common in NLO materials are now reasonably well understood, and it can now be said that materials by design is a reality in this area. One can state with some degree of certainty, that if a class of "super-chromophores" exist, that they will most likely be uncovered with the aid of computational formalisms.

As optimistic as this assessment sounds, a number of questions still remain. At the basic level, there are questions surrounding the requirements (correlation, basis sets) of sophisticated *ab initio* computations on large molecules. Will these computations become computationally economical and user-friendly enough to supplant the more approximate procedures? Another interesting question surrounds the role of chromophore environment in both the linear and nonlinear optical properties. While a decade ago, computed responses within an order of magnitude were regarded as adequate, the accuracy of current methods has caused many researchers concern about factors of 2 and 4 due to problems associated with unit conventions,[36-39] and this is certain to attract attention in the near future. Another important question concerns the mechanism, importance, and tunability of the three-level contributions discussed in this review.

In a more technologically-oriented vein, one wonders if another, more efficient β-mechanism exists. After

all, the conventional π-asymmetric architectures can only be pushed so far before structural/thermodynamic instabilities become a major problem. Thus, nontraditional approaches to increasing β through chromophore–chromophore interactions, organometallic morphologies, or octopolar symmetries offer promising areas for research.

Note Added in Proof

Several recent papers deal with the effects of solvent on hyperpolarizabilities and are useful in interpreting EFISH experiments. Using a very simple Onsager–Kirkwood cavity picture to describe the energy changes upon solvation and using these energy changes in the SOS form of eq 31 in conjunction with a ZINDO model, DiBella et al.[395] have shown that the characteristic underestimate of β for a variety of donor/acceptor π-electron chromophores is indeed caused by solvent-induced energy shifts. Correcting for this, their plot of β_{vec}^{calc} versus β_{vec}^{expt} yields a slope of 0.90 after solvent (CHCl$_3$) energy correction compared to 0.64 before correction. Zerner's group[396] observes similar improvement using a more elaborate semiempirical self-consistent reaction field picture. Finally, an important contribution from Mikkelsen et al.[397] uses *ab initio* reaction-field linear response theory to examine solvent effects on β. They make several important observations including: (1) Ground-state correlation effects on *p*-nitroaniline are very small—CIS is quite accurate. (2) Trancation of the reaction field after the dipolar term is an excellent approximation. (3) The two-state model severely under-represents the dispersion. (4) All of the two-state model parameters ($\Delta\mu_{gn}$, f_{gn}, and ΔE_{gn}) vary strongly with solvation.

VII. Acknowledgements

VIII. References and Notes

(1) Boyd, R. W. Nonlinear Optics; Academic Press: New York, 1992.
(2) Shen, Y. R. The Principles of Nonlinear Optics; Wiley: New York, 1984.
(3) Bloembergen, N. Nonlinear Optics; W. A. Benjamin: New York, 1965.
(4) Bergman, J. G.; Kurtz, S. K. Mater. Sci. Eng. 1969, 5, 235–250.
(5) Franken, P. A.; Ward, J. F. Rev. Mod. Phys. 1963, 35, 23–39.
(6) Zernike, F.; Midwinter, J. Applied Nonlinear Optics; Wiley: New York, 1973.
(7) Lytel, R.; Lipscomb, G. F.; Stiller, M.; Thackara, J. I.; Ticknor, E. J. 1989, 971, 277–289 (Nonlinear Optical Properties of Organic Materials; Proc. SPIE—Int. Soc. Opt. Eng. Khanarian, G., Ed.).
(8) Ulrich, D. R. Mol. Cryst. Liq. Cryst. 1988, 160, 1–31.
(9) Bjorklund, G. J.; Boyd, R. W.; Garter, G.; Garito, A. F.; Lytel, R. S.; Meredith, G. R.; Prasad, P.; Stamatoff, J.; Thakur, M. Appl. Opt. 1987, 26, 227–231.
(10) Zyss, J. J. Mol. Electron. 1985, 1, 25–56.
(11) Kobayashi, T. Nonlinear Opt. 1991, 1, 91–117.
(12) Eaton, D. F. CHEMTECH 1992, 308–316.
(13) Tripathy, S.; Cavicchi, E.; Kumar, J.; Kumar, R. S. CHEMTECH 1989, 620–625.
(14) Tripathy, S.; Cavicchi, E.; Kumar, J.; Kumar, R. S. CHEMTECH 1989, 747–751.
(15) Meredith, G. R. J. Mater. Educ. 1987, 9, 719–750.
(16) Williams, D. J. Thin Solid Films 1992, 216, 117–122.
(17) Eaton, D. F.; Meredith, G. R.; Miller, J. S. Adv. Mater. (Weinheim Fed. Repub. Ger.) 1992, 4, 45–48.

(18) Williams, D. J., Ed. Proc. SPIE—Int. Soc. Opt. Eng. 1992, 1775 (Nonlinear Optical Properties of Organic Molecules V).
(19) Prasad, N. P.; Williams, D. J. Introduction to Nonlinear Optical Effects in Molecules and Polymers; Wiley: New York, 1991.
(20) Eaton, D. F. Science 1991, 253, 281–287.
(21) Marder, S. R.; Beratan, D. N.; Cheng, L.-T. Science 1991, 252, 103–106.
(22) Marder, S. R.; Sohn, J. E.; Stucky, G. D., Eds.; Materials for Nonlinear Optics: Chemical Perspectives; ACS Symposium Series 455, American Chemical Society: Washington, DC, 1991.
(23) Brédas, J. L.; Silbey, R. J., Eds. Conjugated Polymers: The Novel Science and Technology of Highly Conducting and Nonlinear Optically Active Materials; Kluwer: Dordrecht, Neth., 1991.
(24) Khanarian, G., Ed. Proc. SPIE—Int. Soc. Opt. Eng. 1990, 1337 (Nonlinear Optical Properties of Organic Molecules III).
(25) Khanarian, G., Ed. Proc. SPIE—Int. Soc. Opt. Eng. 1990, 1147 (Nonlinear Optical Properties of Organic Molecules II).
(26) Khanarian, G., Ed. Proc. SPIE—Int. Soc. Opt. Eng. 1989, 971 (Nonlinear Optical Properties of Organic Materials).
(27) Messier, J.; Kajar, F.; Prasad, P.; Ulrich, D., Eds. Nonlinear Optical Effects in Organic Polymers; Kluwer Academic Publishers: Dordrecht, 1989.
(28) Heeger, A. J., Orenstein, J., Ulrich, D. R., Eds. Nonlinear Optical Properties of Polymers. Mater. Res. Soc. Symp. Proc. 1988, 109.
(29) Hann, R. A., Bloor, D., Eds. Organic Materials for Nonlinear Optics; Royal Society of Chemistry Monograph 69; Burlington House: London, 1988.
(30) Chemla, D. S., Zyss, J., Eds. Nonlinear Optical Properties of Organic Molecules and Crystals; Academic Press: New York, 1987; Vols. 1 and 2.
(31) Carters, G., Zyss, J., Eds. Nonlinear Optical Processes in Organic Materials. J. Opt. Soc. Am. B, 1987, 4.
(32) Williams, D. J. Angew. Chem., Intl. Ed. Engl. 1984, 23, 690–703.
(33) Williams, D. J., Ed. Nonlinear Optical Properties of Organic Molecules and Polymeric Materials; ACS Symposium Series 233, American Chemical Society: Washington, DC, 1984.
(34) Flytzanis, C. In Treatise of Quantum Electronics; Rabin, H., Tang, C. L., Eds.; Academic Press: New York, 1975.
(35) Blau, W. Phys. Technol. 1987, 18, 250–261.
(36) Stähelin, M.; Burland, D. M.; Rice, J. E. Chem. Phys. Lett. 1992, 191, 245–250.
(37) Willetts, A.; Rice, J. E.; Burland, D. M.; Shelton, D. P. J. Chem. Phys. 1992, 97, 7590–7599.
(38) Burland, D. M.; Walsh, C. A.; Kajzar, F.; Sentein, C. J. Opt. Soc. Am. B: Opt. Phys. 1991, 8, 2269–2281.
(39) Willetts, A.; Rice, J. E. J. Chem. Phys. 1993, 99, 426–435.
(40) Giordmaine, J. A. Sci. Am. 1964, 210 (4), 38–49.
(41) Yariv, A. Quantum Electronics; Wiley: New York, 1975; p 419.
(42) Franken, P. A.; Hill, A. E.; Peters, C. W.; Weinrich, G. Phys. Rev. Lett. 1961, 7, 118–119.
(43) See, for example: Munn, R. W. J. Mol. Electron. 1988, 4, 31–36 and references therein.
(44) Onsager, L. J. Am. Chem. Soc. 1936 58, 1486–1493.
(45) Lorentz, H. A. The Theory of Electric Polarization; Elsevier: Amsterdam, 1952.
(46) Although all 27 components of the β tensor can be computed with the methodologies described herein, only the vector component along the dipole moment direction, the so-called β_{vec}, is sampled experimentally in electric field induced second-harmonic generation (EFISH) experiments:[47,48]

$$\beta_{vec}(-2\omega;\omega,\omega) = \sum_{i=1}^{3} \frac{\mu_i \beta_i}{|\mu|}$$

Here, μ is the ground-state molecular dipole moment and

$$\beta_i = \beta_{iii} + \frac{1}{3}\sum_{j\neq i}(\beta_{ijj} + \beta_{jij} + \beta_{jji})$$

where i and j run over the molecular Cartesian directions x, y, and z. In chromophores where the charge-transfer direction is obviously parallel with the ground-state dipole moment direction (for purposes of illustration, the x direction), some authors label their experimental or theoretical responses as β_x or β_{xxx}. We should mention that the "experimentalist" definition of β_{vec} does vary slightly from that used by many theorists,[37] which we shall label $\beta_{||}$; where $3/5\beta_{vec} = \beta_{||}$. There is another quantity of interest in this work, the total intrinsic quadratic hyperpolarizability, β_{tot},

$$\beta_{tot} = (\beta_x^2 + \beta_y^2 + \beta_z^2)^{1/2}$$

β_{vec} will be identical to β_{tot} when the charge transfer is unidirectional and parallel to the molecular dipole moment. Note that β_{tot} is always a positive quantity regardless of the sign of the individual vectorial components.

(47) Levine, B. F.; Bethea, C. G. Appl. Phys. Lett. 1974, 24, 445–447.
(48) Levine, B. F.; Bethea, C. G. J. Chem. Phys. 1975, 63, 2666–2682.
(49) The units for molecular hyperpolarizabilities can be somewhat complicated.[50–52] Most contributions quote β in either atomic or esu units. Dimensional analysis of the quadratic hyperpolarizability

indicates that it possesses the units of dipole moment^3/energy^2, or in atomic units

$$\beta = e^3 a_o{}^3/E_h{}^2$$

where a_o is the Bohr radius and E_h is the ionization energy of hydrogen (a Hartree). Substituting E_h (Hartree) = e^2/a_o

$$\beta = e^3 a_o{}^3/(e^2/a_o)^2 = a_o{}^5/e$$

in esu units; the second-order response is given as cm^5 statcoulomb^{-1} which is identical to cm^5 esu^{-1}. Sometimes these units are simply referred to as esu. The conversion factor between atomic units and esu is as follows:

$$1 \text{ atomic unit} = \frac{a_o^5}{e}\left(\frac{5.292 \times 10^{-9}\text{cm}}{a_o}\right)^5 \frac{e}{4.803 \times 10^{-10} \text{ esu}}$$

$$1 \text{ atomic unit} = 8.641 \times 10^{-33} \text{ cm}^5/\text{esu}^1$$

in SI units, 1 atomic unit = 3.206×10^{-53} C^3 m^3 J^{-2} and 1 C^3 m^3 J^{-2} = 2.693×10^{20} cm^5 esu^{-1}.

(50) Reference 19, p 303.
(51) Jackson, J. D. Classical Electrodynamics; Wiley: New York, 1975, 811–821.
(52) Bishop, D. M. Rev. Mod. Phys. 1990, 62, 343–374.
(53) There are several technical intricacies associated with deducing β_{vec} from an EFISH experiment.[47,48,54] In the EFISH technique, a static electric field is applied to a solution with the chromophore dissolved in a solvent. The DC field removes the centrosymmetry of the medium through interaction with the dipole moments of the individual chromophores. The experiment creates an SHG signal from the interaction of three waves ($\omega + \omega$ + DC field); thus the EFISH signal is actually a third-order response ($\gamma_{DC\text{-}SHG}$). The intrinsic third-order response (γ_o) must be estimated and subtracted from the experimental number. More importantly, the induced orientational average must be estimated from local field models in order to determine β_{vec} from γ_o. The popular infinite dilution method developed by Singer and Garito[55] minimizes solute–solvent and solute–solute interactions when determining β for solute molecules. However, even when this approach is carried out in relatively apolar solvents (such as dioxane), β is solvent-dependent. A comparison of a gas-phase calculation of β with experimental values could be problematic if such interactions were non-negligible. Thus, when comparing calculated and EFISH values, an internally consistent set of EFISH data should be employed where possible. In using EFISH results from a single laboratory, deviations due to experimental conditions such as differing incident frequencies, solvent polarities, local field models, and data reduction schemes will be minimized.
(54) Reference 19, Chapter 6.
(55) Singer, K. D.; Garito, A. F. J. Chem. Phys. 1981, 75, 3572–3580.
(56) Cheng, L.-T.; Tam, W.; Stevenson, S. H.; Meredith, G. R. J. Phys. Chem. 1991, 95, 10631–10643.
(57) Cheng, L.-T.; Tam, W.; Marder, S. R.; Steigman, A. E.; Rikken, G.; Spangler, C. W. J. Phys. Chem. 1991, 95, 10643–10652.
(58) Oudar, J. L.; Chemla, D. S. Opt. Commun. 1975, 13, 164–168.
(59) Oudar, J. L.; LePerson, H. Opt. Commun. 1975, 15, 258–262.
(60) Chemla, D. S.; Oudar, J. L.; Jerphagnon, J. Phys. Rev. B 1975, 12, 4534–4546.
(61) Everard, K. B.; Sutton, L. E. J. Chem. Soc. 1951, 25, 2818–2826.
(62) Zyss, J. J. Chem. Phys. 1979, 70, 3341–3349.
(63) Rustagi, K. C.; Ducuing, J. Opt. Commun. 1974, 10, 258–261.
(64) Dulcic, A.; Flytzanis, C.; Tang, C. L.; Pépin, D.; Fétizon, M.; Hoppilliard, Y. J. Chem. Phys. 1981, 74, 1559–1563.
(65) Oudar, J. L.; Chemla, D. S. J. Chem. Phys. 1977, 66, 2664–2668.
(66) Oudar, J. L. J. Chem. Phys. 1977, 67, 446–457.
(67) Miller, C. K.; Ward, J. F. Phys. Rev. A 1977, 16, 1179–1185.
(68) For a general discussion on the bond additivity model, see: Buckingham, A. D.; Orr, B. J. Q. Rev. Chem. Soc. 1967, 21, 195–215.
(69) Applequist, J. J. Chem. Phys. 1985, 83, 809–826.
(70) Kajzar, F.; Messier, J. Phys. Rev. A 1985, 32, 2352–2363.
(71) Zyss, J. J. Chem. Phys. 1979, 71, 909–916.
(72) Dulcic, A.; Sauteret, C. J. Chem. Phys. 1978, 69, 3453–3457.
(73) André, J.-M.; Delhalle, J. Chem. Rev. 1991, 91, 843–865.
(74) There are several definitional issues associated with comparing theory to experiment and theory to theory in nonlinear optics.[36–39] These include the following: a. Definition of Molecular Hyperpolarizability. β and $\gamma_{DC\text{-}SHG}$ can be defined though either of the power series expansions (Taylor series or perturbation series convention) of the induced polarization listed below.[36–39] The definitions must be clear for meaningful comparisons.

$$p_i = \sum_j \alpha_{ij} F_j + \sum_{j,k} \beta_{ijk} F_j F_k + \sum_{j,k,l} \gamma_{ijkl} F_j F_k F_l + \dots$$

$$p_i = \sum_j \alpha_{ij} F_j + \frac{1}{2}\sum_{j,k} \beta_{ijk} F_j F_k + \frac{1}{6}\sum_{j,k,l} \gamma_{ijkl} F_j F_k F_l + \dots$$

b. Definition of Electric Fields. NLO susceptibilities can be defined using real (two definitions) or complex fields, and again conventions should be specified.

$$F(\omega) = F_o \cos(\omega t)$$

$$F(\omega) = F_o(e^{i\omega t} + e^{-i\omega t})$$

$$F(\omega) = F_o e^{i\omega t}$$

c. Definition of the Vector Component of β. The vector β_i has been defined as

$$\beta_i = \beta_{iii} + \frac{1}{3}\sum_{j \neq i}(\beta_{ijj} + \beta_{jij} + \beta_{jji})$$

and as

$$\beta_{||} = \frac{3}{5}\left[\beta_{iii} + \frac{1}{3}\sum_{j \neq i}(\beta_{ijj} + \beta_{jij} + \beta_{jji})\right]$$

typically the former is for solution-phase measurements and the latter for gas-phase measurements. d. NLO Response of the Reference Material. It is difficult to measure the absolute NLO response of standards such as quartz, urea, or lithium niobate. Thus, quoted literature values for β will reflect discrepancies in the responses of benchmark materials.

(75) Jørgensen, P.; Simons, J. Second Quantization-Based Methods in Quantum Chemistry; Academic Press: New York, 1981.
(76) Linderberg, J.; Öhrn, Y. Propogators in Quantum Chemistry; Academic Press: London, 1974.
(77) Schatz, G. C.; Ratner, M. A. Quantum Mechanics in Chemistry; Prentice-Hall: Englewood Cliffs, NJ, 1993; Chapter 6.
(78) Stanton, J. F.; Gauss, J.; Watts, J. D.; Lauderdale, W. J.; Bartlett, R. J. ACES II, a program product of the University of Florida, Quantum Theory Project.
(79) Frisch, M. J.; Trucks, G. W.; Head-Gordon, M.; Gill, M. W.; Wong, M. W.; Foresman, J. B.; Johnson, B. G.; Schlegel, H. B.; Robb, M. A.; Replogle, E. S.; Gomperts, D. J.; Andres, J. L.; Raghavachari, K.; Binkley, J. S.; Gonzalez, C.; Martin, R. L.; Fox, D. J.; Defrees, D. J.; Baker, J.; Stewart, J. J. P.; Pople, J. A. GAUSSIAN-92, Gaussian, Inc.: Pittsburgh, PA, 1992.
(80) Dupuis, M.; Rys, J.; King, H. F. J. Chem. Phys. 1976, 65, 111–116.
(81) Dupuis, M.; Farazdel, A.; Karna, S. P.; Maluendes, S. A. HONDO-8.0. In Modern Techniques in Computational Chemistry: MOTECC-90; Clementi, E., Ed.; ESCOM: Leiden, 1990.
(82) Murrell, J. N.; Harget, A. J. Semi-Empirical Self-Consistent-Field Molecular Orbital Theory of Molecules; Wiley: London, 1972.
(83) Pople, J. A.; Beveridge, D. L. Approximate Molecular Orbital Theory; McGraw-Hill: New York, 1970.
(84) Levine, I. N. Quantum Chemistry; Allyn and Bacon: Boston, 1983; Chapter 15.
(85) See, for example: Streitwieser, A. Molecular Orbital Theory for Organic Chemists; Wiley: New York, 1961.
(86) Hoffmann, R. J. Chem. Phys. 1963, 39, 1397–1412.
(87) Wolfsberg, M.; Helmholtz, L. J. Chem. Phys. 1952, 20, 837–843.
(88) Pariser, R.; Parr, R. G. J. Chem. Phys. 1953, 21, 466–471.
(89) Pople, J. A. Trans. Faraday Soc. 1953, 49, 1375–1385.
(90) Pople, J. A.; Santry, D. P.; Segal, G. A. J. Chem. Phys. 1965, 43, S129–S135; S136–S151.
(91) Pople, J. A.; Beveridge, D. L.; Dobosh, P. A. J. Chem. Phys. 1967, 47, 2026–2033.
(92) Ridley, J.; Zerner, M. C. Theoret. Chim. Acta (Berlin) 1973, 32, 111–134.
(93) Bacon, A. D.; Zerner, M. C. Theoret. Chim. Acta (Berlin) 1979, 53, 21–54.
(94) Anderson, W. P.; Edwards, W. D.; Zerner, M. C. Inorg. Chem. 1986, 25, 2728–2732.
(95) Kotzian, M.; Rösch, N.; Schröder, H.; Zerner, M. C. J. Am. Chem. Soc. 1989, 111, 7687–7696.
(96) Dewar, M. J. S.; Thiel, W. J. Am. Chem. Soc. 1977, 99, 4899–4907.
(97) Dewar, M. J. S.; Zoebisch, E. G.; Healy, E. F.; Stewart, J. J. P. J. Am. Chem. Soc. 1985, 107, 3902–3909.
(98) Stewart, J. J. P. J. Comput. Chem. 1989, 10, 209–220, 221–264.
(99) Jaffé, H. H. Acc. Chem. Res. 1969, 2, 136–143.
(100) See for example, Kanis, D. R.; Marks, T. J.; Ratner, M. A. Int. J. Quantum Chem. 1992, 43, 61–82.
(101) Meyers, F.; Brédas, J. L.; Zyss, J. J. Am. Chem. Soc. 1992, 114, 2914–2921.
(102) Morley, J. O.; Docherty, V. J.; Pugh, D. J. Chem. Soc., Perkin Trans. 2 1987, 1351–1355.
(103) Cambridge Structural Database, Cambridge Crystallographic Data Centre, Cambridge.
(104) Feynman, R. Phys. Rev. 1939, 56, 340–343.
(105) Stanton, R. E. J. Chem. Phys. 1962, 36, 1298–1300.
(106) Pople, J. A.; McIver, J. M.; Ostlund, N. S. J. Chem. Phys. 1968, 49, 2960–2964.

(107) Cohen, H. D.; Roothaan, C. C. J. *J. Chem. Phys.* **1965**, *43*, S34–S39.
(108) Hush, N. S.; Williams, M. L. *Chem. Phys. Lett.* **1970**, *5*, 507–510.
(109) Gready, J. E.; Bacskay, G. B.; Hush, N. S. *Chem. Phys.* **1977**, *22*, 141–150.
(110) Pulay, P. *Mol. Phys.* **1969**, *17*, 197–207.
(111) Hurst, G. J. B.; Dupuis, M.; Clementi, E. *J. Chem. Phys.* **1988**, *89*, 385–395.
(112) Dykstra, C. E.; Jasien, P. G. *Chem. Phys. Lett.* **1984**, *109*, 388–393.
(113) Jørgensen, P., Simons, J., Eds. *Geometrical Derivatives of Energy Surfaces and Molecular Properties*; Reidel: Dordrecht, 1986.
(114) Nozières, P.; Pines, P. *Nuovo Cimento* **1958**, *9*, 470–490.
(115) Thouless, D. J. *Quantum Mechanics of Many Body Systems*; Academic: New York, 1961.
(116) Dalgarno, A.; Victor, G. A. *Proc. R. Soc. London Ser. A* **1966**, *291*, 291–295.
(117) Sekino, H.; Bartlett, R. J. *Chem. Phys.* **1986**, *85*, 976–989.
(118) Sekino, H.; Bartlett, R. J. *Chem. Phys.* **1991**, *94*, 3665–3669.
(119) Karna, S. P.; Dupuis, M. *J. Comput. Chem.* **1991**, *12*, 487–504.
(120) Rice, J. E.; Amos, R. D.; Colwell, S. M.; Handy, N. C.; Sanz, J. *J. Chem. Phys.* **1990**, *93*, 8828–8839.
(121) Sekino, H.; Bartlett, R. J. *J. Chem. Phys.* **1993**, *98*, 3022–3037.
(122) Sekino, H.; Bartlett, R. *Int. J. Quantum Chem.* **1992**, *43*, 119–134.
(123) Purvis, G. D.; Bartlett, R. *Phys. Rev. A* **1981**, *23*, 1594–1599.
(124) Bartlett, R.; Purvis, G. D. *Phys. Rev. A* **1979**, *20*, 1313–1322.
(125) Sekino, H.; Bartlett, R. J. *Chem. Phys.* **1986**, *84*, 2726–2733.
(126) Rice, J. E.; Handy, N. C. *Int. J. Quantum Chem.* **1992**, *43*, 91–118.
(127) Hammond, B. L.; Rice, J. E. *J. Chem. Phys.* **1992**, *97*, 1138–1143.
(128) Sim, F.; Chin, S.; Dupuis, M.; Rice, J. E. *J. Phys. Chem.* **1993**, *97*, 1158–1163.
(129) Stähelin, M.; Moylan, C. R.; Burland, D. M.; Willetts, A.; Rice, J. E.; Shelton, D. P.; Donely, E. A. *J. Chem. Phys.* **1993**, *98*, 5595–5603.
(130) Karna, S. P.; Dupuis, M.; Perrin, E.; Prasad, P. N. *J. Chem. Phys.* **1990**, *92*, 7418–7425.
(131) Karna, S. P.; Dupuis, M. *Chem. Phys. Lett.* **1990**, *171*, 201–208.
(132) Daniel, C.; Dupuis, M. *Chem. Phys. Lett.* **1990**, *171*, 209–216.
(133) Karna, S. P.; Prasad, P. N.; Dupuis, M. *J. Chem. Phys.* **1991**, *94*, 1171–1181.
(134) Tsunekawa, T.; Yamaguchi, K. *Chem. Phys. Lett.* **1992**, *190*, 533–538.
(135) Tsunekawa, T.; Yamaguchi, K. *J. Phys. Chem.* **1992**, *96*, 10268–10275.
(136) Meyers, F.; Adant, C.; Brédas, J. L. *J. Am. Chem. Soc.* **1991**, *113*, 3715–3719.
(137) Meyers, F.; Adant, C.; Toussaint, J. M.; Brédas, J. L. *Synth. Met.* **1991**, *43*, 3559–3562.
(138) Brédas, J. L.; Meyers, F. *Nonlinear Opt.* **1991**, *1*, 119–123.
(139) Meyers, F.; Zyss, J.; Brédas, J. L. *Synth. Met.* **1991**, *43*, 3191–3194.
(140) Meyers, F.; Brédas, J. L. *Int. J. Quantum Chem.* **1992**, *42*, 1595–1614.
(141) Bader, M. M.; Hamada, T.; Kakuta, A. *J. Am. Chem. Soc.* **1992**, *114*, 6475–6479.
(142) Keshari, V.; Karna, S. P.; Prasad, P. N. *J. Phys. Chem.* **1993**, *97*, 3525–3529.
(143) Brédas, J. L.; Meyers, F.; Pierce, B. M.; Zyss, J. *J. Am. Chem. Soc.* **1992**, *114*, 4928–4929.
(144) Bloor, J. E.; Yu, J. *J. Phys. Chem.* **1990**, *94*, 5586–5589.
(145) For an excellent reference on basis sets in electronic structure computations, see: Davidson, E. R.; Feller, D. *Chem. Rev.* **1986**, *86*, 681–696.
(146) Dykstra, C. E. *J. Chem. Educ.* **1988**, *65*, 198–200.
(147) Christiansen, P. A.; McCullough, E. A. *Chem. Phys. Lett.* **1979**, *63*, 570–573.
(148) Møller, C.; Plesset, M. S. *Phys. Rev.* **1934**, *46*, 618–622.
(149) Hehre, W. J.; Radom, L.; Schleyer, P. v. R.; Pople, J. A. *Ab-Initio Molecular Orbital Theory*; Wiley: New York, 1986; Chapter 2.
(150) See, for example: Bartlett, R. J. *Ann. Rev. Phys. Chem.* **1981**, *32*, 359–401.
(151) Dalgaard, E. *J. Chem. Phys.* **1980**, *72*, 816–823.
(152) Dalgaard, E. *Phys. Rev. A* **1982**, *26*, 42–52.
(153) Yeager, D. L.; Jørgensen, P. *Chem. Phys. Lett.* **1979**, *65*, 77–80.
(154) Olsen, J.; Jørgensen, P. *J. Chem. Phys.* **1985**, *82*, 3235–3264.
(155) Hettema, H.; Jensen, H. J. Aa.; Jørgensen, P.; Olsen, J. *J. Chem. Phys.* **1992**, *97*, 1174–1190.
(156) Luo, Y.; Agren, H.; Vahtras, O.; Jørgensen, P. *Chem. Phys. Lett.* **1993**, *190–194*.
(157) Jaszuński, M.; Jørgensen, P.; Jensen, H. J. Aa. *Chem. Phys. Lett.* **1992**, *191*, 293–298.
(158) Parkinson, W. A.; Oddershede, J. *J. Chem. Phys.* **1991**, *94*, 7251–7258.
(159) Aiga, F.; Sasagane, K.; Itoh, R. *Chem. Phys.* **1992**, *167*, 277–290.
(160) Sadlej, A. J. *Theor. Chim. Acta* **1991**, *79*, 123–140.
(161) Ward, J. F.; Miller, C. K. *Phys. Rev. A* **1979**, *19*, 826–833.
(162) Dudley, J. W.; Ward, J. F. *J. Chem. Phys.* **1985**, *82*, 4673–4677.
(163) Bishop, D. M. *J. Chem. Phys.* **1991**, *95*, 5489.
(164) Schweig, A. *Chem. Phys. Lett.* **1967**, *1*, 195–199.
(165) Zyss, J. *J. Chem. Phys.* **1979**, *70*, 3333–3340.
(166) Zyss, J.; Berthier, G. *J. Chem. Phys.* **1982**, *77*, 3635–3653.
(167) Parkinson, W. A.; Zerner, M. C. *J. Chem. Phys.* **1991**, *94*, 478–483.

(168) Sen, R.; Majumdar, D.; Bhattacharyya, S. P.; Bhattacharyya, S. N. *Chem. Phys. Lett.* **1991**, *181*, 288–292.
(169) Mestechkin, M. M.; Whyman, G. E. *Opt. Commun.* **1993**, *95*, 92–96.
(170) Waite, J.; Papadopoulos, M. G. *J. Phys. Chem.* **1990**, *94*, 1755–1758.
(171) Nicolaides, C. A.; Papadopoulos, M. G.; Waite, J. *Theor. Chim. Acta* **1982**, *61*, 427–436.
(172) Waite, J.; Papadopoulos, M. G. *J. Mol. Struct. (Theochem)* **1989**, *202*, 121–128.
(173) Waite, J.; Papadopoulos, M. G. *J. Chem. Phys.* **1985**, *82*, 1427–1434.
(174) Waite, J.; Papadopoulos, M. G. *Z. Naturforsch* **1990**, *45a*, 189–190.
(175) Kurtz, H. A.; Stewart, J. J. P.; Dieter, K. M. *J. Comput. Chem.* **1990**, *11*, 82–87.
(176) Matsuzawa, N.; Dixon, D. A. *Int. J. Quantum Chem.* **1992**, *44*, 497–515.
(177) Matsuzawa, N.; Dixon, D. A. *J. Phys. Chem.* **1992**, *96*, 6232–6241.
(178) Chandra, A. K.; Banerjee, M. *J. Mol. Struct. (Theochem)* **1991**, *83*, 261–269.
(179) Williams, G. R. J. *J. Mol. Struct. (Theochem)* **1987**, *36*, 215–222.
(180) Lu, Y. J.; Lee, S. L. *Int. J. Quantum Chem.* **1992**, *44*, 773–784.
(181) Kondo, K.; Goda, H.; Takemoto, K.; Aso, H.; Sasaki, T.; Kawakami, K.; Yoshida, H.; Yoshida, K. *J. Mater. Chem.* **1992**, *2*, 1097–1102.
(182) Subramaniam, G.; Polashenski, S.; Kennedy, K. *Ferroelectrics* **1991**, *122*, 229–238.
(183) Risser, S. M.; Ferris, K. F. *Nonlinear Opt.* **1991**, *1*, 195–200.
(184) Ryu, U.; Choi, D.; Kim, N.; Lee, Y. S. *J. Korean Chem. Soc.* **1993**, *37*, 62–67.
(185) Yoshimura, T. *Appl. Phys. Lett.* **1989**, *55*, 534–536.
(186) Yoshimura, T. *Phys. Rev. B* **1989**, *40*, 6292–6298.
(187) Yoshimura, T. *Mol. Cryst. Liq. Cryst.* **1990**, *182*, 43–50.
(188) Marder, S. R.; Gorman, C. B.; Tiemann, B. G.; Cheng, L.-T. *J. Am. Chem. Soc.* **1993**, *115*, 3006–3007.
(189) Barzoukas, M.; Fort, A.; Serbutoviez, C.; Oswald, L.; Nicoud, J. F. *Chem. Phys.* **1991**, *153*, 457–464.
(190) Barzoukas, M.; Fort, A.; Klein, G.; Servutoviez, C.; Oswald, L.; Nicoud, J. F. *Chem. Phys.* **1992**, *164*, 395–406.
(191) Armstrong, J. A.; Bloembergen, N.; Ducuing, J.; Pershan, P. S. *Phys. Rev.* **1962**, *127*, 1918–1939.
(192) Ward, J. F. *Rev. Mod. Phys.* **1965**, *37*, 1–18.
(193) Orr, B. J.; Ward, J. F. *Mol. Phys.* **1971**, *20*, 513–526.
(194) Allen, S.; Morley, J. O.; Pugh, D.; Docherty, V. J. *Proc. SPIE-Int. Soc. Opt. Eng.* **1987**, *682*, 20–26.
(195) Reference 77, Chapter 11.
(196) Pariser, R.; Parr, R. G. *J. Chem. Phys.* **1953**, *21*, 466–471.
(197) Pople, J. A. *Trans. Faraday Soc.* **1953**, *49*, 1375–1385.
(198) Morley, J. O.; Pugh, D. *Spec. Publ. - R. Soc. Chem.* **1989**, *69*, 28–39.
(199) Ulman, A.; Willand, C. S.; Kohler, W.; Robello, D. R.; Williams, D. J.; Handley, L. *J. Am. Chem. Soc.* **1990**, *112*, 7083–7090.
(200) Kanis, D. R.; Ratner, M. A.; Marks, T. J. *J. Am. Chem. Soc.* **1992**, *114*, 10338–10357.
(201) Risser, S. M.; Beratan, D. N.; Marder, S. R. *J. Am. Chem. Soc.* **1993**, *115*, 7719–7728.
(202) Marder, S. R.; Cheng, L.-T.; Beratan, D. N. *AIP Conf. Proc.* **1992**, *262*, 252–264.
(203) Marder, S. R.; Cheng, L.-T.; Tiemann, B. G.; Beratan, D. N. *Proc. SPIE-Int. Soc. Opt. Eng.* **1991**, *1560*, 86–97.
(204) Dirk, C. W.; Twieg, R. J.; Wagnière, G. *J. Am. Chem. Soc.* **1986**, *108*, 5387–5395.
(205) Soos, Z. G.; Ramasesha, S. *J. Chem. Phys.* **1989**, *90*, 1067–1076.
(206) Li, D.; Marks, T. J.; Ratner, M. A. *Chem. Phys. Lett.* **1986**, *131*, 370–375.
(207) Li, D.; Marks, T. J.; Ratner, M. A. *J. Am. Chem. Soc.* **1988**, *110*, 1707–1715.
(208) Li, D.; Ratner, M. A.; Marks, T. J. *J. Phys. Chem.* **1992**, *96*, 4325–4336.
(209) Li, D.; Marks, T. J.; Ratner, M. A. *Mat. Res. Soc. Symp. Proc.* **1988**, *109*, 1707–1715.
(210) Hutter, J.; Wagnière, G. *J. Mol. Struct.* **1988**, *175*, 159–164.
(211) Matsuoka, M.; Furushow, M.; Iida, S.; Kitao, T. *Nonlinear Opt., Proc. Toyota Conf. Nonlinear Opt. Mater., 5th.* **1992**, 231–236.
(212) Taketani, Y.; Shouji, A.; Iwata, K. *Nonlinear Opt., Proc. Toyota Conf. Nonlinear Opt. Mater., 5th.* **1992**, 249–254.
(213) Sales, T. R. M.; deMelo, C. P.; Dossantos, M. C. *Synth. Met.* **1991**, *43*, 3751–3754.
(214) de Melo, C. P.; Silbey, R. *J. Chem. Phys.* **1988**, *88*, 2567–2571.
(215) Ramasesha, S.; Das, P. K. *Chem. Phys.* **1990**, *145*, 343–353.
(216) Ramasesha, S.; Albert, I. D. L. *Phys. Rev. B: Condens. Matter* **1990**, *42*, 8587–8594.
(217) Ramasesha, S.; Albert, I. D. L. *Chem. Phys. Lett.* **1992**, *196*, 287–293.
(218) Albert, I. D. L.; Das, P. K.; Ramasesha, S. *Chem. Phys. Lett.* **1991**, *176*, 217–224.
(219) Hetherington, W. M., III; Mazely, T. L. *J. Chem. Phys.* **1987**, *86*, 3640–3647.
(220) Atkins, K. J.; Honeybourne, C. L. *Spec. Publ. - R. Soc. Chem.* **1991**, *91* (Org. Mater. Nonlinear Opt 2), 121–127.
(221) Joffre, M.; Yaron, D.; Silbey, R. J.; Zyss, J. *J. Chem. Phys.* **1992**, *97*, 5607–5615.

(222) Morrell, J. A.; Albrecht, A. C. *Chem. Phys. Lett.* **1979**, *64*, 46–50.

(223) Morrell, J. A.; Albrecht, A. C.; Levin, K. H. *J. Chem. Phys.* **1979**, *71*, 5063–5068.

(224) Willand, C. S.; Albrecht, A. C. *Opt. Commun.* **1986**, *57*, 146–152.

(225) Sen, R.; Majumdar, D.; Bhattacharyya, S. P. *Chem. Phys. Lett.* **1992**, *190*, 443–446.

(226) Maslyanitsin, I. A.; Shigorin, V. D.; Shipulo, G. P. *Chem. Phys. Lett.* **1992**, *194*, 355–358.

(227) Kodaka, M.; Fukaya, T.; Yonemoto, K.; Shibuya, I. *J. Chem. Soc., Chem. Commun.* **1990**, 1096–1098.

(228) Lalama, S. L.; Garito, A. F. *Phys. Rev.* **1979**, *20*, 1179–1194.

(229) del Bene, J.; Jaffe, H. H. *J. Chem. Phys.* **1968**, *48*, 1807–1813.

(230) Lipari, N. O.; Duke, C. B. *J. Chem. Phys.* **1975**, *63*, 1748–1757.

(231) There are two important typographical errors in ref 228: (1) The first summation in eq 9a, p 1181, should not be primed. (2) The second summation in eq 9a should have two terms, a diagonal term and an off-diagonal term. Therefore, this crucial equation should read as follows:

$$r_{nn'} = \sum_{i,j,k,l} A_{n,i \to j} A_{n',k \to l} \int \chi_{i \to j} M^i \chi_{k \to l} d\tau$$

$$= \sum_{i,j,k,l}' A_{n,i \to j} A_{n',k \to l} (\delta_{ik} m_{jl}^i - \delta_{jl} m_{ik}^i)$$

$$+ \sum_{i,j} A_{n,i \to j} A_{n',i \to j} (\langle \text{ground} | M^i | \text{ground} \rangle + m_{jj}^i - m_{ii}^i)$$

(232) Teng, C. C.; Garito, A. F. *Phys. Rev. B* **1983**, *28*, 6766–6773.

(233) Teng, C. C.; Garito, A. F. *Phys. Rev. Lett.* **1983**, *50*, 350–352.

(234) Garito, A. F.; Teng, C. C.; Wong, K. Y.; Zamani-Khamiri, O. *Mol. Cryst. Liq. Cryst.* **1984**, *106*, 219–258.

(235) Lipscomb, G. F.; Narang, R. S.; Garito, A. F. *J. Chem. Phys.* **1981**, *75*, 1509–1516.

(236) Lalama, S. J.; Singer, K. D.; Garito, A. F.; Desai, K. N. *Appl. Phys. Lett.* **1981**, *39*, 940–942.

(237) Garito, A. F.; Wong, K. Y.; Cai, Y. M.; Man, H. T.; Zamani-Khamiri, O. *Proc. SPIE-Int. Soc. Opt. Eng.* **1987**, *682*, 2–11.

(238) Docherty, V. J.; Pugh, D.; Morley, J. O. *J. Chem. Soc., Faraday Trans. 2* **1985**, *81*, 1179–1192.

(239) Pugh, D.; Morley, J. O. *Nonlinear Opt. Prop. Org. Mol. Cryst.* **1987**, *1*, 193–225.

(240) Morley, J. O. *Ann. Soc. Sci. Bruxelles, Ser. 1* **1990**, *103*, 109–124.

(241) Morley, J. O. *Springer Proc. Phys.* **1989**, *36*, 86–97.

(242) Morley, J. O.; Pavlides, P.; Pugh, D. *NATO ASI Ser., Ser. E* **1991**, *194*, 37–52.

(243) Morley, J. O.; Pavlides, P.; Pugh, D. *Int. J. Quantum Chem.* **1992**, *43*, 7–26.

(244) Morley, J. O.; Docherty, V. J.; Pugh, D. *J. Chem. Soc., Perkin Trans. 2* **1987**, 1357–1360.

(245) Morley, J. O.; Docherty, V. J.; Pugh, D. *J. Chem. Soc., Perkin Trans. 2* **1987**, 1361–1363.

(246) Morley, J. O.; Docherty, V. J.; Pugh, D. *J. Mol. Electron.* **1989**, *5*, 117–121.

(247) Morley, J. O. *J. Am. Chem. Soc.* **1988**, *110*, 7660–7663.

(248) Morley, J. O. *J. Chem. Soc., Perkin Trans. 2* **1989**, 103–106.

(249) Hurst, M.; Munn, R. W.; Morley, J. O. *J. Mol. Electron.* **1990**, *6*, 15–19.

(250) Morley, J. O. *J. Chem. Soc., Faraday Trans. 2* **1991**, *87*, 3009–3013.

(251) Morley, J. O. *J. Chem. Soc., Faraday Trans. 2* **1991**, *87*, 3015–3019.

(252) Morley, J. O.; Pugh, D. A. *J. Chem. Soc., Faraday Trans. 2* **1991**, *87*, 3021–3025.

(253) Morley, J. O. *Proc. SPIE-Int. Soc. Opt. Eng.* **1992**, *1775*, 2–12.

(254) Morley, J. O. *Int. J. Quantum Chem.* **1993**, *46*, 19–26.

(255) Barzoukas, M.; Josse, D.; Fremaux, P.; Zyss, J.; Nicoud, J. F.; Morley, J. O. *J. Opt. Soc. Am. B: Opt. Phys.* **1987**, *4*, 977–986.

(256) Cao, Y.; Qui, G.; Wang, Y. *Huaxue Xuebao* **1992**, *50*, 783–787.

(257) Kanis, D. R.; Griffin, F.; O'Neal, P.; Ratner, D.; Shoemaker, B.; Marks, T. J.; Ratner, M. A. Submitted to *J. Phys. Chem.*

(258) Most of the variation in slope is believed due to experimental issues. Such a measurement will reflect modification of the isolated chromophore response due to the presence of solvent (and, perhaps, the effect of other chromophores). For most organic chromophores that exhibit reasonable nonlinear responses, the excited-state dipole moments are larger than the ground-state dipole moments (Figure 17); therefore, stabilization effects due to simple solvent polarization should lower the energies of the excited states more than the ground states, thereby reducing the denominator of eq 10 and increasing the nonlinear response—this is reminiscent of the generally observed red-shifting of spectra due to polarization effects in solution, and it results in increased response in solvent compared to that expected for isolated molecules.

(259) Ulman, A. *J. Phys. Chem.* **1988**, *92*, 2385–2390.

(260) Gao, X. L.; Feng, J. K.; Sun, C. C. *Int. J. Quantum Chem.* **1992**, *42*, 1747–1758.

(261) Gao, X.; Feng, J.; Li, J.; Fei, H.; Sun, J. *Huaxue Xuebao* **1991**, *49*, 644–648.

(262) Feng, J.; Gao, X.; Li, J.; Sun, C. *Wuli Huaxue Xuebao* **1992**, *8*, 156–161.

(263) Feng, J.; Gao, X.; Sun, J. *Gaodeng Xuexiao Huaxue Xuebao* **1992**, *13*, 809–812.

(264) Yu, H.; Feng, J.; Li, J.; Li, Z. *Huaxue Xuebao* **1993**, *51*, 334–340.

(265) Feng, J.; Gao, X.; Sun, J. *Chin. Sci. Bull.* **1992**, *37*, 1441–1445.

(266) Kanis, D. R.; Marks, T. J.; Ratner, M. A. *Mol. Cryst. Liq. Cryst. Sci. Technol.-Sec. B: Nonlinear Opt.*, in press.

(267) Kanis, D. R.; O'Neal, P.; Griffin, F.; Wong, J.; Ratner, M. A.; Marks, T. J. Manuscript in preparation.

(268) Kanis, D. R.; Ratner, M. A.; Marks, T. J.; Zerner, M. C. *Chem. Mater.* **1991**, *3*, 19–22.

(269) Murphy, D. M.; Mingos, D. M. P.; Haggitt, J. L.; Powell, H. R.; Westcott, S. A.; Marder, T. B.; Taylor, N. J.; Kanis, D. R. *J. Mater. Chem.* **1993**, *3*, 139–148.

(270) Kanis, D. R.; Ratner, M. A.; Marks, T. J. *J. Am. Chem. Soc.* **1990**, *112*, 8203–8204.

(271) Kanis, D. R.; Lacroix, P. A.; Ratner, M. A.; Marks, T. J. Submitted to *J. Am. Chem. Soc.*

(272) DiBella, S.; Fragalá, I. L.; Ratner, M. A.; Marks, T. J. *J. Am. Chem. Soc.* **1993**, *115*, 682–686.

(273) DiBella, S.; Ratner, M. A.; Marks, T. J. *J. Am. Chem. Soc.* **1992**, *114*, 5842–5849.

(274) Jain, M.; Chandrasekhar, J. *J. Phys. Chem.* **1993**, *97*, 4044–4049.

(275) Szabo, A.; Ostlund, N. S. *Modern Quantum Chemistry*; McGraw-Hill: New York, 1989, Chapter 4.

(276) Reference 149, Chapter 4.

(277) Linderberg, J.; Öhrn, Y. *J. Chem. Phys.* **1967**, *49*, 716–727.

(278) Jørgensen, P.; Linderberg, J. *Int. J. Quantum Chem.* **1970**, *4*, 587–602.

(279) Tomonari, M.; Ookubo, N.; Takada, T.; Feyereisen, M. W.; Almlöf, J. *Chem. Phys. Lett.* **1993**, *203*, 603–610.

(280) Stanton, J. F.; Bartlett, R. J. *J. Chem. Phys.* **1993**, *99*, 5178–5183.

(281) Charton, M. *Prog. Phys. Org. Chem.* **1981**, *13*, 119–251.

(282) Taft, R. W.; Topsom, R. D. *Prog. Phys. Org. Chem.* **1987**, *16*, 1–84.

(283) Topsom, R. D. *Prog. Phys. Org. Chem.* **1987**, *16*, 85–124.

(284) Hansch, C.; Leo, A.; Taft, R. W. *Chem. Rev.* **1991**, *91*, 165–195.

(285) The oscillator strength (f_{ge}) is related to the extinction coefficient by the formulas $f_{ge} \approx 4.319 \times 10^{-9}$ (ϵ_{max}) $(\Delta \nu)_{1/2}$, where $\Delta \nu$ is the half-band width. See, for example: Suzuki, H. *Electronic Absorption Spectra and Geometry of Organic Molecules*, Academic Press: New York, 1967; p 9.

(286) Burland, D. M.; Rice, J. E.; Stähelin, M. *Mol. Cryst. Liq. Cryst.* **1992**, *216*, 27–32.

(287) Burland, D. M.; Miller, R. D.; Reiser, O.; Twieg, R. J.; Walsh, C. A. *J. Appl. Phys.* **1992**, *71*, 410–417.

(288) Burland, D. M.; Rice, J. E.; Downing, J.; Michl, J. *Proc. SPIE-Int. Soc. Opt. Eng.* **1991**, *1560*, 111–119.

(289) Buncel, E.; Rajagopal, S. *Acc. Chem. Res.* **1990**, *23*, 226–231.

(290) Buncel, E.; Rajagopal, S. *J. Org. Chem.* **1989**, *54*, 798–809.

(291) Benson, H. G.; Murrell, J. N. *J. Chem. Soc., Faraday Trans. 2* **1972**, *68*, 137–143.

(292) Levine, B. F.; Bethea, C. G.; Wasserman, E.; Leenders, L. *J. Chem. Phys.* **1978**, *68*, 5042–5045.

(293) Wrighton, M. S.; Abrahamson, H. B.; Morse, D. L. *J. Am. Chem. Soc.* **1976**, *98*, 4105–4109.

(294) Cheng, L.-T.; Tam, W.; Eaton, D. F. *Organometallics* **1990**, *9*, 2856–2857.

(295) See for example, Paley, M.; Harris, J.; Looser, H.; Baumert, J.; Bjorklund, G.; Jundt, D.; Tweig, R. *J. Org. Chem.* **1989**, *54*, 3774–3778.

(296) Burland, D. M.; Downing, J.; Michl, J. *Mol. Cryst. Liq. Cryst. Sci. Technol. -Sec. B: Nonlinear Opt.* **1992**, *3*, 195–203.

(297) Beratan, D. N. in ref 22, pp 89–102.

(298) More precisely, the sum-over-states expression (eq 31) can be partitioned into two contributions, $\beta_{ijk,2}$ (two-level terms) and $\beta_{ijk,3}$ (three-level terms). The components of each along the dipole moment direction ($\beta_{vec,2}$ and $\beta_{vec,3}$) can be obtained from the 27 individual tensorial elements in a fashion completely analogous to extracting β_{vec} from β_{ijk}. Ultimately, of course, $\beta_{vec} = \beta_{vec,2} + \beta_{vec,3}$.

(299) Kanis, D. R.; Marks, T. J.; Ratner, M. A. Manuscript in preparation.

(300) Slama-Schwok, A.; Blanchard-Desce, M.; Lehn, J.-M. *J. Phys. Chem.* **1990**, *94*, 3894–3902.

(301) Blanchard-Desce, M.; Ledoux, I.; Lehn, J.-M.; Malthete, J.; Zyss, J. *J. Chem. Soc., Chem. Commun.* **1988**, 736–739.

(302) André, J. M.; Brédas, J. L.; Delhalle, J.; Vanderveken, D. J.; Vercauteren, D. P.; Fripiat, J. G. In *Modern Techniques in Computational Chemistry: MOTECC-90*; Clementi, E., Ed.; ESCOM: Leiden, 1990; pp 745–783.

(303) Jones, R. O.; Gunnarson, O. *Rev. Phys.* **1989**, *61*, 689–746.

(304) Parr, R. G.; Yang, W. *Density-Functional Theory of Atoms and Molecules*; Oxford University: New York, 1989.

(305) Moullet, I.; Martins, J. L. *J. Chem. Phys.* **1990**, *92*, 527–535.

(306) Jasien, P. G.; Fitzgerald, G. *J. Chem. Phys.* **1990**, *93*, 2554–2560.

(307) Sim, F.; Salahub, D. R.; Chin, S. *Int. J. Quantum Chem.* **1992**, *43*, 463–479.

(308) Westin, E.; Rosén, A. *Surf. Sci.* **1992**, *269/270*, 577–582.

(309) Dixon, D. Personal communication.

(310) Guan, J.; Duffy, P.; Carter, J. T.; Chong, D. P.; Casida, K. C.; Casida, M. E.; Wrinn, M. *J. Chem. Phys.* **1993**, *98*, 4753–4765.

(311) Colwell, S. M.; Murray, C. W.; Handy, N. C.; Amos, R. D. *Chem. Phys. Lett.*, in press.

(312) Barzoukas, M.; Blanchard-Desce, M.; Josse, D.; Lehn, J.-M.; Zyss, J. *Chem. Phys.* **1989**, *133*, 323–329.
(313) Huijts, R. A.; Hesselink, G. L. J. *Chem. Phys. Lett.* **1989**, *156*, 209–212.
(314) See, for example: Platt, J. R. *Systematics of the Electronic Structure of Conjugated Molecules: A Source Book*; Wiley: New York, 1964.
(315) See, for example: Albright, T. A.; Burdett, J. K.; Whangbo, M. H. *Orbital Interactions in Chemistry*; Wiley: New York, 1985; Chapter 12.
(316) Kanis, D. R.; Brewer, L.; Griffin, F.; Marks, T. J.; Ratner, M. A. Manuscript in preparation.
(317) Stiegman, A. E.; Graham, E.; Perry, K. J.; Khundkar, L. R.; Cheng, L.-T.; Perry, J. W. *J. Am. Chem. Soc.* **1991**, *113*, 7658–7666.
(318) Dehu, C.; Meyers, F.; Brédas, J. L. *J. Am. Chem. Soc.* **1993**, *115*, 6198–6206.
(319) Graham, E. M.; Miskowski, V. M.; Perry, J. W.; Coulter, D. R.; Stiegman, A. E.; Schaefer, W. P.; Marsh, R. E. *J. Am. Chem. Soc.* **1989**, *111*, 8771–8779.
(320) Yitzchaik, S.; Roscoe, S. B.; Kakkar, A. K.; Allan, D. S.; Marks, T. J.; Xu, Z.; Zhang, T.; Lin, W.; Wong, G. K. *J. Phys. Chem.* **1993**, *97*, 6958–6960.
(321) Kakkar, A. K.; Yitzchaik, S.; Roscoe, S. B.; Kubota, F.; Allan, D. S.; Marks, T. J.; Lin, W.; Wong, G. K. *Langmuir* **1993**, *9*, 388–390.
(322) Li, D.; Marks, T. J.; Zhang, C.; Yang, J.; Wong, G. K. *Proc. SPIE-Int. Soc. Opt. Eng.* **1990**, *1337*, 341–347.
(323) Li, D.; Ratner, M. A.; Marks, T. J.; Zhang, C.; Yang, J.; Wong, G. K. *J. Am. Chem. Soc.* **1990**, *112*, 7389–7390.
(324) Marginggele, W. In *The Chemistry of Inorganic Homo- and Heterocycles*; Haiduc, I., Sowerby, D. B., Eds.; Academic Press: London, 1987; p 17.
(325) Nelson, J. T.; Pietro, W. *J. Inorg. Chem.* **1989**, *28*, 544–548.
(326) Molecule 33 represents a linear analogue of a B–O heterocycle; see Haiduc, I. in ref 324, pp 109–141.
(327) Molecule 34 represents a linear analogue of a B–S heterocycle; see Siebert, W. in ref 324, pp 143–165.
(328) Miller, R. D. *Angew. Chem. Int., Ed. Engl.* **1989**, *28*, 1733–1740.
(329) West, R. J.; Maxka, J. *ACS Symp. Series* **1988**, *360*, 6–20.
(330) Miller, R. D.; Rabolt, J. R.; Sooriyakumaram, R.; Fleming, W.; Fickes, G. N.; Farmer, B. L.; Kuzmany, H. *ACS Symp. Ser.* **1988**, *360*, 43–60.
(331) Klingensmith, K. A.; Dawning, J. W.; Miller, R. D.; Michl, J. *J. Am. Chem. Soc.* **1986**, *108*, 7438–7439.
(332) Baumert, J.-C.; Bjorklund, G. C.; Jundt, D. H.; Jurich, M. C.; Looser, H.; Miller, R. D.; Rabaolt, J.; Sooriyakumaran, R.; Swalen, J. D.; Twieg, R. *J. Appl. Phys. Lett.* **1988**, *53*, 1147–1149.
(333) Lever, A. B. P. *Inorganic Electronic Spectroscopy*, 2nd ed.; Elsevier: Amsterdam, 1984; Chapter 5.
(334) Geoffroy, G. L.; Wrighton, M. S. *Organometallic Photochemistry*; Academic Press: New York, 1979; Chapter 1.
(335) Marder, S. R.; Perry, J. W.; Schaefer, W. P.; Tiemann, B. G.; Groves, P. C.; Perry, K. *Proc. SPIE-Int. Soc. Opt. Eng.* **1990**, *1147*, 108–115.
(336) Green, M. L. H.; Marder, S. R.; Thompson, M. E.; Bandy, J. A.; Bloor, D.; Kolinsky, P. V.; Jones, R. J. *Nature* **1987**, *330*, 360–362.
(337) Pollagi, T. P.; Stoner, T. C.; Dallinger, R. F.; Gilbert, T. M.; Hopkins, M. D. *J. Am. Chem. Soc.* **1991**, *113*, 703–704.
(338) Wright, M. E.; Toplikar, E. G.; Kubin, R. F.; Seltzer, M. D. *Macromolecules* **1992**, *25*, 1838–1839.
(339) Zyss, J.; Dhenaut, C.; Chauvan, T.; Ledoux, I. *Chem. Phys. Lett.* **1993**, *206*, 409–414.
(340) Laidlaw, W. M.; Denning, R. G.; Verbiest, T.; Chauchard, E.; Persoons, A. *Nature* **1993**, *363*, 58–60.
(341) Thami, T.; Bassoul, P.; Petit, M. A.; Simon, J.; Fort, A.; Barzoukas, M.; Villaeys, A. *J. Am. Chem. Soc.* **1992**, *114*, 915–921.
(342) Marcy, H. O.; Warren, L. F.; Webb, M. S.; Ebbers, C. A.; Velsko, S. P.; Kennedy, G. C.; Catella, G. C. *Appl. Opt.* **1991**, *31*, 5051–5060.
(343) Matsuo, T.; Nakamura, H.; Nakao, T.; Kawazu, M. *Chem. Lett.* **1992**, 2363–2366.
(344) Coe, B. J.; Kurek, S. S.; Rowley, N. M.; Foulon, J. D.; Hamor, T. A.; Harman, M. E.; Hursthouse, M. B.; Jones, C. J.; McCleverty, J. A.; Bloor, D. *Chemotronics* **1991**, *5*, 23–28.
(345) Li, S. X.; Wang, Z. M.; Chen, J. Z.; Su, W. Y. *Chin. Chem. Lett.* **1992**, *3*, 397–398.
(346) Yuan, D.; Zhang, N.; Tao, X.; Xu, D.; Jiang, M.; Shao, Z. *Chin. Sci. Bull.* **1991**, *36*, 1401–1404.
(347) Chiang, W.; Thompson, M. E.; Van Engen, D. *Spec. Publ.—R. Soc. Chem.* **1991**, *91* (Org. Mater. Non-linear Opt. 2), 210–216.
(348) Lamberth, C.; Murphy, D. M.; Mingos, D. M. P. *Spec. Publ.—R. Soc. Chem.* **1991**, *91* (Org. Mater. Non-linear Opt. 2), 183–189.
(349) Copley, R. C. B.; Lamberth, C.; Machell, J.; Mingos, D. M. P.; Murphy, D. M.; Powell, H. *J. Mater. Chem.* **1991**, 583–589.
(350) Lesley, G.; Yuan, Z.; Stringer, G.; Jobe, I. R.; Taylor, N. J.; Koch, L.; Scott, K.; Marder, T. B.; Williams, I. D.; Kurtz, S. K. *Spec. Publ.—R. Soc. Chem.* **1991**, *91* (Org. Mater. Non-linear Opt. 2), 197–203.

(351) Sakaguchi, H.; Nagamura, T.; Matsuo, T. *Appl. Organomet. Chem.* **1991**, *5*, 257–260.
(352) Chollet, P. A.; Kajzar, F.; Moigne, J. L. *Proc. SPIE-Int. Soc. Opt. Eng.* **1990**, *1273*, 87–95.
(353) Zhang, N.; Jiang, M. H.; Yuan, D. R.; Xu, D.; Tao, X. T.; Shao, Z. S. *J. Cryst. Growth* **1990**, *102*, 581–584.
(354) Coe, B. J.; Jones, C. J.; McCleverty, J. A.; Bloor, D.; Kolinsky, P. V.; Jones, R. J. *J. Chem. Soc., Chem. Commun.* **1989**, 1485–1487.
(355) Tam, W.; Eaton, D. F.; Calabrese, J. C.; Williams, I. D.; Wang, Y.; Anderson, A. G. *Chem. Mater.* **1989**, *1*, 128–140.
(356) Cheng, L.-T.; Tam, W.; Eaton, D. F. *Organometallics* **1990**, *9*, 2856–2857.
(357) Tam, W.; Calabrese, J. C. *Chem. Phys. Lett.* **1988**, *144*, 79–82.
(358) Tao, X.; Zhang, N.; Yuan, D.; Xu, D.; Yu, W.; Jiang, M. *Spec. Publ.—R. Soc. Chem.* **1988**, *69* (Org. Mater. Non-linear Opt. 2), 385–389.
(359) Eaton, D. F.; Anderson, A. G.; Tam, W.; Wang, Y. *J. Am. Chem. Soc.* **1987**, *109*, 1886–1888.
(360) Calabrese, J. C.; Tam, W. *Chem. Phys. Lett.* **1987**, *133*, 244–245.
(361) Anderson, A. G.; Calabrese, J. C.; Tam, W.; Williams, I. D. *Chem. Phys. Lett.* **1987**, *134*, 392–396.
(362) Frazier, C. C.; Harvey, M. A.; Cockerham, M. P.; Hand, H. M.; Chauchard, E. A.; Lee, C. H. *J. Phys. Chem.* **1986**, *90*, 5703–5706.
(363) Cheng, L.-T.; Tam, W.; Meredith, G. R.; Marder, S. R. *Mol. Cryst. Liq. Cryst.* **1990**, *189*, 137–153.
(364) Ledoux, I. *Synth. Met.* **1993**, *54*, 123–137.
(365) Houlton, A.; Miller, J. R.; Silver, J.; Jassim, N.; Ahmet, M. J.; Axon, T. L.; Bloor, D.; Cross, G. H. *Inorg. Chim. Acta* **1993**, *205*, 67–70.
(366) Bunting, H. E.; Green, M. L. H.; Marder, S. R.; Thompson, M. E.; Bloor, D.; Kolinsky, P. V.; Jones, R. J. *Polyhedron* **1992**, *11*, 1489–1499.
(367) Bandy, J. A.; Bunting, H. E.; Garcia, M. H.; Green, M. L. H.; Marder, S. R.; Thompson, M. E.; Bloor, D.; Kolinsky, P. V.; Jones, R. J. *Polyhedron* **1992**, *11*, 1429–1435.
(368) Houlton, A.; Jasin, N.; Roberts, R. M. G.; Silver, J.; Cunningham, D.; McArdle, P.; Higgins, T. *J. Chem. Soc., Dalton Trans.* **1992**, 2235–2241.
(369) Loucif-Saiebi, R.; Delaire, J. A.; Bonazzola, L.; Doisneau, G.; Balavoine, G.; Filleebeen-Khan, T.; Ledoux, I.; Puccetti, G.
(370) Kimura, M.; Abel-Halim, H.; Robinson, D. W.; Cowan, D. O. *J. Organomet. Chem.* **1991**, *403*, 365–372.
(371) Yamazaki, Y.; Hosono, K.; Matsuda, H.; Minami, N.; Asai, M.; Nakanishi, H. *Biotechnol. Bioeng.* **1991**, *38*, 1218–1222.
(372) Yamazaki, Y.; Minami, N. *Bio. Ind.* **1991**, *8*, 626–636.
(373) Qin, J.; Gong, X.; Wu, X.; Liao, J.; Dai, C.; Gu, J.; Ma, S.; Liu, D. *C-MRS Int. Symp. Proc.* **1991**, *1*, 409–412.
(374) Doisneau, G.; Balavoine, G.; Filleebeen-Khan, T.; Clinet, J. C.; Delaire, J.; Ledoux, I.; Loucif, R.; Puccetti, G. *J. Organomet. Chem.* **1991**, *421*, 299–304.
(375) Calabrese, J. C.; Cheng, L.-T.; Green, J. C.; Marder, S. R.; Tam, W. *J. Am. Chem. Soc.* **1991**, *113*, 7227–7232.
(376) Marder, S. R.; Perry, J. W.; Schaefer, W. P.; Tiemann, B. G. *Organometallics* **1991**, *10*, 1896–1901.
(377) Richardson, T.; Roberts, G. G.; Polywka, M. E. C.; Davies, S. G. *Thin Solid Films* **1989**, *179*, 405–411.
(378) Bandy, J. A.; Bunting, H. E.; Garcia, M. H.; Green, M. L. H.; Marder, S. R.; Thompson, M. E.; Bloor, D.; Kolinsky, P. V.; Jones, R. J. *Spec. Publ.—R. Soc. Chem.* **1988**, *69* (Org. Mater. Non-linear Opt. 2), 225–231.
(379) Marder, S. R. *Inorg. Mater.* **1992**, 115–164.
(380) Nalwa, H. S. *Appl. Organomet. Chem.* **1991**, *5*, 349–377.
(381) Gilbert, T. M. Private communication (manuscript in preparation).
(382) Curtiss, L. A.; Naleway, C. A.; Miller, J. R. *J. Phys. Chem.* **1993**, *97*, 4050–4058.
(383) Jordan, K. D.; Paddon-Row, M. *J. Phys. Chem.* **1992**, *96*, 1188–1196.
(384) Michl, J. Private communication.
(385) Zyss, J. *Nonlinear Opt.* **1991**, *1*, 3–18.
(386) Zyss, J. *J. Chem. Phys.* **1993**, *98*, 6583–6599.
(387) Clays, K.; Persoons, A. *Phys. Rev. Lett.* **1991**, *66*, 2980–2983.
(388) Verbiest, T.; Clays, K.; Persoons, A.; Meyers, F.; Brédas, J. L. *Opt. Lett.* **1993**, *18*, 525–527.
(389) Munn, R. W. *Mol. Phys.* **1988**, *64*, 1–20.
(390) Hurst, M., Munn, R. W., Aviram, A., Eds. *Molecular Electronics*; Engineering Society: New York, 1989.
(391) Yasukawa, T.; Kimura, T.; Uda, M. *Chem. Phys. Lett.* **1990**, *169*, 219–222.
(392) Waite, J.; Papadopoulis, M. G. *Z. Naturforsch.* **1988**, *43a*, 253–261.
(393) Mikkelsen, K. V.; Ratner, M. A. *J. Phys. Chem.* **1989**, *93*, 1759–70.
(394) Wong, M. W.; Wiberg, K. B.; Frisch, M. *J. J. Am. Chem. Soc.* **1992**, *114*, 623–29, and references therein.
(395) DiBella, S.; Marks, T. J.; Katner, M. A. *J. Am. Chem. Soc.*, in press.
(396) Yu, J.; Zerner, M. J. Manuscript in preparation. (We thank these authors for information in advance of publication.)
(397) Mikkelsen, K. V.; Luo, Y.; Aagren, H.; Jorgensen, P. J. *J. Chem. Phys.*, in press. (We thank these authors for information in advance of publication.)